

Investigation on the Effect of Trap States Signature on the Charge Transport Mechanism of Some Natural Organic Semiconducting Material based Devices

Thesis submitted for the Doctor of Philosophy (Science) of Jadavpur University, 2023

By

Kushal Chakraborty

Research Scholar, Department of Physics, Jadavpur University



Jadavpur University

**Condensed Matter Physics Research Centre
Department of Physics
Jadavpur University
Kolkata-700032**

The thesis is dedicated to the source of supreme power, my parents and rest of my family members.

Declaration by the Author

I hereby declare that this submission of the thesis entitled **“Investigation on the effect of trap states signature on the charge transport mechanism of some natural organic semiconducting material based devices”** is my own work and that, to the best of my knowledge and belief, it contains no material previously published or written by another person nor material which has been accepted for the award of any other degree of the university or other institute of higher learning, except where due acknowledgement has been made in the text.

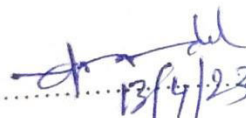
(Kushal Chakraborty)

Date:

Place: Kolkata

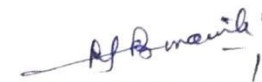
CERTIFICATE FROM THE SUPERVISORS

This is to certify that the thesis entitled “**Investigation on the effect of trap states signature on the charge transport mechanism of some natural organic semiconducting material based devices**”, submitted by Mr. Kushal Chakraborty, who got his name registered on 26th November, 2019 for the award of PhD (Science) degree of Jadavpur University, is absolutely based upon his own work under the supervision of **Prof. Dulal Krishna Mandal and Prof. Nabin Baran Manik** that neither his thesis nor any part of it has been submitted for any degree / diploma or any other academic award anywhere before.


.....
Signature of the Supervisor

&
Date with Official Seal

Professor
Dept. of Mechanical Engineering
Jadavpur University, Kolkata-32


.....
13.04.23

Signature of the Supervisor

&
 Dr. NABIN BARAN MANIK
Date with Official Seal
Professor
Department of Physics
Jadavpur University
Kolkata - 700 032

Acknowledgement

I would like to thank my mother who is the first guide of my life. I am grateful to my mother who envisioned me to set up a goal of doctoral degree. I am grateful to my father who supports me with his all contribution in my life. I thank to my elder sister for her assistance. One thing should definitely be mentioned that without the patience and constant support of my wife, I was unable to fulfill my dream of doctorate degree. So I am especially thankful to all of them.

I am thankful to my supervisor Prof. Dulal Krishna Mandal. Without acknowledgement of Prof. D.K.Mandal, it was certainly not possible to me to frequently walk on the way of research work. My heartiest gratitude for him to permit me to express myself with own scientific creativity.

I am thankful to Prof. Nabin Baran Manik for being my mentor and advisor. I am grateful to Prof. Manik for giving me valuable advice and research guidance on the techniques of preparing scientific manuscripts and how to express scientific presentations in a proper way. His guidance and rigorous scientific attitude of research is unrivalled and it claims obvious appreciation. My respect and heartiest gratitude for him for all assistance to develop a research based mind and way of finding the meaning of research.

I would like to thank to Prof. Ratan Mandal, Professor and Director, School of Energy Studies, Jadavpur University for providing kind cooperation to access energy studies laboratory whenever required and thoroughly advice me to enrich my quality of research. I highly appreciate his cooperation in my thesis.

I would like to thank Mr. Alope Das for giving me assistance in different experimental investigations. I am thankful to my childhood friend Mr. Arnab Basu who brought me first there in the campus of Jadavpur University to join in doctoral work. I am undoubtedly very glad that I had the opportunity to stay here. I would also like to thank all of my lab members for their heartiest cooperation and constant encouragement in my research work.

Further, I like to convey my gratefulness to all the people who have contributed directly or indirectly towards the enrichment as well as completion of my doctorate degree and obviously the formation of the thesis. My heartiest gratitude to all of them because it would never been possible without your kind cooperation.

List of Tables

- Table.3.1 Estimated electrical parameters for Indigo dye based natural organic device
- Table.3.2 Estimated reduction percentage (%) of electrical parameters obtained in indigo dye based herbal device over other reported organic dye based devices
- Table.4.1 Estimated electrical parameters for Turmeric dye based natural organic device
- Table.4.2 Estimated reduction percentage (%) of E_t and ϕ obtained in Al/Turmeric/Cu device over RB and MG dye based organic diodes
- Table.5.1 Comparison of electrical parameters of PALD and ETLD
- Table.5.2 Comparison of photovoltaic parameters of PALD and ETLD

List of Figures

- Fig 1.1 Chemical structure of Turmeric dye
- Fig 1.2 Chemical structure of Indigo dye
- Fig 2.1 Energy level of organic semiconductor based device
- Fig 2.2 Schematic diagram of bond structure of carbon in an organic molecule
- Fig 2.3 Chemical structure of some organic semiconductors
- Fig 2.4 Pictorial representation of amplitude of wave function of (a) atomic orbitals and (b) molecular orbitals
- Fig 2.5 Schematic representation of energy levels of two distinct atoms, one bi-atomic molecule and a solid
- Fig 2.6 Energetic diagram for disorder organic material
- Fig 2.7 Schematic representation of three types of exciton: (a) Frenkel exciton, (b) Wannier-Mott exciton, (c) charge transfer excitons (CTE)
- Fig 2.8 Schematic representation of potential energy vs nuclear coordinate relationship where three different positions has been given providing the excited state and charge separation state of a D-A system
- Fig 2.9 Traps Density of States presentation represents shallow traps at tail states (black color) and deep traps (red color) in the band gap (left side of the diagram). Schematic representation of Energy diagram of OSC with localized trap states has been depicted in the band gap region. Acceptor and donor like shallow trap states are drawn (blue color) at top and bottom of deep traps (red color). Arrows express different conduction regime like: Band like transport, MTR and hopping transport
- Fig 2.10 Schematic representation of different trapping and anti-trapping states of guest-host molecules in a lattice
- Fig 2.11 Schematic diagram of Anderson localization due to a Gaussian distribution of quantum well depths
- Fig 2.12 Schematic representation of MTR mechanism

- Fig 2.13 Carrier hopping between two sites having Miller-Abraham hop rate estimated by energy-space separation
- Fig 2.14 NNH and VRH in Energy-Space curve
- Fig 2.15 Typical I-V characteristics used to SCLC measurements of trap energy of discrete shallow traps
- Fig 3.1 Chemical structure of Indigo dye
- Fig 3.2 Dark current measurement set up where Al and Cu has been used as front and back electrodes respectively whereas the Indigo dye has been selected as active layer sandwiched between the electrodes
- Fig 3.3 I-V Characteristics of Indigo dye based diode
- Fig 3.4 G(V)-V plot of Indigo dye based diode. Multiple distortions in the figure explain the presence of multiple discrete traps. The first in the plot is quite suppressed and is generated due to V_{bi} . Remaining peaks arise from other deeper traps; (b) logI-logV plot for Indigo dye based device used to calculate trap energy
- Fig 3.5 (a)(dV/dlnI)-I plot and (b) H(I)-I plot of Indigo dye based diode
- Fig 3.6 lnI vs $V^{1/2}$ plot for Indigo dye based diode
- Fig 4.1 Chemical structure of Turmeric dye
- Fig 4.2 Schematic current-voltage measurement set up where Al and Cu are selected to utilize as front and back electrodes respectively. Thin film Turmeric dye is used as active semiconducting layer deposited between the mentioned electrodes
- Fig 4.3 V_x -V Characteristics of Al/Turmeric/Cu device where trap assisted charge conduction with distinct nature at different regime has been shown with clear signature of trapping distribution is shown with comparison to ideal trap free conduction for better realization
- Fig 4.4 G(V)-V characteristics of Al/Turmeric/Cu based device. Multiple distortions in such figure represent multiple discrete traps, first of which is quite suppressed and is generated due to V_{bi} . Remaining peaks arise due to the existence of other deeper traps
- Fig 4.5 Energy band diagram at different states at different voltage limit. a) Quasi equilibrium, b) $E_F < E_{TD}$, c) $E_F \approx E_{TD}$, d) $E_F > E_{TD}$

- Fig 4.6 InI-lnV plot of Al/Turmeric/Cu based device
- Fig 4.7 Schematic representation of interfacial band bending at electrodes having different work function along with relating built in potential and barrier height together
- Fig 4.8 Semilog I-V plot of Al/Turmeric/Cu based device
- Fig 4.9 InI vs $V^{1/2}$ plot for Al/Turmeric/Cu based diode
- Fig 5.1 Block diagram representation of organic dye based photovoltaic measurement setup (a) in experiment and (b) in GPVDM simulation
- Fig 5.2 I-V characteristics of PALD and ETLD obtained in GPVDM (plotted in origin 5.0)
- Fig 5.3 $I \frac{dV}{dI}$ vs I characteristics of PALD and ETLD
- Fig 5.4 Absorption of photon energy generates dynamic holes and electrons that travel through acceptor and donor phases and its consequent energy level diagram where E_v represents the energy at vacuum level and E_F expresses the energy of Fermi level
- Fig 5.5 Hopping movement of carriers in different materials as per work function into ETLD
- Fig 5.6 InI-lnV characteristics of PALD and ETLD
- Fig 5.7 G(V)-V characteristics of PALD and ETLD
- Fig 6.1 (a).Dark I-V characteristics obtained for SM (simulation modeling is abbreviated as SM) based device. V_L and V_H notify are low and high voltage zone respectively and the mentioned zones are separated by dotted line in first figure. V_L is basically diffusion conduction dominated regime whereas V_H is influenced by drift dominated conduction regime.(b)lnI-V characteristics of SM based device at low voltage regime. From the slope of the characteristics ideality factor is determined.(c).I and n has been plotted with respect to V. In region-(i) n is increasing with increasing voltage while reduction of n is found with increasing voltage in region-(ii). Dotted line in this figure is used to distinguish these two regions
- Fig 6.2 Schematic diagram of band bending at diffusion regime towards drift regime
- Fig 6.3 $\log(P_t)$ vs V plot of SM based device. $\log(P_t)$ follows inverse linearity with

increasing voltage which shows consistency with the theoretical aspect

- Fig 6.4 E_t vs n plot of SM based device at low voltage zone. Low voltage zone has been segmented into two different regions. In region 1, the plot n shows highly disordered nature with increasing E_t whereas n faces exponential decay in region 2 with increasing value of E_t
- Fig 6.5 $\ln I$ - V characteristics at low voltage regime of 5.(a) ID based 5.(b) TD based device. From the slope of the characteristics ideality factor is determined for both devices. V - I - n plot of 5.(c) ID based 5.(d) TD based device
- Fig 6.6 E_t vs n plot of ID and TD based devices at low voltage zone

List of Abbreviations

OSCs	Organic semiconductors
Al	Aluminium
Cu	Copper
R_s	Series resistance
n	Ideality factor
E_t	Trap energy
Θ	Trap factor
ϕ	Barrier height
V_{bi}	Built-in Potential
MG	Mott-Gurney equation
SCLC	Space Charge Limited Current
TCLC	Trap Charge Limited Current
OPV	Organic photovoltaic
HOMO	Highest Occupied Molecular Orbital
LUMO	Lowest Unoccupied Molecular Orbital
CTL	Carrier Transport Layer
TEC	Thermal Expansion Coefficient
TSC	Thermal Stimulation Current
CTE	Charge Transfer Excitons
LCAO	Linear Combination of Atomic Orbital
BO	Bonding Orbital
ABO	Anti- Bonding Orbital
DOS	Density of States
GPVDM	General Purpose Photovoltaic Device Model
MTR	Multiple Trapping and Release
MA	Miller-Abraham
VRH	Variable Range of Hopping
PAL	Photoactive Layer

PALD	Photoactive Layer based Device
ETL	Electron Transport Layer
ETLD	Electron Transport Layer based Device
SRH	Shockley_Read_Hall
V_{oc}	Open Circuit Voltage
J_{sc}	Short-circuit Current
SM	Simulation Modeling
DLTS	Deep Level Transient Spectroscopy
TE	Transpotations Charges
ME	Mobility Edge
PCE	Photo Conversion Efficiency

Contents

Chapter-1

Aim of the present work and Thesis outline	6
1.1. Introduction	7
1.2. Brief of Experimental Natural Dyes	7
1.3. Motivation of the present work	8
1.4. Objective of the present work	9
1.5. Thesis outline	10

Chapter-2

Overview on Trap Induced Charge Conduction in Organic Semiconductors	15
2.1. Introduction	16
2.2. Earlier works on organic semiconductors	16
2.3. Organic semiconductors: Chemical properties	19
2.4. Organic semiconductors: Electrical structure	21
2.5. Carrier Generation	25
2.5.1. CTE Generation	26
2.5.2. CTE dissociation	27
2.6 Carrier Recombination	28
2.6.1. Type of recombination in organic semiconductors	28
2.7. Natural organic Material used in our research work	29
2.8. Theoretical aspect of charge transport in organic semiconductors	30
2.9. Traps in organic semiconductors-underlying physics	40
2.9.1. Definition of Traps	41
2.9.2. Different sources of Traps	42
2.10. Trap assisted Transport Models	48

2.10.1. Anderson localization	48
2.10.2. Mobility Edge model	49
2.10.3. Hopping Transport model	50
2.10.4. Percolation model	52
2.11. Trap characterization techniques and measurement methodology	53
2.11.1. Electrical measurements	54
2.11.2. Optical measurements	56
2.12. Concluding remarks	57
2.13. References	59

Chapter-3

Interpretation of Trap Assisted Conduction with Estimation of Electrical Parameters of Thin Indigo Film Based Semiconducting Device 68

3.1. Introduction	69
3.2. Experimental Arrangement	69
3.2.1. Material description	69
3.2.2. Experimental method	70
3.3. Results and Discussions	71
3.4. Conclusive remarks	79
3.5. References	79

Chapter-4

Investigation on Trapping Signature in Organic Semiconductor Turmeric Film Introducing Different Current-Voltage Analysis 82

4.1. Introduction	83
4.2. Materials and Experiments	83
4.3. Results and Discussions	85
4.4. Conclusive remarks	97
4.5. References	97

Chapter-5

Utility of Carrier Transportation Layer P3HT:PCBM for Efficiency Improvement of Organic Photovoltaic Devices using GPVDM Modeling	101
5.1. Introduction	102
5.2. Numerical Modeling and Experiments	103
5.3. Results and Discussions	104
5.4. Conclusive remarks	112
5.5. References	113

Chapter-6

An Analytical Study on Low Voltage Regime of Natural Organic Semiconductor Based Device: Physics of Trap energy and Ideality Factor	117
6.1. Introduction	118
6.2. Materials and Methods	119
6.2.1. GPVDM simulation	119
6.2.2. Experimental arrangements	119
6.3. Results and discussions	120
6.4. Conclusive remarks	130
6.5. Reference	131

Chapter-7

Conclusion of the thesis	135
7.1. Introduction	136
7.2. Work summary and objectives	136
7.3. Concluding remarks	139
7.4. Scope of the future work	141
List of publications	143

Preface

The present thesis entitled “**Investigation on the effect of trap states signature on the charge transport mechanism of some natural organic semiconducting material based devices**” is submitted for the degree of Doctor of Philosophy at Faculty of Science, Jadavpur University, Kolkata. The research work presented here was carried out under joint supervision of Prof. Dulal K Mandal and Prof. Nabin Baran Manik at Department of Physics, Jadavpur University.

To best of my knowledge this work is original. Neither this nor any substantially similar thesis has been or is been submitted for any other degree, diploma or other qualification at any other University.

The thesis illustrates the charge conduction into natural semiconducting dye based organic diode. Since the semiconducting signature in natural product based dye solutions draws the significant attention nowadays, so detail investigation still remains to be done in order to completely understand the chemistry regulating the whole process. Variation of their anisotropic critical molecular structures, interesting electronic properties, metal-semiconductor interfacial charge dynamics, photo-induced carrier transition mechanism adjoins additional importance to carry out more research over such material based devices. But rapid development of such kind of semiconducting substances is getting challenged as because their performance struggles to reach the satisfactory level due to the presence of trapping states. Trap state is basically the energy state below the state of carrier conduction energy arises due to spatial disorder which has a significant impact on all such type of based devices. Moreover, field effected lower mobility with respect to the hole mobility is attributed to the presence of huge amount of trap states in organic elements. Current-Voltage (I-V) relationship is distorted distinctly with the existence of high concentration of trapping. This perspective claims to have a better knowledge on trap assisted charge conduction is primarily required to resolve such problem.

Considering all above aspects, we have introduced current-voltage relationship to determine the charge transport mechanism for two different natural dyes (Turmeric dye and Indigo dye). Detail of the experimental arrangement and process of device characterization has been mentioned. The analytical illustration of charge trapping signature in charge transport process of abovementioned dyes has been given here in the work. Different electronic parameters related to both of drift

dominated charge conduction above threshold voltage and diffusion dominated charge carrier dynamics below threshold voltage and their relevance with impact of trap distribution have also been analyzed. In this context, different type transport modeling has been reviewed and information obtained by analyzing the experimental data has been validated with suitable theoretical techniques.

We have organized from objective to all experimental findings of present investigations sequentially in different chapters. Summary of the whole investigation has been concluded at last chapter named as “conclusion of the thesis”. Future scope of the research along with avenues of its practical application has also been mentioned there.

Finally, a list of publications has also attached at the end of the thesis.

Chapter-1

Aim of the present work and Thesis outline

- 1.1 Introduction**
- 1.2 Brief of Experimental Natural Dyes**
- 1.3 Motivation of the present work**
- 1.4 Objective of the present work**
- 1.5 Thesis outline**

1.1. Introduction

Invention of electronic conductivity in organic materials, a section of such materials which previously assumed to be extremely isolating, recently opened a fascinating field of profound research. Interesting properties of different organic semiconductors hold challenges of drawing attention of researchers by their different optoelectronic properties, amorphous structure, charge transformation and interfacial level transition related physics. Moreover, the natural materials used in experiments become a concern of intensive research because of their light weight, flexibility, easy sample preparation technology and cheap rate. Interest has been grown when it has been observed that some common natural organic dyes are indicating suitable semiconducting properties. Some of the natural organic dyes have been investigated in present thesis also.

1.2. Motivation of the present work

Organic semiconductors have chemical and electronic properties which radically differentiate the materials from inorganic ones and justify themselves to provide great effort on their possibilities of rapid development in device application. But still organic light emitting diode (OLED) and organic photovoltaic (OPV) diode seem to require more time in transforming from research phase to commercialization level. Several problems have been encountered which resists the rapid growth of organic materials as a perfect replacement of inorganic ones in device application. Electronic trap has been observed as most fundamental parameter in this context. Thin amorphous structure of organic thin film often has localized trapping distribution into the band energy gap of material that influences on the device performance. Such organic devices show poor performance due to the presence of traps.

There are intensive investigations concentrated upon organic materials and devices made of organic materials. Most of the researches provide the outcome related to material characterization technique, material preparation and synthesis. On the other hand, a constant improvement can be observed on physical models explaining theoretical aspect with

experimental validation of organic semiconductors. Unfortunately, only a limited connection has been encountered to sort out the basic problems related to trapping states which inherently impact device efficiency. This leads to a lack of consistency for improvement of organic semiconductor based device resolving the trapping problem. A recent trend has been followed where it has been found that some natural organic dyes exhibit charge conduction. The interesting phenomenon certainly draws the attention of the researcher to go insight of this issue. We have also intended to investigate in this aspect. A unified realization of physics related to traps is illustrated in our work to fill up the gap of consistency between theoretical proposals and experimental validation. Charge conduction at low voltage regime is very less attracted issue to the researchers always due to very low amount of charge concentration at this regime. Only a very few works can be found in this context. Finally, we have initiated to put some additional relevant information regarding conduction mechanism at this low voltage regime.

1. 3. Objective of the present work

In this thesis, we have studied the trap assisted charge transport mechanism of different natural dye based organic diode configuration. To solve this purpose, Turmeric and Indigo dye have been taken into account. Electrical characterization has been executed of experimentally formed device structures to estimate the trap energy. We also have measured a series of other relevant electrical parameters like series resistance, ideality factor, trap factor, barrier height etc for both dyes. We have compared the experimental outcomes with the results of some other reported organic dye based devices. Experimental outcome of our research signifies that the experiment natural organic dyes have significant less trap energy and subsequently these dyes exhibit promising improvement in outcome of conduction related electrical parameters in comparison to some earlier reported organic semiconductors.

Secondly, a comparative study on the electrical parameters of organic photovoltaic device has been taken into consideration for unified realization about the need of carrier transportation layer (CTL) in organic photovoltaic devices. The parameters have been extracted by modeling the devices using GPVDM simulation technique. Possible reason of such improvement in device efficiency has been explained in terms of trapping states concentration. Differential technique of

current voltage relationship has also been implemented to explain the trapping distribution for both devices. We found that trap factor increases and subsequently trap energy reduces for CTL inserted device which concludes better conduction into the device.

Conduction follows diffusion dominated mechanism at injection regime. We have explained the theoretical aspect in this domain on the basis of which simulation modeling has been implemented to validate the approach. Simulation outcome shows high consistency with the theoretical concepts which indicates the reliability of the simulation approach. Based on simulation result, we have further extended our observation to relate the dependence of ideality factor on trap energy. Output of the simulation shows quite interesting physics of the parameters at diffusion domain. Reason of such outcome has been predicted theoretically. Experimental approach has also been undertaken on aforesaid natural organic sample based semiconducting devices to verify the reliability of the prediction. Results of the experiments show satisfactory consistency with the theoretical estimations as well as simulation result.

1.4. Brief of Experimental Natural Dyes

Turmeric dye:

Turmeric is natural compound with bright yellow color belongs to the botanical Curcuminoid group. The chemical compounds of the dye extracted from *Curcuma Longa* consist mainly of diarylheptanoid and natural phenol. Chemical formula of Turmeric is $C_{21}H_{20}O_6$. The dye shows promising semiconducting properties besides several medical applications. Recently, the dye under consideration is utilized as natural semiconductor in organic photovoltaic devices. It has excellent UV absorption property. Estimated Optical band gap of turmeric dye solution is 2.85 eV. Structure of the chemical configuration of the dye has been shown in fig.1.1.

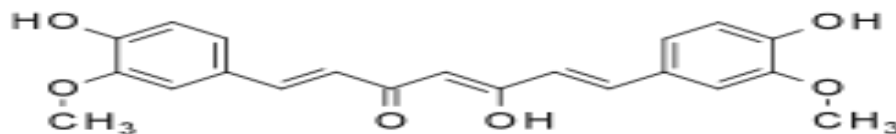


Fig.1.1. Chemical structure of Turmeric dye

Indigo dye:

Indigo dye is a herbal compound with distinctive blue color combination. Chemical formula for indigo is $C_{16}H_{10}N_2O_2$. Indigo is a natural dye extracted from the leaves of certain plants. A variety of plants have provided indigo throughout history, but most natural indigo was obtained from those in the genus *Indigofera*, which are native to the tropics. The primary commercial indigo species in Asia was true indigo. This dye is taken into consideration for its significant semiconducting properties, good quantum yield and quite satisfactory spectral response. The dye shows the latest peak of absorption spectra at 268 nm at UV light region whereas characteristic peak can be observed at 612 nm in visible light range. Reported optical bandgap of the dye is 1.689 eV. Fig.1.2 shows the chemical structure of Indigo dye.

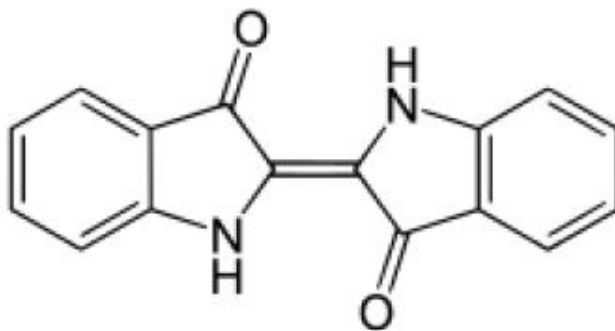


Fig.1.2. Chemical structure of Indigo dye

1. 5. Thesis outline

Chapter-I

The thesis starts with aims and objectives of the whole research work in Chapter I. Overview of experimental dyes has been provided here in this chapter. The chapter briefly focuses on the effect of traps in different optoelectronic devices and reason of requirement of intensive research over the physics of charge trapping and its role in charge conduction mechanism in organic semiconductor based diode.

Chapter-II

This chapter provides a thorough explanation about organic semiconductor. Earlier works on this occasion have been referred. Materialistic properties and their relevant electronic structures have been discussed further. Degrees of disorder have been classified into three categories in this subsection. The mechanism regulating free carrier generation and process of carrier recombination has been explained at the last section of this chapter. Name of the natural organic semiconductors studied in present work have been mentioned before conclusion part.

Further we have focused on charge transport mechanism in organic semiconductor like disordered system. Gaussian distribution model has been implemented in this regard. It has been observed that carriers are diffused at lower concentration regime into the material and a transition of diffusion to drift motion is encountered with increasing carrier density. Nature of the current flow at different regime (injection level, interfacial zone, space charge limited zone) of the bulk zone of the material has been explained with theoretical validation.

In the next section, a comprehensive discussion on the physics of traps in organic semiconductors has been provided in this chapter. Possible source of trap generation and important properties of trapping states are discussed in next section. Source of charge trapping ranges from defects in molecular structure and chemical impurities to environmental impact are categorized in this subsection. Next, the discussion of different proposed theoretical modeling of trap assisted charge conduction is elucidated. Finally, the experimental techniques available for characterization of different trapping states have been focused. Significant development in constructive research work in terms of proposed theory and different measurement technique has been observed in this context. Most renowned SCLC measurements have been employed to demonstrate our trap related measurement works. There are several other experimental methods like Impedance spectroscopy, Optical and Thermal methods which have been explained briefly here also.

Chapter-III

We have reported trap assisted charge conduction mechanism of Indigo dye based organic schottky diode in this chapter. Existence of trapping tendency has been examined by $G(I,V)$ vs V characteristics. Non-monotonous nature of the characteristics indicates the signature of traps

states of different energy levels during charge conduction process. The trap energy (E_t) is determined for the device. Extrapolated value of E_t is found 0.073 eV. The abovementioned value indicates the improved result of 16.09 % and 3.95% comparatively than other two previously reported organic dyes. Electrical parameters of the device have been estimated by Cheung-Cheung method which has been used to calculate the series resistance (R_s), ideality factor (n) and barrier height (ϕ) of the device. Analyzing the obtained data, Recharadson-Schottky effect on charge transport mechanism has been interpreted in this context.

Chapter-IV

We elucidate the analytical description of trap signature in charge conduction process of Turmeric dye based organic semiconductor has been presented in this chapter. Experiments have been performed here with Turmeric dye. Interpretation of explicit relationship between band bending energy and trap states has been mentioned. V_x - V graph has been elucidated to emphasis on the presence of trapping distribution. Differential analysis of I-V characteristics has also been employed to verify the signature of trapped carrier in the device. Non monotonous decrement of $G(V)$ - V plot ensures the signature of trapping. Trap energy (E_t) and trap factor (Θ) has been extrapolated from log I-V relationship. Determination of barrier height (ϕ_{bi}) of the device has been executed By analyzing semilog I-V plot. The overall I-V curve has been taken into account to examine the Recharadson-Schottky effect and Poole-Frankel effect into trap assisted charge conduction process. Schottky effect is found to be effective in the experiment which leads to bulk limited conduction procedure.

Chapter-V

This chapter has been taken into account to demonstrate the impact of traps on device efficiency of organic semiconductor based practical photovoltaic application. A comparative investigation on the electronic parameters of organic photovoltaic device has been considered in presence of P3HT:PCBM through GPVDM (GPVDM (abbreviated form of General purpose photovoltaic model which is considered as a reliable and renowned software simulation tool) technique. The parameters have been measured by modeling the devices using aforementioned simulation. Device efficiency of P3HT:PCBM incorporated device has been obtained increasing comparatively. Possible reason of such improvement in device efficiency has been demonstrated

on the basis of theoretical point of view. Series resistance and ideality factor has been estimated from $I_dV/dI-I$ plot. About three times reduction of the following has been encountered with addition of P3HT:PCBM compound. Such significant reduction of series resistance (R_s) and trap energy (E_t) are found to be responsible for the probable reason of improvement of device efficiency which are calculated by analyzing Current-Voltage (I-V) characteristics. Differential technique of current voltage relationship has also been implemented to explain the trapping distribution for both devices. It has been found that trap factor increases for P3HT:PCBM compound device comparatively which concludes better conduction into the device.

Chapter-VI

From relevant literature review related to the topic of the thesis, it has been concluded that most of those earlier investigations had a tendency to focus on current conduction and its related physics at space charge limited high voltage regime. Our research work demonstrated in earlier chapters follows up the trend. Very few researches can be found which emphasizes at the diffusion driven low voltage zone. So many aspects in this regard still remain vexed question. From this point of view, we intend to contribute this chapter with our final research work to add relevant information about trap effect at low voltage regime.

As a consequence, we have demonstrated the physics of trap prone low voltage region of natural organic semiconductor based single layer device in present chapter. Theoretical explanation of diffusion driven current equations has been implemented as an efficient way to study the charge transport mechanism in that regime. GPVDM software simulation technique of organic devices has been introduced to obtain current voltage relationship and fitted with diffusion assisted equation. The plot shows high consistency with theoretical explanation which indicates reliability of the plot. Simulation based observation on trap assisted conduction at low voltage and its relation with corresponding ideality factor at that region has been explained on the basis of theoretical point of view. It has been found that ideality factor decays exponentially with increasing trap energy at low voltage. Experimental approach has finally been employed on Turmeric and Indigo dye based single layer natural semiconducting diodes to validate the outcome of the proposal. Results of the experiment lead to great similarity with the outcomes of both theoretical and simulation approach.

Chapter-VII

Overall conclusion of the entire research work has been presented with a description in order to obtain a better performance of organic semiconductor based devices reducing the trapping problem. Although a compact substantial work has been intended to represent in present thesis, but there are still many avenues which were not covered in this research work. Photovoltaic performance, transient response, carrier lifetime measurement and performance of different optoelectronic devices made of such natural components are the possible avenue of further research work. Such unsolved aspects have been mentioned in this chapter. Thus these research works were kept open to the future researchers on this exciting topic.

Chapter-2

Overview on Trap Induced Charge Conduction in Organic Semiconductors

- 2.1 Introduction**
- 2.2 Earlier works on organic semiconductors**
- 2.3 Organic semiconductors: Chemical properties**
- 2.4 Organic semiconductors: Electrical structure**
- 2.5 Carrier generation**
- 2.6 Carrier recombination**
- 2.7 Natural organic materials used in our research work**
- 2.8 Theoretical aspect of charge transport in organic semiconductors**
- 2.9 Traps in organic semiconductors-underlying physics**
- 2.10 Traps assisted transport models**
- 2.11 Trap characterization techniques and measurement methodology**
- 2.12 Conclusive remarks**
- 2.13 References**

2.1. Introduction

Science and technology in recent age are truly the witness of proper execution of emergence concepts and techniques applied in micro to nano scale level semiconductors. The field in concern has proved tremendous potential over last two decades. Initially the studies were based on the optical, magnetic and electronic properties at bulk and interfacial regime of different inorganic semiconducting materials. But the invention of charge conductivity in organic material has opened such a new fascinating field in research. Organic materials exhibit distinct electrical properties that differentiate such elements from inorganic materials and claim to justify obvious effort to research the possibilities of their utility as a semiconductor in different device application. Studies over these materials have opened up very new avenue to the material scientists for utilizing them as active material in fabrication of different devices. High availability, low cost, ease film fabrication technique and flexibility generate additional interest of extensive research to realize its applicability in optoelectronic devices. Still the materials are facing some fundamental limitation about its extensive usage in device application. Some devices made of such materials exhibit low stability when they are exposed to large current over extended time duration. Moreover, organic semiconductors are prone to traps due to their disordered nature which is one of the most crucial reasons of its low current conduction. Conduction into the materials suffers high series resistive impact in presence of trapping states. So emphasis should be given on role of traps and its impact on charge conduction mechanism of organic semiconductors. The following point of view draws the attraction of the author to carry out investigation over the fact. The outcome of the research work over this issue has been described in various chapters of the thesis.

2.2. Earlier works on organic semiconductors

Traditionally the investigation on organic semiconducting materials focused onto the molecules belongs in crystalline state. Anthracene and naphthalene like molecular crystals were found to exhibit semiconducting properties [1]. Photosensitive conductivity in organic molecules and anthracene based electroluminescent devices have been described in 1960s [2-4]. However, organic materials were generally taken as exotic materials with low potentiality in device

application for their disordered amorphous structure generated poor semiconducting properties then that time. After a few years later, polymers were characterized by taking chromophores in the polymer as element of side group and also in the polymer chain. In 1970s, amorphous selenium and silicon were replaced by multilayer photosensitive organic semiconductors because of their variation in material utility, safe use in environment [5].

The first significantly high conducting polymer, known as doped polyacetylene, was reported in the year of 1977 [6]. Initially the doped polymers were really unstable in air and it was very difficult to process. However, new ungraded generations of the aforementioned materials are able to be processed and stable in nature. Electrical conductivity obtained in this generation ranges from $<10^{-10}$ S/cm for typical insulators to 10^{-5} S/cm for typical semiconductors like Silicon. Such polymer began to exhibit their emerging application from that era which includes coating and blends as well as for the electrostatic dissipation and interference of electromagnetic shielding, conducting layer of optoelectronic devices and coatings of anticorrosion in different metallic surfaces [7]. However, due to some fundamental limitations, rapid utilization of organic semiconductors in electronics has been restricted. Strong coupling force acting over a long range of constituting atoms enforces the electronic states to be delocalized and allows the formation of energy gap between valence and conduction band in inorganic crystals. Generation of free electrons in conduction level, living positive holes in valence band, is to be done with the execution of photo-excitation or thermal activation process. Conduction of these free charges can be explained by Bloch function, k-space dispersion relation of solid state physics [8].

In organic semiconductors, interactions at intermolecular level are generally covalent but such interactions are significantly weaker because of London forces and van-der waals forces. So naturally the transport bands are narrower enough compare to the inorganic materials. So energy bands are disrupted easily in presence of disorder into the system. Thus excitations as well as inherent interactions stated on atoms of molecular crystals have a crucial role than the relevance of energy band conception. Organic materials basically hold π - conjugated electronic features formed by the overlap of pz orbitals of carbon atoms. P-electrons suffer delocalization due to such overlap in orbits and the energy band gap becomes relatively small between highest occupied molecular orbital (HOMO) and lowest unoccupied molecular orbital (LUMO).

Lower value of coupling in the molecules belonging in solid states leads to the fact which concludes the charges in such materials are localized enough. Conduction takes place in such a sequence which steps from one to another molecular state, very similar to hopping transport in different defect states belongs in inorganic semiconductors [9].

Furthermore, excitons are formed by the light absorption in organic semiconductors which do not dissociate thermally into free carriers at normal temperature. Therefore, stable charge states formation following absorption of photon seldom takes place but charges form with quenching of excitons by impurities in material. These were the factors which were responsible for very low device efficiency.

After a certain time interval, a breakthrough invention came with the work of Tang et al. [10], creating donor-acceptor interface (D-A interface) formed at the junction between bi-layer of two organic substances having different electro negativity. Such difference in electron affinity produces an effective force for transformation of carriers towards excited states by splitting the excitons formed by absorption of photons into charge carriers. A schematic representation of the D-A interface has been given below.

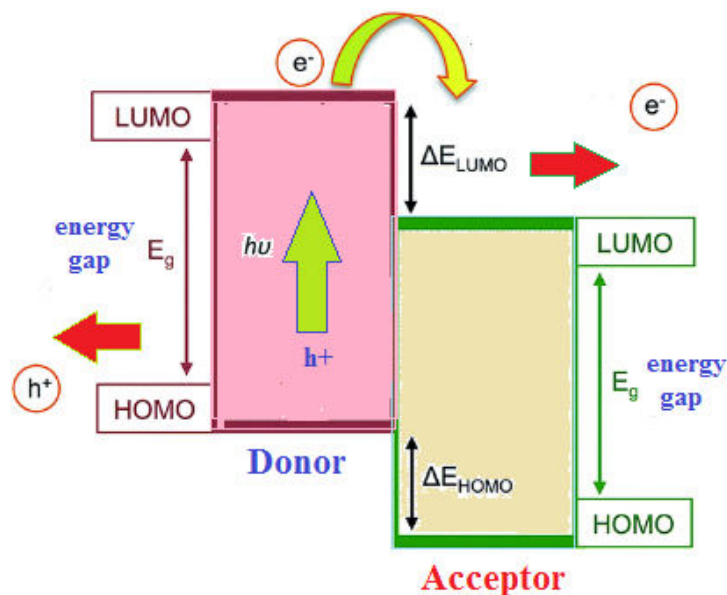


Fig.2.1 Energy level of organic semiconductor based device

The anomalous behavior of organic semiconductors accelerates the thrust of realization of the physics for both organic polymers and small organic molecules at late 1980s. The fact leads to (i) the illustration of upgraded performance (to increase the luminescent efficiency nearly about two orders of its magnitude to 1% at nearly 10 volt of operating voltage) of electroluminescent devices formed by multilayer vacuum-sublimed organic dye based thin films at Eastman Kodak [11], (ii) the explanation of the report of conjugated oligomers and organic polythiophene based transistors [12-13], (iii) discovery of optoelectronic device from conjugated polymers at Cambridge University [14], (iv) hetero-structure based efficient solar cell. As a consequence of that, Kojima et al. in 2009 found organic dye metal halide perovskite photosensitive device and Kim et al. in 2012 and Li et al. in 2016 draws highest reported device efficiency of similar organic dye based perovskite configuration which was certified also by National Renewable Energy Laboratory. [15, 39-41]. One information should be mentioned in this regard that in 2000s, Nobel prize has been won by Heeger-McDiarmid-Shirakawa for their remarkable work on development and application of organic semiconductors.

2.3. Organic semiconductors: Chemical properties

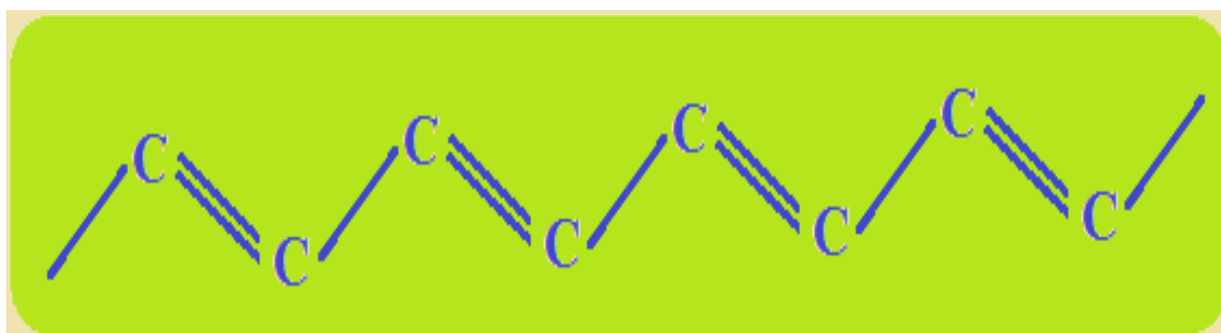
All organic semiconducting materials have carbon atoms as a common component. Carbon atoms (C) are closely bonded together through a covalent bond. There may be the presence of ionic interactions partially to other atomic elements. The electronic orientation of C is $He\ 2s^2 2p^2$. Such configuration consists of four electrons in valence band, the p ones, are found to distinct bonds. Such structure would form two equivalent bonding whereas experimental research observes that C can form maximum four equivalent bonding. Theory of hybridization of valence bands is employed to resolve the issue which considers that the electron in S orbit is promoted to the last p orbital, obtaining thus four single occupied valence bands whereas the rest S and remained P orbital are kneaded together to obtain newly formed equivalent orbital. Hybridized orbitals are a combination of the initial orbital. Hybridized p shells define the structural properties of different polymers. Hybridization can be classified into three types: sp^1 , sp^2 and sp^3 ,

the numbers mentioned in the superscripts denote the actual number of p shells participate in hybridization.

Four single occupied orbital, able to form same number of S bonding, can be obtained in sp^3 hybridization where an electron cloud inherently distributed around the axis of bonding, obtaining a structure of geometrical tetrahedral shape. sp^3 hybridization based polymers contain single bond only along its backbone. These type of materials are not able to exhibit semiconducting properties. At least 6 eV amount of energy requires for transformation of an electron from bonding S orbital to its anti-bonding.

The sp^2 hybridization consists of double bonds where three electrons of carbon atom are directed to produce S bonds; while non-hybridized fourth electron is employed to form p bond. Schematic diagram of bonding structure of an organic material has been shown below in Fig 2.2..

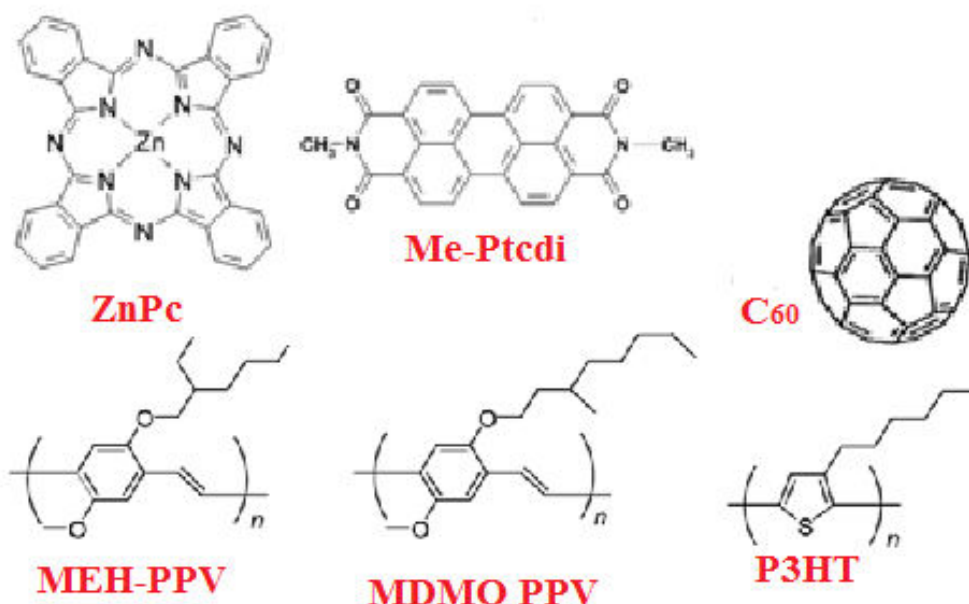
Organic semiconductors showing sp^2 hybridization are known as conjugated substances as it can alter its double and single bonds. Conjugation among the bonds produces a delocalization of those electrons which are said to be situated above and below the molecular plane. The π bonds in this plane are either empty, termed as-(LUMO) or filled up by electrons, termed as- (HOMO).



2.2 Schematic diagram of bond structure of carbon in an organic molecule

Organic semiconductors are classified into two types: small molecule organic materials and organic polymers. Polymeric molecules are form by repetition of a basic monomer and they are

gradually soluble in organic composition based solvents. Such materials are known as molecular materials. Structure of some molecular materials and polymers are shown below.



2.3 Chemical structure of some organic semiconductors

Organic semiconductors can be categorized into two types: n-type and p-type semiconductors. Nevertheless, doping mechanism of organic semiconductors are completely different from inorganic materials, a direct comparison between these two type of materials should not have relevance in this regard. MDMO-PPV, P3HT and PFB behave like p-type whereas MEH-PPV, F8BT, C₆₀ and Me-Ptcdi act as n-type organic semiconductors. Based on their chemical properties, it has been obtained that the polymers can be solution processed. Such p-type polymer mixture and usually n-type small molecular materials processed by the solution have potential application in photosensitive devices [16-17].

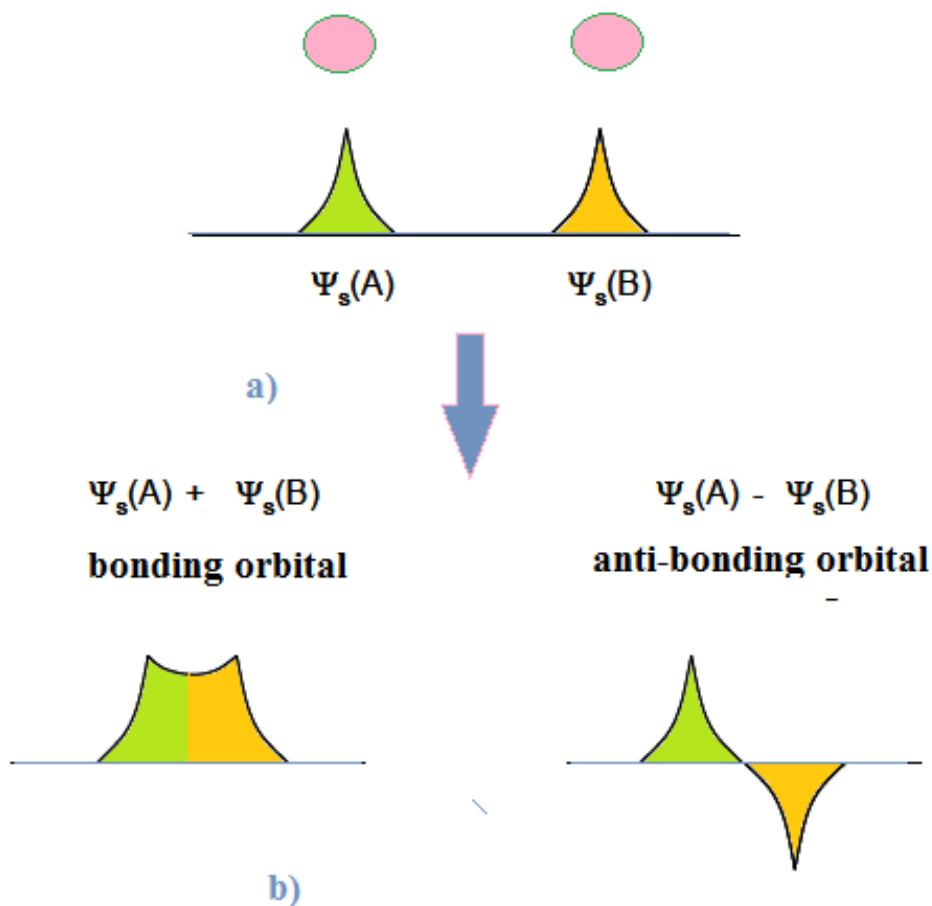
2.4. Organic semiconductors: Electrical structure

In order to illustrate electronic structures of organic semiconducting materials, we have to deal with ideal molecular system consisting two atoms. Molecular orbital model is used to describe

the molecular system. According to the model, when two atoms of equal energy interact together then their level of energies are isolated by creating two distinct energy levels in such a way that one level would stay lower than original energy state while the other state belongs in higher state of energy. Such molecular states are approximated by the principle of Linear Combination of Atomic Orbital (LCAO). LCAO demonstrates that molecular orbital can be compared as like as isolated atom. There is the expression of the wave-function of two hydrogen atoms:

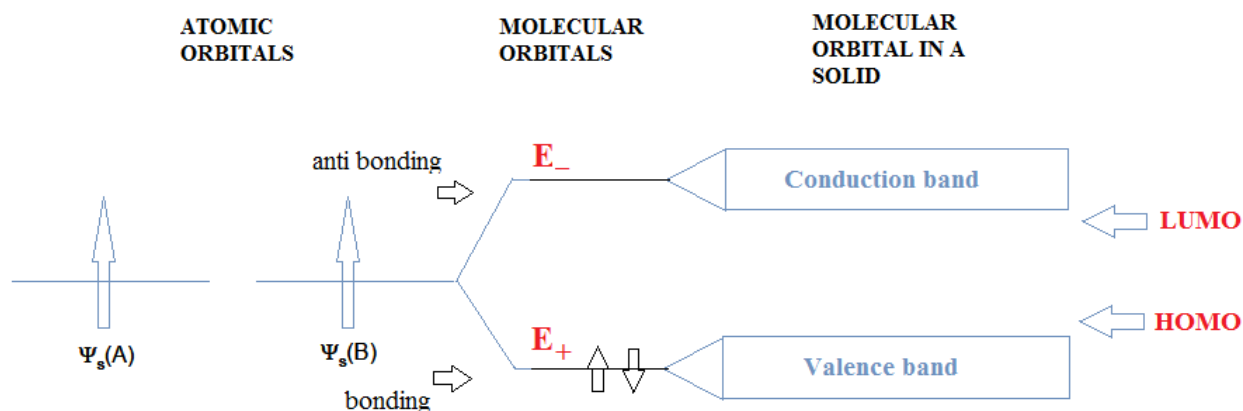
$$\Psi_{\pm} = \Psi_{1s}(A) + \Psi_{1s}(B) \quad (2.1)$$

Here $\Psi_{1s}(A) = \sqrt{\frac{1}{\pi a_0^3}} e^{-r_A/a_0}$, A and B are considered as atom and r_A is the distance between atom A and electron and r_B is the distance between electron and atom B.



2.4 Pictorial representation of amplitude of wave function of (a) atomic orbitals and (b) molecular orbitals

Two molecular orbital can be found from linear combination of wave functions for both A and B. Molecular orbital are of two types: bonding orbital (abbreviated as BO), Ψ_+ and anti bonding orbital (abbreviated as ABO), Ψ_- . Such atomic and molecular orbital have been depicted in Fig. 2.4. Addition of atomic orbital forms the BO. BO has high electron density between two nuclei. Such orientation enhances the energy of atomic bond and is favorable enough as its energy E_+ is comparatively lower than one of the isolated atomic orbital. On the other hand, ABO is obtained from the difference between the atomic orbital. Such orientation is very unfavorable on the basis of molecular stability as its energy E_- is comparatively high than one of the isolated atomic orbital.



2.5 Schematic representation of energy levels of two distinct atoms, one bi-atomic molecule and a solid

Superposition occurs for all molecular orbital in polymer chain like compounds having many covalently attached atoms. Such interaction leads to further splitting with appearance of different bands as can be seen in Fig 2.5 where difference between HOMO and LUMO corresponds to energy gap (E_g).

Energetic diagram of linear organic molecules is quite similar to crystalline inorganic molecules where forbidden gap with different energy bands exist. But remarkable modification can be observed for energy diagram of many organic molecule based solids. Intermolecular interactions in organic solids are much weaker than covalently bounded intra-molecular interactions. Since intermolecular interactions depends on London force and van der Waals impact, resulting

diagram of energy strongly depends upon the degree of disorder in different organic molecular system. Degree of disorder of organic materials can further be classified into three categories:

- (i) Highly ordered system
- (ii) Slightly disordered system
- (iii) Highly disordered system

(i) Highly ordered system

Solid state molecules in this system ensure that carriers of such materials are localized. So transport bands of such materials are narrow enough comparatively its inorganic counterparts due to strong localized molecules. Band structure can easily be disrupted by introducing quality disorder. Thus introducing allowed excitons in molecular system on localized molecules maintain a crucial role.

(ii) Slightly disordered system

If a chain made of polymer is planar in nature, delocalization of charge carriers can be observed over the chain. However, p-conjugated system is segmented into different localized states by the chemical and structural defects in a polymer chain based compounds. Various conjugation length of the system is the reason of disordered nature. The appeared formation can be compared with a number of quantum well having different size. Energetic value of such disordered states basically depends upon the execution of the defects. Ion implantation based doping of electro-active polymers in disordered organic semiconductor based device fabrication technique omit discontinuity over a long range observed at band edges of polymer chain [18-19]. Forbidden energy states in the middle band zone can be incorporated to permit for dangling groups (i.e., structural deformation). Such deformation can occur during radiation and thermal treatments. Pictorial representation of the band scheme has been shown in Fig. 2.6.

(iii) Highly disordered system:

The properties of all conjugated organic molecules having short conjugation length are quite same. Wave-function of electrons of such materials is limited by the length of π -bond conjugated chain.

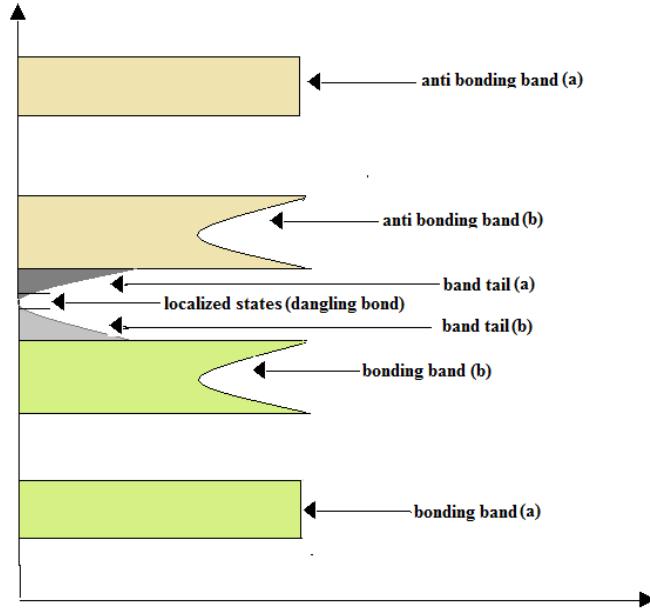


Fig.2.6 Energetic diagram for disorder organic material

Site of such conjugated molecules has a little bit of different energy states. The following fact leads to a relevant statistical distribution of localized states ensemble, known as Gaussian distribution of density of states (DOS):

$$\rho(\varepsilon) = \frac{1}{\sqrt{2\pi w_G^2}} \exp \left[-\frac{(\varepsilon - \varepsilon_c)^2}{2w^2} \right] \quad (2.2)$$

w_g denotes the width of distribution which corresponds to the energetic disorder in polymer molecules, ε_c is the energy at the centre of DOS. Energy of disordered orientation is lower in tiny organic molecules than in polymers [20]. Lower value of energetic disorder is fruitful for any physical process. Such disorder can be found experimentally in inhomogeneous broadening of transition spectra in optics.

2.5 Carrier Generation

In inorganic semiconductors, photon absorption leads to the sharp jump of an electron from valence band towards conduction band which results a free hole in valence band and free electron in conduction band. Pair of such carriers does not influenced by mutual force of electrostatic attraction due to the screening impact of surrounding material. But formation of bound state takes place when the kinetic energy of the carriers is relatively lower than their effective Coulomb attraction at a very low temperature. Such bound states lead to the generation

of exciton [19]. There is actually no existence of free carriers in OSCs. In OSCs, exciton formed by electron-hole pair, basically correspond to the excited states. Excitons formed by light absorption can be classified in different types, such as: Frenkel, Wannier-Mott, charge transfer excitons (CTE). The classification basically depends upon the average distance between hole and electron. Frenkel exciton hold on same molecule and their movement is considered as a unit through a lattice. The separation distance between carriers in Wannier-Mott exciton is at least one magnitude greater than Frenkel exciton. Interaction energy and dielectric constant in such of excitons are relatively high. CTE are the most common excitons in organic semiconductors. These types of excitons are delocalized on different lattice constants. It is relevant in this regard to mention that exciton binding energy in inorganic semiconductors ranges from 1 to 40 meV whereas it ranges from 100 to 300 meV in organic semiconductors having stability at normal temperature [20-21, 23-24].

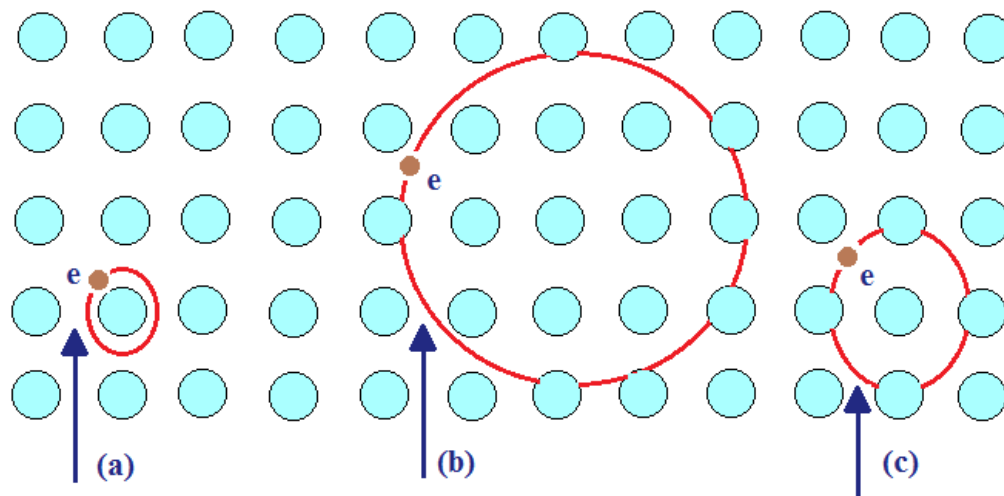
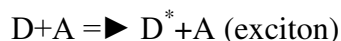
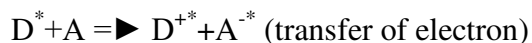


Fig.2.7 Schematic representation of three types of exciton: (a) Frenkel exciton, (b) Wannier-Mott exciton, (c) charge transfer excitons (CTE)

2.5.1. CTE Generation

In this case, electrons are transferred from donor element (D) to acceptor (A) by energy induced electron transfer procedure. One of the components is taken to the excited state in presence of photon prior to the conduction of electron carriers:





The state of charge transformation is formed subsequently to transfer of the electron. It can be described as the jumping of electrons from D to A to hop around or injection towards an acceptor.

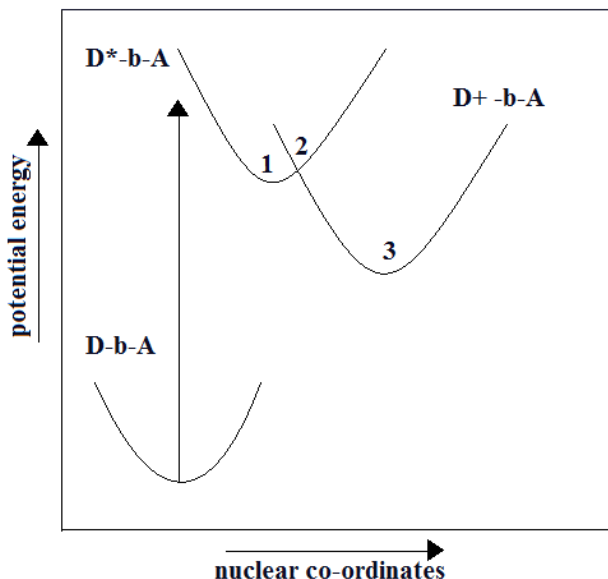


Fig.2.8 Schematic representation of potential energy vs nuclear coordinate relationship where three different positions has been given providing the excited state and charge separation state of a D-A system

An electron transformation state of a system has been explained in Fig. 2.8. which consists of a donor and an acceptor. Three positions of CTE on potential energy graph are represented as ground state (D-b-A), excited state (D^* -b-A) and charge separation state (D+ -b-A), where donor and acceptor are connected by a bridge (b).

2.5.2. CTE dissociation

Free carriers are obtained by the dissociation of exciton. It can be found by blending of two organic materials having different energy level. It is quite easy for an electron to go through a charge-transfer procedure from bound exciton state to a less tightly attached CTE. Common example of this condition is pure polymer. Electron-hole distance is enhanced after CT due to which binding energy decreases leading to dissociation of charges under the influence of thermal

activation or external electric fields. Onsager et al., [22] was the first who explained the temperature and field assisted CTE dissociation and later the theory was modified by Braun et al., [20] and Tachiya et al., [21]. Coulombic binding energy corresponds to the barrier of dissociation at the distance of separation between CT. The value of dissociation barrier generally ranges from 0.1 eV to 0.5 eV. Carrier separation distance in this regard in CTE generally ranges from 1 to 4 nm [25].

2.6 Carrier Recombination

Opposite type of charge carriers in OSc move towards together by Coulombic interactions in presence of external electric field and Coulombic bond formation accordingly takes place when the distance between a hole and an electron becomes smaller comparatively than capture radius, r_c . The specific distance where the Coulombic force becomes equal to the thermal energy $k_B T$ and is expressed by $r_c = e^2 / (4\pi\epsilon_r k_B T)$, where ϵ_r is dielectric constant of organic substance. A probability of recombination arises when electron and holes bounded together. An exciton appears when pair of such opposite charges belongs at the same site. Decay of the appeared exciton leads to the radiative recombination of electron-hole pair which results emission of energy in form of photon. The way of energy may also be non-radiative in nature in case of organic semiconductors.

2.6.1 Type of recombination in organic semiconductors

I) Langevin, bimolecular recombination

Charge carriers are confined in material phases of organic semiconductor blends in some cases which result interfacial recombination. Such interfacial state of action reduces the rate of recombination. Incorporation of an additional factor into Langevin type recombination rate should be required which accounts for area of interfacial contact, typically ranges 10^{-1} - 10^{-3} [26-30]. In order to explain the fact as illustrated above, charge density dependent mobility can be stated. Mobility of carriers depend on the charge density which leads to additionally effected carrier density dependence rate of recombination. Assuming the case of ideal semiconductors where $n=p$, recombination rate can be expressed as:

$$R = \vartheta \frac{(\mu_e + \mu_h)}{\varepsilon \varepsilon_0} n^2 \quad (2.3)$$

According to modified Langevin theory, recombination rate applicable to organic semiconductor blends is explained by:

$$R = \vartheta \frac{(\mu_e + \mu_h)}{\varepsilon \varepsilon_0} n^{\lambda+1} \quad (2.4)$$

It is not easy to predict the prefactor and the order of reaction ($\lambda + 1$) depends on morphology of the material sample that can be influenced by properties of material as well as conditions of sample preparation.

II) Auger recombination

Auger recombination is recombination of a hole associated an electron with a third carrier. Energy appeared by recombination of electron-hole opposite type charge carriers, transfer to third charge carrier due to which the carrier jumps higher into the band before back to the regime of band edge. The energy of the initial charge pair dissipates as thermal heating (phonons).

In practical, trapped carrier situated in a defect recombines with counter charge forming a trapped CT state. Auger process can occur when any free carrier interacts to such trapped CT states. Recombination energy is totally utilized to its corresponding kinetic energy to the added free charge carrier in this process. Photoemission can be observed when such type of recombination takes place near surface area [31].

2.7. Natural organic Material used in our research work

The experimental research work of the thesis consists of a pair of herbal organic semiconducting materials:

- Turmeric dye
- Indigo dye

Photosensitive response and UV absorption spectra of Turmeric dye is quite satisfactory while relatively low band gap of Indigo dye draws the attention of the researchers to carry forward the work. Informative discussion over the properties of the aforesaid dyes has already been provided in Chapter-I.

2.8. Theoretical aspect of charge transport in organic semiconductors

It has been observed in general that most of the research work in this field is based on either material synthesis related experimental works or simulation modeling of charge conduction of OSCs. But there is limited connection between these two different approaches. So to set up a bridge by experimental validation of theoretical concepts followed by simulation modeling would be a better way of justification of applicability of such organic materials. But before proceeding in this way, a clear conception about charge transport mechanism is much required. In this chapter, some theoretical study on the some relevant charge transport modeling in different segments of organic semiconducting materials used in organic diode like devices has been provided. This in turn helps also to further realization of different physical parameters and materialistic properties associated to charge conduction at the bulk regime of organic devices. Some basic approaches have been considered in order to study the charge conduction in such OSCs. OSCs have significantly low carrier concentration. However, generation of carriers can be occurred by injection process or by optical agitation or by doping. Theoretical modeling is extensively concerned with first criteria following precise discussion of charge conduction mechanism at different regime of organic semiconductor based diode.

Transport theory

Drift-diffusion model can define charge transport mechanism in a very simple way. The differential equations used in the model uses space charge in a continuous way. Theory of such model is derived from the equations of Boltzmann transport applying assumption of thermal equilibrium [42]. Therefore presence of quasi-therrmal equilibrium has its strong impact on the applicability of the model. It is obviously difficult to consider the effect of percolation of charge carriers which is crucial for conduction in organic substances. Drift-diffusion model can be very effective in modeling of charge transport in OSCs [43-47]. The variables used in the equations have been taken into account due to disorder effect [48-49].

Drift-diffusion model can be explained by the following form:

$$\Delta\psi = -\frac{q}{\epsilon_0\epsilon_r}(n) \quad (2.5)$$

$$\frac{\partial}{\partial t}(n) = -\frac{1}{q}\Delta j_n \quad (2.6)$$

$$j_n = -q(D\Delta n - \mu n\Delta\phi) \quad (2.7)$$

Where ϕ is electrostatic potential, n is charge carrier density, q is elementary charge, ϵ_0 is permittivity at free space and ϵ_r relative permittivity of dielectric. Eq. (2.6) represents the equation of continuity where j_n is charge current. Total conduction has been represented in Eq. (2.7) by the sum of drift and diffusion based contribution. Diffusion coefficient D is related to charge mobility μ by renowned Einstein relation.

If we consider n as an independent term then Eq. (2.8) can be represented as

$$j_n = -q\mu nF \quad (2.8)$$

Where F denotes electric field and is expressed as $F = -\Delta\phi$. And n denotes electronic conductivity of carriers. However, if carrier concentration varies accordingly then conductivity is taken into account as an aspect of macroscopic quantity.

Organic materials are sandwiched between two electrodes in diode application. Effective dimension of those electrodes are much greater than thickness of experimental film of organic substances. So it is justified in such cases to simplify the issue of dependence on space in the aforementioned system of equations to the one dimensional facts. Hence the equation can be written in the following form:

$$\frac{d^2\phi}{dx^2} = -\frac{q}{\epsilon_0\epsilon_r}(n) \quad (2.9)$$

$$\frac{\partial}{\partial t}(n) = -\frac{1}{q}\frac{\partial j_n}{\partial x} \quad (2.10)$$

$$j_n = -q\left(D\frac{\partial n}{\partial x} - \mu n\frac{\partial\phi}{\partial x}\right) \quad (2.11)$$

Illustration of charge conduction can be initiated using the equations. While the equations interpret the conduction mechanism, profound application needs the insertion of boundary conditions in this occasion.

$$\phi(x=0) = 0 \quad (2.12)$$

$$\phi(x = L) = V \quad (2.13)$$

$$n(x = 0) = n(x = L) = n_0 \quad (2.14)$$

Where n_0 is carrier density, V is applied voltage and L is sample thickness.

However more complex term could be added while considering complex phenomenon like trapping effect, dual electron-hole conduction, formation of photo-carriers, carrier recombination etc.

Space-charge-limited current (SCLC)

A simple case should be taken into consideration where current flows into a layer sandwiched in ideal ohmic contacts. Analytical treatment of the condition will gradually follow the drift-diffusion Eq. (2.11). Charge particle current j_n is equal to observed current j in steady state situation. Substituting the terms, $-\frac{d\phi}{dx} \rightarrow F$, $j_n \rightarrow j$ we get

$$\frac{dF}{dx} = \frac{q}{\epsilon_0 \epsilon_r} n \quad (2.15)$$

$$j = q\mu n F \quad (2.16)$$

Combining the above two equations, we obtain,

$$F \frac{dF}{dx} = \frac{j}{\mu \epsilon_0 \epsilon_r} \quad (2.17)$$

$$\frac{dF^2}{dx} = \frac{2j}{\mu \epsilon_0 \epsilon_r} \quad (2.18)$$

Injection approaching electrode at $x=0$ is said to be ohmic, which leads to the boundary conditions as follows [9] :

$$F(0) = 0 \quad (2.19)$$

Consideration of the following boundary condition leads to

$$F = \left(\frac{2j}{\mu \epsilon_0 \epsilon_r} x \right)^{\frac{1}{2}} \quad (2.20)$$

Drop of voltage across the sample can be expressed as

$$V = \int_0^L F(x) dx = \left(\frac{8j}{9\mu \epsilon_0 \epsilon_r} \right)^{\frac{1}{2}} \quad (2.21)$$

From Eq. (3.17), Mott-Gurney equation can be stated by

$$j = \frac{9}{8} \epsilon_0 \epsilon_r \mu \frac{V^2}{L^3} \quad (2.22)$$

The above equation has high significance to describe the current density j flowing through the organic sample having layer thickness L at voltage V . It can be observed that V and L have strong influence on current density j . j is proportional to the square of the applied voltage and inversely proportional to the cube of the layer thickness. $j \propto V^2$ is applicable at the low voltage diffusion regime neglecting SCLC [50-51] where space charge density can be determined as

$$n(x) = \frac{1}{2} \left(\frac{L}{x}\right)^{1/2} \langle n \rangle \quad (2.23)$$

$$\langle n \rangle = \frac{1}{L} \int_0^L n(x) dx = \frac{3}{2} \left(\frac{\epsilon_0 \epsilon_r V}{qL^2}\right) \quad (2.24)$$

Therefore, current is limited when passing through the sample due to the formation of space charge in presence of ohmic contact in one side. As follows in Eq. (2.22), critical influence of mobility of carriers can be observed on carrier conduction ($j \propto \mu$). Therefore, the amount of current conducting at the bulk regime of organic diode is driven by low mobility which leads to the SCLC. It is necessary to illustrate the SCLC while analyzing the performance of characterization of experimental organic material. Field dependent mobility has been observed in this conduction regime where conduction varies quite peculiarly along with externally applied voltage [52].

Significance of carrier diffusion

We have shown in upcoming chapters that the precise variation of ideality factor with trap energy in organic dye based diode. But before that, few lines about diffusion driven current conduction in thin film of organic materials is required. Generally diffusion current is not considered for SCLC dominated conduction mechanism. But it has obvious impact at low voltage regime where the applied voltage is considerably less than the thermal voltage. Also the diffusion current becomes dominant with increasing thickness of organic layer [51]. Diffusion is the reason of enhancement of current density at small external voltage far exceeding the prediction of Mott-Gurney law (MG law). Current- Voltage plots (I-V) are validated with MG

law for comparatively higher level. The larger electric field is required for the thinner sample to obtain the agreement given above.

Metal-Organic interface

Zero field interfacial ohmic contact and expression of charge density have been considered in Eq. (2.19) and (2.23) respectively. This type of contact acts as a reservoir of infinite carriers in such idealized case. But in order to study the interfacial phenomena finite value of carrier density and obvious non zero value of field effect across the interface should be taken into account. Electrodes used in almost all application and measurement technique are made of different type of conducting materials (either different metals: gold, copper, silver, aluminum or materials such as ITO, PEDOT:PSS). Metal-organic interface influences highly on the device performance. Different work functions of metal and organic layer govern the electrical properties at junction [53]. When the aforesaid elements are said to be in contact, Fermi level of their materialistic energy aligns at the interfacial regime. It can be possible by the accumulation of the charges on each side of the contact. Organic substances are devoid of carriers completely at the initial position of the interfacial regime. Fermi level is found to be undefined and consequently its respective conception of alignment is not applicable. It is essential to use such an electrode which injects charges into the bulk region of the organic layer to have ohmic contact into the device. An injection barrier forms at the contact area due to the mismatch of work function of two distinct materials and two states of energy levels: HOMO and LUMO. Numerous models have been proposed to describe the physics of such contact regime [53-54].

Due to the contribution of image potential effect, potential $U(x)$ in the adjacent contact of electrode is given by the formula such as follows [13-14]:

$$U(x) = \phi_B - qF_x - \frac{q^2}{16\pi x \epsilon_0 \epsilon_r} \quad (2.25)$$

where F is electric field applied across, q is elementary charge and ϕ_B is the potential barrier height. Considering thermionic emission followed by surface recombination, a current density equation can be reformed [54]:

$$J(F) = 4\psi^2 N_0 \exp\left(-\phi_B/kT\right) \exp\sqrt{f} \quad (2.26)$$

$$f = eFr_c/kT \quad (2.27)$$

$$\Psi = f^{-1} + f^{-\frac{1}{2}} - f^{-1}(1 + 2f^{\frac{1}{2}})^{\frac{1}{2}} \quad (2.28)$$

$$r_c = \frac{q^2}{4\pi\epsilon_0\epsilon_r kT} \quad (2.29)$$

Here, r_c is Coulomb radius and f is reduced field. The set of equations described above was successfully applied to study the contact effect [43-44].

Injection limited current (ILC)

Here, another conduction possibility draws the attention next to SCLC conduction. Such conduction is known as injection limited current (ILC) where magnitude of current is limited by contact. In such cases SCLC is not very suitable. ILC conduction takes place to represent the situation where ohmic contact is not formed by electrodes. This can only happen when ϕ_B is very high to withstand ohmic injection of carriers from one electrode to bulk regime of organic material layer. For high value of ϕ_B , contact barrier results a drastic decrement of current. Presence of such contact barrier is not intended for injected carrier conduction towards material. It is quiet difficult to provide a very clear prediction about device performance for organic material based devices with ohmic contact [43]. But it is true that performance of such devices struggles for a long range comparatively than pure SCLC conduction. Though the graph of characteristic nature may have some similarities but to differentiate between SCLC and ILC based conduction undoubtedly has great practical relevance.

Gaussian Disorder Model

The overall discussion was limited within macroscopic point of view neglecting the microscopic mechanism effective in charge conduction. Microscopic level of transport in OSCs is subject for research for a long time. Multiple theoretical models have been proposed regarding this fact [56]. Gaussian Disorder Model and its extension were able to explain most successfully the physics of conduction [57]. The model basically deals with all localized states on a Cartesian grid. The grid is used to define different sites separated by a small distance “ a ”. So the whole density of states (DOS) is defined as $N_0 = a^{-3}$. Energy occupied by the states is random in nature to produce the energetic disorder in Gaussian distribution is defined by the following equation:

$$\sigma^{\wedge} = \sigma/kBT \quad (2.30)$$

Such disordered values ranges between 50meV to 150 meV.

Hopping is the way for carrier transportation in this model where the model under discussion deals with Miller-Abrahams rate. The rate of conduction through such sharp jump from state i to state j is

$$v_{ij} = v_0 \exp\left(-2\gamma_{ij} \frac{\partial r_{ij}}{a}\right) B(\varepsilon(j) - \varepsilon(i)) \quad (2.31)$$

Here v_0 is the hopping frequency, γ_{ij} is wave function overlapping factor of electronic states and ∂r_{ij} is the distance measured between i and j.

Here $\varepsilon(i)$ is the total amount of energy of state i which is represented by

$$\varepsilon(i) = E(i) - q\varphi(i) \quad (2.32)$$

$E(i)$ represents specific energy of state i obtained in Gaussian distribution

$$p(E) = \frac{1}{\sqrt{2\pi}\sigma} \exp\left(\frac{-(E(i)-E_0)^2}{2\sigma^2}\right) \quad (2.33)$$

Here E_0 is the average energy and the related term $B(x)$ is Boltzmann factor

$$B(x) = \begin{cases} \exp\left(-\frac{x}{kT}\right) & \text{for } x \geq 0 \\ 1 & \text{for } x \leq 0 \end{cases} \quad (2.34)$$

The factor shows that upward hoping requires some energy from heat source and hopping along downward direction is unaffected by the following conditions.

In Gaussian model, several considerations have been taken into account. Firstly, polaronic impacts are neglected, yet coupling to heat source is considered to be strong enough to allow jumps along upward direction [57-58]. Secondly, distribution of energy state is assumed in Gaussian form which leads to theory of central limitations of molecular interactions in disordered organic solids. Experimental arguments based on Gaussian Curve draw wide acceptance in terms of density of state, hence stress has presently been given on Gaussian Density of states distribution to best judgment of amorphous solids. Estimation of disordered nature is possible for field and temperature dependent distribution for many materials.

Gaussian disorder model provides the prediction given hereunder that depends on temperature (T) based charge carrier mobility and electric field (E)

$$\mu(\sigma, \delta, E) = \begin{cases} \exp C(\sigma^2 - \delta^2) E^{\frac{1}{2}} & \delta \geq 1.5 \\ \exp C(\sigma^2 - 2.25) E^{\frac{1}{2}} & \delta < 1.5 \end{cases} \quad (2.35)$$

Since hopping conduction is activated thermally, increment of mobility is encountered with temperature variation. In absence of electric field mobility can be stated as

$$\mu \propto \exp\left(-\left(\frac{2}{3} \frac{\sigma}{k_B T}\right)^2\right) \quad (2.36)$$

One very significant property of Gaussian model is field dependent mobility of conducting charges. Enhancement of mobility could be observed for δ less than 1.5. The conditions correspond to Poole-Frankel effect and related to the lowering of barrier potential by electric field. Electronic transition along the field driven direction is likely to be across downward in this distribution. Carrier mobility is assumed to be decreasing with value of disorder related parameter σ . The fact can be illustrated associated to percolation. Transition occurs for the electrons directed towards the direction of high applied field which inherently reduces the possibility to penetrate through some relatively easier way of percolation by such jump of carriers.

Master Equation approach

Gaussian model is well satisfied rather than time-of-flight experiments to analyze the charge concentration dependent space charge limited conditions. Consideration of charge concentration is very important to realize the devices operating in SCLC zone. Mobility is influenced by carrier concentration in case of Gaussian density of states. It is assumed that lower energy states are occupied by a fraction of charges. Consequently, conduction of majority of carriers will not be touched anymore by the presence of single charge occupied lower energy states. This is because the required time for upward hopping from lower energy states is related exponentially to its energy depth, a tail of distribution function of states which is withholding the drift velocity. The tail is almost filled up in high carrier concentration condition and hence, does not try to resist the fluent conduction of charges. This inherently enhances the mobility of charge carriers with increasing concentration of charges. Effects of carrier concentration on mobility of same material has been experimented in different type of devices with variation of carrier density in the work of Tanase et al. [58]

Master equation approach is introduced to investigate the influence of carrier concentration on mobility of charge carriers. The aforementioned equation takes the form given below in Gaussian model:

$$\frac{dp_i}{dt} = \sum_{j \neq i} -p_i(1 - p_j)v_{ij} + (1 - p_i)p_jv_{ji} \quad (2.37)$$

p_i is probability of occupation at site i , v_{ij} and v_{ji} are hopping rates from one site to another. The Eq. (2.37) gives time dependent probability of occupied sites. The following differential equation is reduced to its corresponding algebraic form of equation for constant electric field which can easily be solved. Carrier mobility (μ) can be extracted from the solution of abovementioned equation.

$$\mu = \frac{\sum_{j \neq i} -p_i(1-p_j)\Delta r_{ij}}{(\sum_i p_i)F} \quad (2.38)$$

where F is external applied field.

It has been obtained that μ can approximately be factorized between the factor $g_1(T, c)$ and $g_2(T, E)$. $g_1(T, c)$ and $g_2(T, E)$ are termed as concentration dependent factor and field dependent factor respectively.

$$\mu(T, E, c) \approx \mu_0 g_1(T, c) g_2(T, E) \quad (2.39)$$

It has been reported that effect of applied field and carrier concentration on charge mobility enhances with disorder increment [49]. Mobility remains constant in absence of disorder. Some fundamental facts of both enhancement factors can be encountered on the basis of such disorder. g_2 approaches to unity for lower field intensity. It is in contrast to g_1 , which, in presence of high disorder, exceeds unity even for low concentration of carriers. Undoubtedly, effect of charge concentration play a significant role in disordered organic materials.

On the other hand, process of charge injection occurs basically in two consecutive steps. At first a pair of image charge is appeared and transition occurs accordingly from Fermi level of metal electrode towards organic layer. Next, the injected charge is conducted by hopping into a potential. The aforementioned potential gains a maximum value because of superposition of image and external potentials. Maximum obtained values of different electrical parameters well exceed the dimension of sites. A number of hopping of the charge carriers can be scheduled to take place to exit the active electrode regime. So in a nutshell, the first step becomes more significant for high electric field and potential barrier value. Such values dominate the current magnitude.

The next equations mentioned below denote the relation of charge carrier concentrations with potential barrier.

$$n_{con} = N_0 \int_{-\infty}^{+\infty} \frac{p(E)}{1 + \exp\left[\frac{E + \Delta'}{kT}\right]} dE \quad (2.40)$$

Where n_{con} is the charge carrier concentration and Δ' is the potential barrier of the electrode Δ modified with image charge in the following form such as follows

$$\Delta' = \Delta - q \sqrt{\frac{qF}{4\pi\epsilon_0\epsilon_R}} \quad (2.41)$$

Here, F is electric field and p(E) means density of states function.

The following relation is well fitted with drift-diffusion model. Further investigation using Master equation on conduction mechanism of three dimensional grid has been carried out to compare with expected outcomes of drift-diffusion model using aforementioned boundary conditions. In Master equation approach, total site energy is assumed as the sum of Gaussian density of states based specific energy of sites and applied field dependent electrostatic energy with image charge effect.

$$q\phi = q(\phi_i + \phi_{im}) \quad (2.42)$$

Where $q\phi_i$ and $q\phi_{im}$ are the applied electric field and image charge prone field respectively.

Potential at electrode planes are termed as

$$q\phi(i_x = 1) = qV \quad (2.43)$$

$$q\phi(i_x = m_x) = 0 \quad (2.44)$$

ϕ_i and ϕ_{im} can be calculated from Poisson equation and the formula stated below:

$$q\phi_{im} = \frac{-q^2}{16\pi\epsilon_0\epsilon_R a} \left(\frac{1}{m_x - i_x} + \frac{1}{i_x - 1} \right) \quad (2.45)$$

Where i_x denotes the index of the layer.

Solution of the Poisson's equation was found by utilizing the average value calculation of carrier concentration in each layer. The Gaussian density of states is assumed to be equal to barrier of the electrode Δ . Same hopping rate is assumed also to and from the each electrode. The obtained outcomes of one dimensional drift diffusion model reveals good agreement with Master equation approach with lowering of image charge potential barrier.

2.9. Overview on traps

The inherently weak molecular interactions in organic semiconductors (OSCs) lead to the formation of defects which causes localized states in band-gap regime [59-61]. These localized states are able to trap carriers. Thus trapping is ubiquitous in such organic materials and can deeply influence on the performance of OSC based optoelectronic devices [62-63]. OSCs include conjugated molecules with delocalized electrons formed during the overlapping of p-orbital. Such spatial overlapping determines the electronic coupling among the molecules and thereby charge transport mechanism [64-67]. Binding energy of intermolecular interactions in OSCs is low enough which is highly intended for application in flexible electronics. Such materials are undoubtedly exciting, proving a wealth of technically attractive facts and intriguing a strong base to explore innovative research. But there are some challenges also that require to be carefully addressed before its widespread development and rapid adoption. Low mobility related problem of OSCs can be taken for a suitable example in this regard. Localization of carriers alters the narrow shaped band initiating from van der waals intermolecular interactions is encountered as one of the major cause for such low mobility. The carrier localization in organic molecules has been attributed to polarization in earlier research works. Charges interact to nearby electrons in molecular crystals generates “polarons” and the corresponding theory has been modeled by polaron band theory [68-70]. Most crystalline organic molecules showed hopping dominated activate charge conduction which was widely accepted in early years. However, this acceptance has been challenged by recent observations. The fact is justified by the investigation on power-law dependence of mobility in single crystals which reminiscent the delocalized band transport [70-71]. Such band transport in semi classical theory implies that the charges are delocalized over a long distance comparatively than the lattice spacing which are scattered occasionally by lattice vibration and presence of impurities. However, since delocalization is limited in OSCs so that “band like” term has been introduced to demonstrate the charge carrier transport mechanism in such materials.

The mean free path of carriers in OSCs is comparatively lower than the intermolecular spacing which results localization of carriers and low mobility. It has been recently observed that thermal motion driven dynamic disorder impact on molecules which is the main barrier of high carrier mobility in organic system. Such transient localization, generated by amorphous disorder nature

of OSCs, survives up to the time limit of molecular vibrations. Several models have been given to reconcile the idea of coexistence of localized carriers and band like carrier transport conception which builds a strong theoretical realization of charge transport mechanism in OSCs [70-73]. Besides that, electronic states formation is held in the band gap regime by disorder generated defect. Carriers are subsequently trapped in such in-gap states during conduction. Traps are ubiquitous phenomenon having enormous repercussions on stability and performance of OSC based optoelectronic devices. Naturally, understanding the facts regarding trap formation mechanism and its impact on free carrier conduction is decisive in determining the fundamental limitations of performance of the OSCs. This chapter aims to demonstrate a clear and comprehensive review on trapping phenomena in OSCs emphasizing on the impact of the mentioned parameter on device operation.

2.9.1. Definition of Traps

Electronic traps are a kind of imperfection into the semiconductors which form spatially distributed localized electronic states. These states are well oriented within the band gap based on their energetic distribution. The distance of their relative energetic positions from band edge or trap depth gives the idea about the nature of the traps at a given temperature. Traps are shallow when they lie in the band edges vicinity regime (a few kT) or deep if located further from band edge (at several kT), where k is Boltzmann's constant and T is operating temperature. The diagram given in fig. 2.9 illustrates this very well. Localized tails in band gap region are considered shallow in general with acceptor states at LUMO and donor states at HOMO expressing states of the trap distributions for electrons and holes respectively. Carriers can be captured and restrained temporally by traps until it is released to the band by the influence of electric energy or thermal energy. If the concentration of traps is high enough, trapping carriers conducts by thermal activated hopping or tunneling from one localized energy state to another. Releasing from trapping charges can be held if the trap depth is too low. Shallow traps are comparatively high responsive than the deep charge carriers [74-75]. Charge carriers trapped in shallow traps get back into the band by thermal excitation. But probability of such occurrence is very low for charge carriers in deep traps and such traps inherently reduce the lifetime of the carriers acting as recombination centers [76]. It is to be noted in this perspective that shallow trap

is relatively more deep trapping states as it interrupts the mobility of charge carriers more than the deep trapping centers.

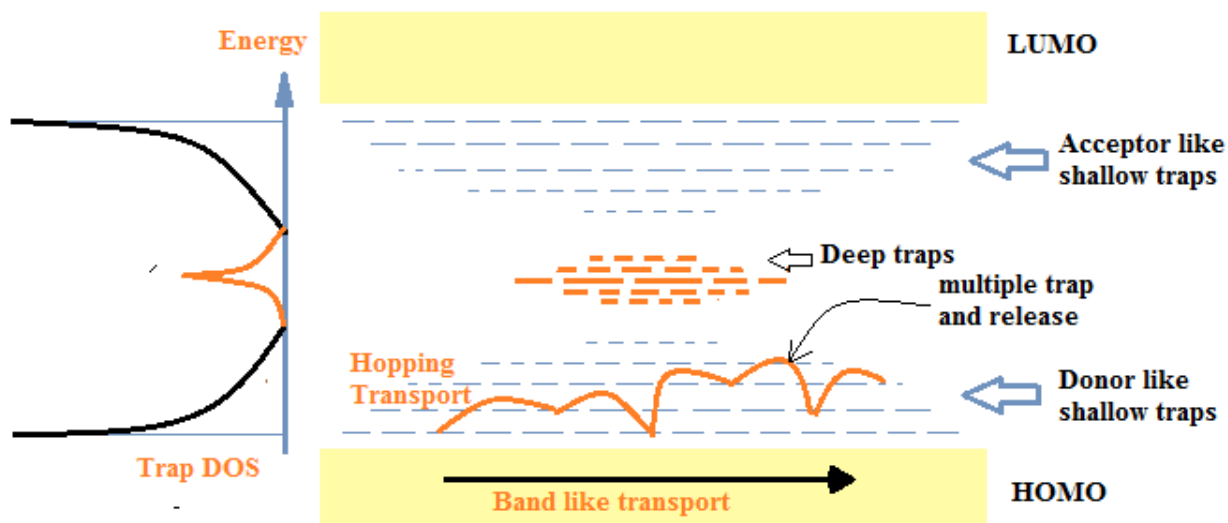


Fig.2.9. Traps Density of States presentation represents shallow traps at tail states (black color) and deep traps (red color) in the band gap (left side of the diagram). Schematic representation of Energy diagram of OSC with localized trap states has been depicted in the band gap region. Acceptor and donor like shallow trap states are drawn (blue color) at top and bottom of deep traps (red color). Arrows express different conduction regime like: Band like transport, MTR and hopping transport [77]

A DOS function defines localized states into the band gap zone of an OSC. Distribution of traps is also represented by this function. Traps acquire quasi-continuous or discrete energy level which can be explained by using Gaussian distribution function [78-79]. As can be seen in the figure, the left segment of the diagram shows Gaussian distribution of deep trap states in the band gap regime (shows in red color) and extension of disorder dominated tail states (black color curve) acts as shallow traps in that regime.

2.9.2. Different sources of Traps

There are different sources from which traps can be originated. The most crucial source of traps is disorder in OSCs. Static disorder appears due to impurities and structural defects. Such traps are defined as intrinsic source of trapping distribution in OSCs. Formation of the intrinsic sources holds during film formation. On the other hand, extrinsic traps can be introduced by

interfacial mismatch caused by interfacing with other materials like OSCs, dielectrics or metals. Detail of the trap sources has been discussed in next subsections.

2.9.2. i) Disorder

Imperfections in crystal structure can strongly impact on translational symmetry, thereby forming disorder into the molecular system. Spatial distribution of molecular structure results off diagonal structural disorder. If the disorder introduces fluctuations in energy differences between energy levels of HOMO and LUMO of a molecular segment, it can be referred as energetic disorder. This type of disorder can be explained by Gaussian distribution of energy. An exponential DOS is also often referred to model such disorder introduced tail states in band gap regime [80-81]. Disorder can be classified into two types: dynamic disorder and static disorder. These disorders can be distinguished on the basis of site energy variations and transfer integrals of crystal. Dynamic disorders appear due to thermal influence and interaction between photon and electron and orient itself on the entire crystal regime causing destruction of electronic energy bands with localization of carriers whereas static disorder is introduced by impurities and structural defects and locates only defects affected specific locations [82-84]. Both type of disorders introduce localized band tail states with additionally forming in-gap states into the band gap regime due to inhomogeneties in molecular structure. Disorder dominated band tail states formed in OSC crystals express performance limiting issue in such materials [85, 97]. Density of band tail states has a significant role in determining the detail explanation of charge conduction mechanism in comparatively weak electronic coupling based organic molecules [84]. Theoretical investigations confirm the band tail existence in gap states near the valence band edge causing thermal motion of molecules [85-87]. Such states have been observed experimentally in different organic materials but their source of origin is still remain a vexed question [88-89]. Troisi et al. found that the states have similarity with intrinsic disorder prone inorganic molecules [70]. Role of band tail states in trapping of carriers in OSCs have been discussed in succeeding sections.

2.9.2. i) a) Structural defect

Structural defects in both of crystal and thin film have been discussed in this section. Defect in uniformity in crystal structure of OSC can yield the formation of intrinsic traps. Lattice

imperfections present in every crystal [90]. Such defects can be classified as extended defects. Extended defects take the form of line defects due to dislocation or planer defect. These defects are deviated from their position of equilibrium and the polarization energy of such carriers placed on these molecules changes. This change in polarization energy leads to the formation of the sites of localized traps with quasi-continuously distribution of energies in the band gap regime held between LUMO and HOMO level. Anti-traps is also a crucial fact in this context which appears when the aforementioned states are inactive energetically. These Anti-traps disturbs the fluent motion by scattering the carriers to and fro from their movement. Such variation in electronic polarization energy also influences the electronic coupling sites. Stronger coupling can be observed in narrow spaced regime while dilated zone in the lattice is weaker coupling prone in nature [91-92].

On the other hand, grain boundaries (GBs) in thin film of OSCs incorporate structural defects and disturb the charge conduction accordingly [93-95]. They serve as trapping impact on the carrier which leads to thermally activated charge transport mechanism [96-97]. Marohn et al. applied electron force microscopy to investigate spatial trapping distribution in thin film transistors [96-98]. They observed that the traps are distributed not only in GBs but also on the entire film. Observation of Frisbie et al. was little bit different. Frisbie found that static potential in GBs surface is sufficiently lower in crystallites [99] which show consistency with the work of Horowitz et al. [102-105]. Kaake et al. demonstrates that GBs acts as barriers for the trapped carriers while charges are trapped into the grains [97].

Kinks like structural defects introduce both deep and shallow trapping state in the polymer [104]. Kinks produce energetic disorder with sequential conjugated segments having different HOMO and LUMO energy levels. Such effects lead to hopping occasionally through p-stacks. Long ranged amorphous polymers consist of crystalline domains obeying law of crystalline polymer physics [105].

2.9.2. i) b) Chemical impurities

Dopants are added deliberately in a host by existing chemical impurities of guest molecules which inherently produce traps with significantly high energy in band gap. Generally the guest molecular energy levels differ from the host and trapping states are formed on the basis of such

energy states. The localized traps have a discrete nature on zero order approximation. Hence, for trapping of holes, trap energy E_{th} is measured from the guest-host energy level difference. Similarly, electron affinity difference between host and guest level concludes the electron trapping energy E_{te} .

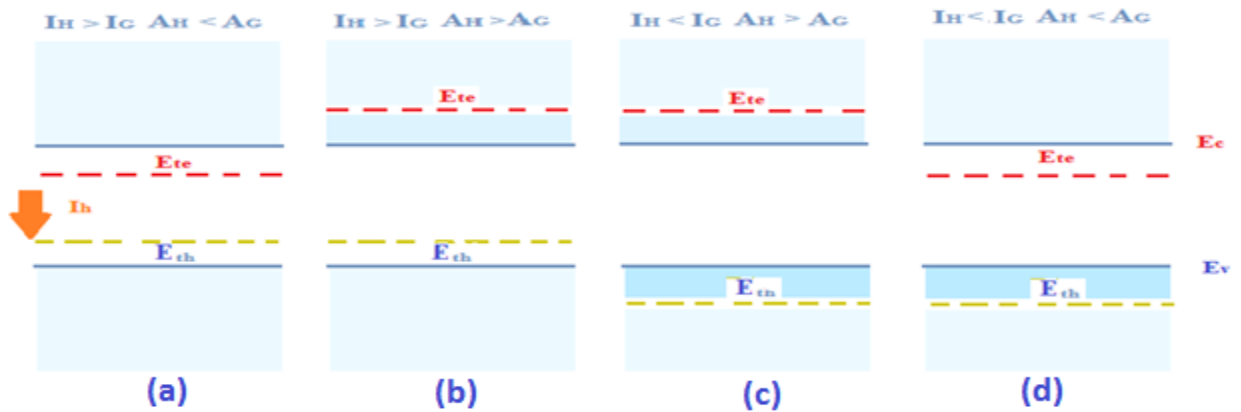


Fig.2.10 Schematic representation of different trapping and anti-trapping states of guest-host molecules in a lattice

Fig.2.10 illustrates different hypothetical states in which several trapping states of conducting charges are generated due to the presence guest-host molecules. In the first case Fig.2.10 (a) host molecular band gap is the place of energy levels of guest molecules (HOMO and LUMO). This generates trapping states for carriers. In second case Fig. 2.10 (b), traps are introduced by guest molecules for holes only where the concentration of trapping states can be found in the vicinity of HOMO. Fig. 2.10 (c) represents inert chemical impurities having ionization energy and electron affinity is respectively greater and less than host molecules. Such impurities contribute local distortion in the lattice which results scattering of carriers during conduction. Dopants or impurity concentrations provide the estimation of scattering events [78, 106]. In the last figure Fig.2.10 (d), explanation of introduction of traps for electrons has been explained in order to emphasize on the influence of the guest molecules.

Traps are also driven by chemical degradation acts in the form of oxidation. Oxidation is produced due to increasing concentration of impurities [107]. Trapping density is lowered in presence of reduction [108]. On the other hand, environmental contaminants results discrete traps by high electron affinity. Molecules of water cluster having low ionization energy caused by

dipole moment stabilization from other surrounding molecules can form potential hole trapping states [109].

2.9.2. ii) Interfacial fact

Organic semiconductor based device contains consecutive dissimilar layers and architecture of their orientation has different levels of complexity based on their work function. Interfacial phenomena between two adjacent layers like electrode/semiconductor, semiconductor/dielectric and two distinct organic layers deliberately adds carrier trapping. Interfacial trapping states has profound impact on the device performance.

2.9.2. ii) a) Semiconductor-dielectric interface

Dielectric layer roughness alters the molecular orientation and ordering which in addition scatters the accumulated carriers and results defects in surface structure and energy of surface by dislocations. Trap is produced in another way at interface which is related to impurities absorption like water (H_2O), O^+ and OH^- groups. Passivation of bonding at the vicinity of the SiO_2 gate-dielectric interface result trapping of interfacial carriers by OH^- absorption. This was main challenge of significantly achieving charge conduction in SiO_2 based transistor [111-112]. Investigation of Mei et al. concludes that the thermal expansion coefficient (CTE) mismatch between consecutive layers of thin film introduces interfacial strain. Such interfacial disturbance generates localized states prone to traps [113]. They observed a crossover between temperature dependent activated transport and band transport upon enhancing interfacial CTE mismatch which is associated to thermal strain driven carrier trapping [114-115].

2.9.2. ii) b) Metal-Semiconductor interface

Trapping of conducting charges also takes place at metal electrodes-semiconductor interfacial regime. Such trapping inherently impacts upon carrier injection and fluent conduction. The band localized states of OSCs influences the charge transport which leads to the injection barrier enhancement and the increasing barrier manifest itself as significant contact resistance. Band electronic tail states is introduced by such energetic disorder in OSCs which pin the metal Fermi level and resist it to reach the band edge of the injection barrier. Further extension of the disorder measures the band edge to Fermi level distance. Incorporation of buffer layer between metal and

OSC can unpin the Fermi level energy lowering injection barrier [116]. Charge carrier utilizes energy gap states as energy ladder to hop towards the level of energy transport [116-117]. The surface of the organic materials are prone to defects. When a contact is made of metallic surface and OSC surface, localized states are formed at the interfacial contact. These states are responsible for the generation of surface potential which subsequently enhances the injection barrier. According to Baessler et al., surface potential generated at low work function electrodes is strongly influenced by trapping of charge carriers [118]. Boer and Morpurgo investigated the surface trap states impact by analyzing the SCLC measurement on Tetracene crystal inserted in sandwich like structure where Al and Au are used as top and bottom electrode respectively. It has been observed in their experiment that injection of carriers was more prominent from bottom surface contact. They concluded that interaction between X-rays used in electron beam evaporation procedure and electrons damages the surface of the Tetracene crystal which results a high level of trap concentration in comparison to the bottom surface. These trapping states lead to the surface traps processing which further influence the conduction process.

2.9.2. ii) c) Environmental impact

Different exposure related to environment often impacts the quality of the device performance formed by OSC and lead to the formation of traps. Temperature, electromagnetic radiation, moisture and ambient gaseous particles are the sources of trapping. Temperature affected trapping states manifest themselves due to shifting in sub-threshold and turn-on voltage [119]. Shallow and deep traps can be distinguished by temperature effect i.e., traps behave like shallow traps at sufficiently high temperature and vice versa [120-121]. Water molecules acts as traps for conducting carriers. Bias stress like untended instabilities in opto-elctronic devices was caused by such traps [122-123]. In pentacene crystal, trap states are generated during bias stress. Observation of Nikolka et al. also demonstrates that such bias stress acts as carrier traps in polymer films [124]. Gomes et al., investigated that the bias stress impact is strongly related to temperature function and presents only above 200 K [65].

Oxygen related trapping states also takes place in different organic materials [125-127]. Northrup et al. explains that formation of trapping states complete with the replacement of H-atom by O-atom forming a double bond shape along with C-atoms [125]. Oxygen driven trapping impact on DOS spectrum of thin organic layer based transistor has also been studied.

Knipp et al. found that exposed thin organic film faces continuous bias stress in presence of oxygen atmosphere [127]. Such stress leads to induced discrete trap states in OSCs.

OSCs are characterized by exposing under X-ray treatment or by some other ionization radiation. Several studies reports that such radiations involving to elucidate surface morphology and device metrics causes shifts in threshold voltage V_{th} without disturbing mobility of carriers, concludes the generation of deep trapping states into the bandgap. These generated traps were attributed to breaking of C-H bonding with hydrogen loss.

2.10. Trap assisted Transport Models

This section provides an overview of different proposed models for explaining trap assisted carrier transport in organic semiconductors. The discussion in this context has been given below:

2.10.1. Anderson localization

Localization of different energy states are followed by Anderson formula by assuming three dimensional quantum well arrays. Depths of the quantum well are distributed randomly based on its Gaussian distribution energy characterized by mean energy E_m , schematically represented below:

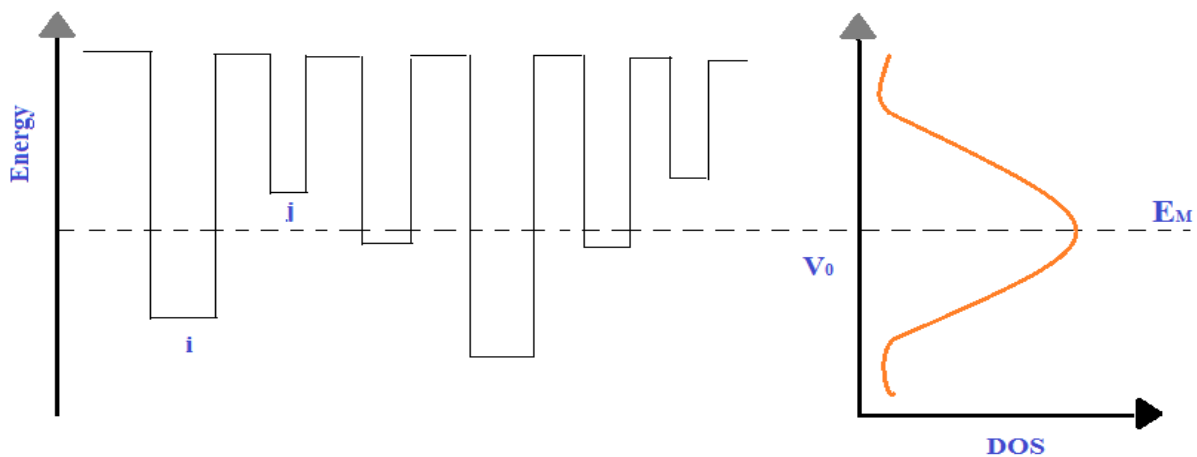


Fig.2.11 Schematic diagram of Anderson localization due to a Gaussian distribution of quantum well depths

Wave function ψ_i of trapped carrier in a quantum well i exponentially decays with respect to x such as:

$$\psi_i(x) = \left(\sqrt{\pi}\alpha^{-\frac{3}{2}}\right)^{-1} \exp\left(-\frac{x-x_i}{\alpha}\right) \quad (2.46)$$

Where x_i is position of localized site and α is localized length. In case of $V_0=0$, all quantum well depth remains same and the system indicates no disorder in nature. Overlaps are encountered in the wave function leading to band formation in bandwidth regime. Increment in DOS can be found with increasing value of V_0 and hence the distribution spreads over the energy space with less overlapping. Transfer integral becomes proportional to the localization length. Anderson stated that all quantum states are localized beyond a certain limit of V_0 with respect to bandwidth B . The critical ratio of $V_0/B=1.6$ for total localization of states [128]. However, complete DOS localization is not essential for execution of incoherent hopping as dominated charge conduction mechanism. The separation between delocalization and localization states can be done when the transport energy lies below the range of mobility edge.

2.10.2. Mobility Edge model

DOS sites places below the range of certain energy is termed as mobility edge, E_{ME} . E_{ME} is assumed as localized site and serves as carrier trapping whereas all existing states lie above E_{ME} are extended or delocalized states with continuous band distribution in which conduction of carriers are disturbed only by scattering. Fermi level lies close to mobility edge at high concentration that leads to the thermally activated charge transport from E_F to E_{ME} . Carriers face multiple trapping at lower level of DOS during band transport into OSCs [129]. Such type of conduction is typically stated as multiple trapping and release (MTR). Schematic representation of MTR has been depicted in Fig.4. In presence of large disorder, the localized state to extended state ratio is best suited to describe the analogy of trap driven transport mechanism. Explanation of charge conduction will be more specific in terms of hopping model or transport energy (TE) model [130-131] in polymer chain or crystalline OSCs where π -orbital along with wave function of occupied states of carriers can be more extended leading to trap driven conformational defects with separation in chain segment or in disorder amorphous phase of crystal molecular structure

[132]. Temperature based conductivity and thermal release of carriers in band transport can be elucidated by MTR model.

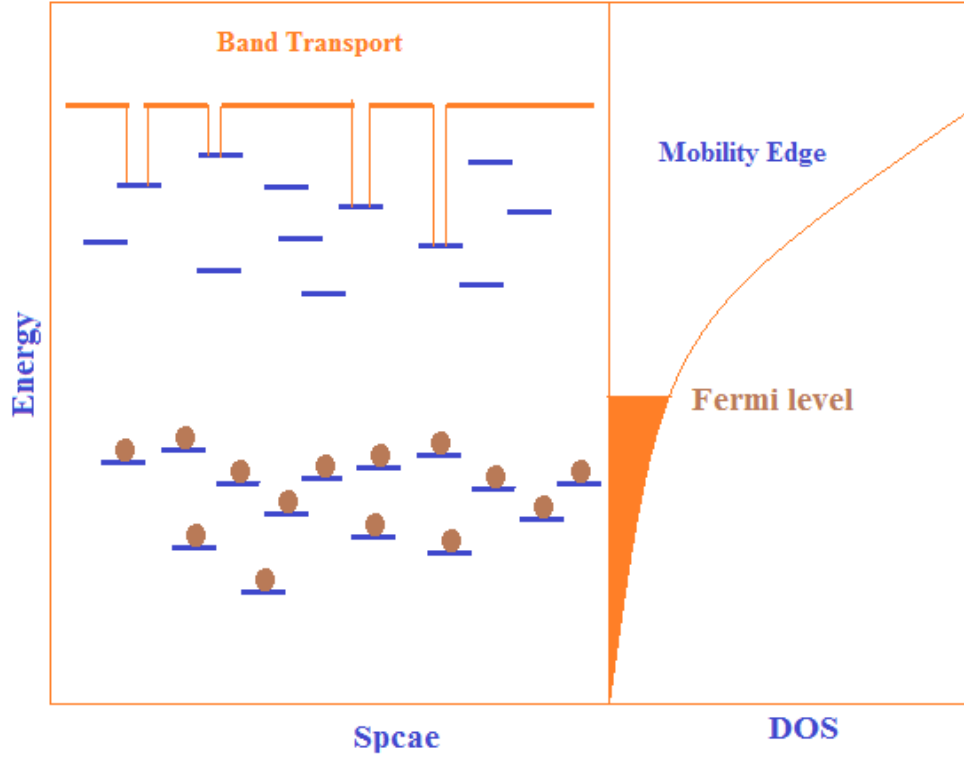


Fig.2.12 Schematic representation of MTR mechanism

2.10.3. Hopping Transport model

Thermal activated charge tunneling in localized states was proposed by researchers to demonstrate the procedure of charge conduction in amorphous inorganic materials [133-134]. Large disorder in OSCs results localization of carrier states. Conduction in these localized states of OSCs are referred as hopping. Thermally activated hopping in such localized states with hopping rate between two mentioned sites i and j and that was expressed by Marcus formalism or by Miller-Abraham (MA) expression such as follows:

$$\vartheta_{ij} = \vartheta_0 \exp\left(-\frac{2r_{ij}}{\alpha} - \frac{|E_i - E_j| + |E_i - E_F| + |E_j - E_F|}{2k_B T}\right) \quad (2.47)$$

Here, r_{ij} is site of separation between energies E_i and E_j . ϑ_0 is a material dependent factor used to refer as attempt-to-hopping frequency. The first exponential term of the above equation represents spatial distribution dependent tunneling rate driven term which denotes the tendency of wave function overlapping. Difference between different sites and the level of Fermi energy E_F to the probability of hopping events are indicated by the second exponential term of the aforementioned equation. However, downward hopping struggles with their spatial separation and hops along two unoccupied or occupied energy sites and hence therefore not associated to a penalty in rate of hopping. The corresponding fact can take the shape of the following equation:

$$\vartheta_{ij} = \vartheta_0 \exp\left(-\frac{2r_{ij}}{\alpha}\right) f(x) = \begin{cases} \exp\left(-\frac{E_j - E_i}{k_B T}\right), & E_j > E_i \\ 1, & E_j \leq E_i \end{cases} \quad (2.48)$$

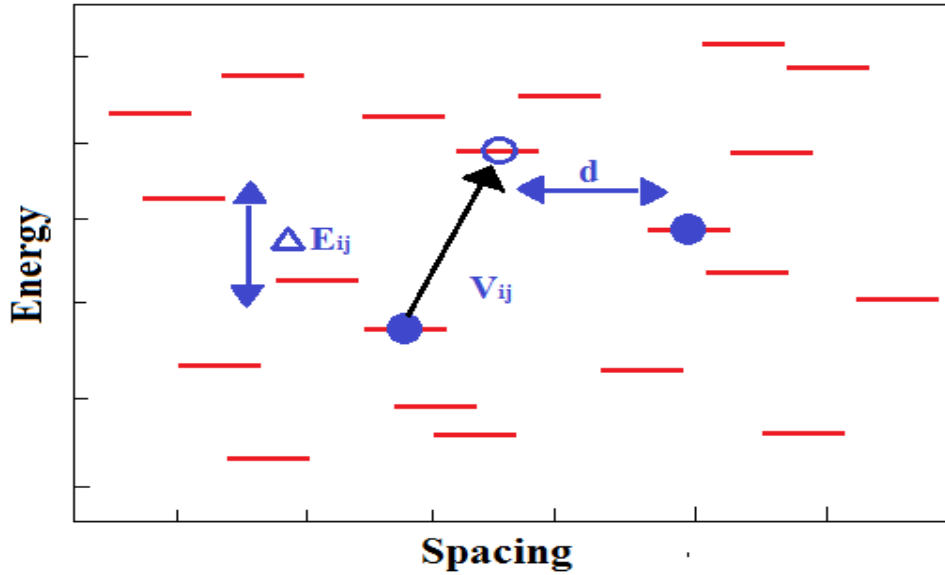


Fig.2.13 Carrier hopping between two sites having Miller-Abraham hop rate estimated by energy-space separation

If a positive carrier is directed along the direction of the applied field F , the charge acquires energy which leads to the lowering of energy difference $(E_j - E_i)$ perceived by dynamic carrier and enhances accordingly the probability of hopping rate.

2.10.4. Percolation model

Miller-Abraham (MA) approach estimates the charge dynamics due to hopping of percolated carriers through a resistive network. Each carrier hopping is replaced by junction electrical node distributed on overall space in random manner. A pair of adjacent sites or nodes i and j is associated with a resistor R_{ij} . R_{ij} follows inverse relation to probability of MA hopping such as

$$R_{ij} = \frac{k_B T}{q^2} \cdot \frac{1}{\vartheta_{ij}} \quad (2.49)$$

ϑ_{ij} is the equilibrium transition rate between i and j sites. Upward hopping is considered only as rate-limiting factor in hopping conduction. Electric field in such model is assumed to be small enough and a perturbation to the resistances [135]. In order to obtain a fluent conduction, a continuous percolation pathway is required and that can be formed by overcoming the critical resistance into the system. Problems in percolation can be resolved by geometry considering a sphere surrounded by each sites. The threshold value for charge percolation can be obtained by increasing r until it reaches to its critical value or $r = r_c$. Average number of sites within percolation limit can be written as:

$$\frac{4\pi}{3} g(E_F) r_c^3 = B_C \quad (2.50)$$

Where B_C is average bond numbers per sites require to form threshold percolation and $g(E_F)$ is the DOS located at Fermi level. Being a thermal activated procedure, hopping becomes energetically favorable for charges to tunnel towards non-nearest hopping sites (NNH) from lower energy state even at low $k_B T$, as depicted in Fig.2.14. Hopping occurs at variable ranges based on different energy sites and is termed as variable range of hopping (VRH). VRH can be introduced in criterion of percolation formalism such as follows:

$$\frac{4\pi}{3} r_c^3 \int_{E_i}^{E_f} g(E') dE' = B_C \quad (2.51)$$

Solution of the percolation formalism equation for VRH leads to renowned Mott-equation for low temperature based conductivity such as:

$$\sigma = \sigma_0 \exp \left\{ - \left(\frac{T_0}{T} \right)^{\frac{1}{1+d}} \right\} \quad (2.52)$$

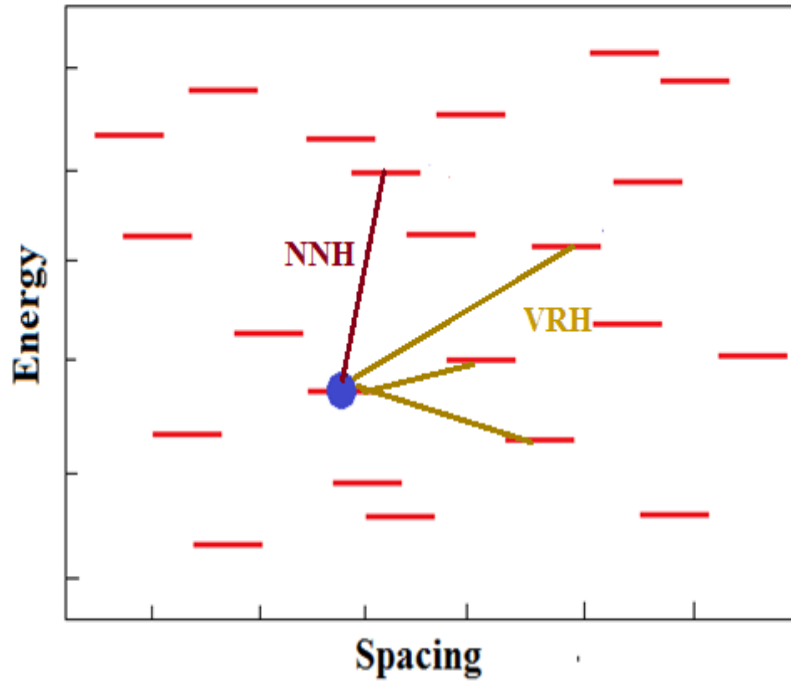


Fig.2.14 NNH and VRH in Energy-Space curve

Where σ_0 conductivity pre-factor and T_0 is characteristic temperature. Mott equation is valid in constant DOS approximation around Fermi level energy whereas the VRH in this law is strongly dependent on disorder of the DOS [75].

2.11. Trap characterization techniques and measurement methodology

Determining the different sources and spatial distribution of trapping states remain a strong challenge in spite of efforts dedicated over last few years. Nevertheless, remarkable progress has been observed to access to the carrier trapping concentration has indicated to device performance

improvements and reliability. Implementation of different experimental methods have been encountered which include different levels of assumptions with varying sensitivities and energy distribution. The present section implies some popular methods employed in trap characterization among which we have applied SCLC measurement technique in experimental part of our research work.

2.11.1. Electrical measurements

2.11.1.1. Space Charge Limited Current (SCLC) measurements

SCLC measurement is most renowned process to obtain better insight about trap related issues. The measurement is based on the consideration of carrier injection along unipolar direction. When injected carriers move towards semiconductor junction, a space charge regime is set up that subsequently changes the mellifluous flow of carriers. The signature of trapping states causes the appearance of series resistive impact upon the fluency of charge conduction. Measurement of current voltage (I-V) relationship is utilized to have insights in the charge carrier trapping. The experimental arrangement required for SCLC measurement is simple enough which involves sandwiching of semiconducting materials between two electrodes having different work function. We have used Al and Cu metal electrodes as front and back electrode respectively in our experiments.

The phenomenological theory of SCLC measurement emphasizes an idealized model that considers ohmic contacts and diffusion free unipolar directional charge conduction for discrete trap distribution. The I-V relationship in this context is given by:

$$J_{SCLC} = \frac{9}{8} \frac{\mu \epsilon_r \epsilon_0 \theta}{L^3} V^2 \quad (2.53)$$

Where μ is the drift mobility of carrier, ϵ_r is material permittivity, L is spacing between front and back electrodes and θ is trap factor.

Fig.2.15 illustrates SCLC conduction based I-V curve from which trap energy can be determined. It is observed from the following curve that the current at the low voltage is small enough and shows ohmic nature and then it changes its nature at SCLC zone with increasing bias voltage, followed by trap free conduction at high voltage.

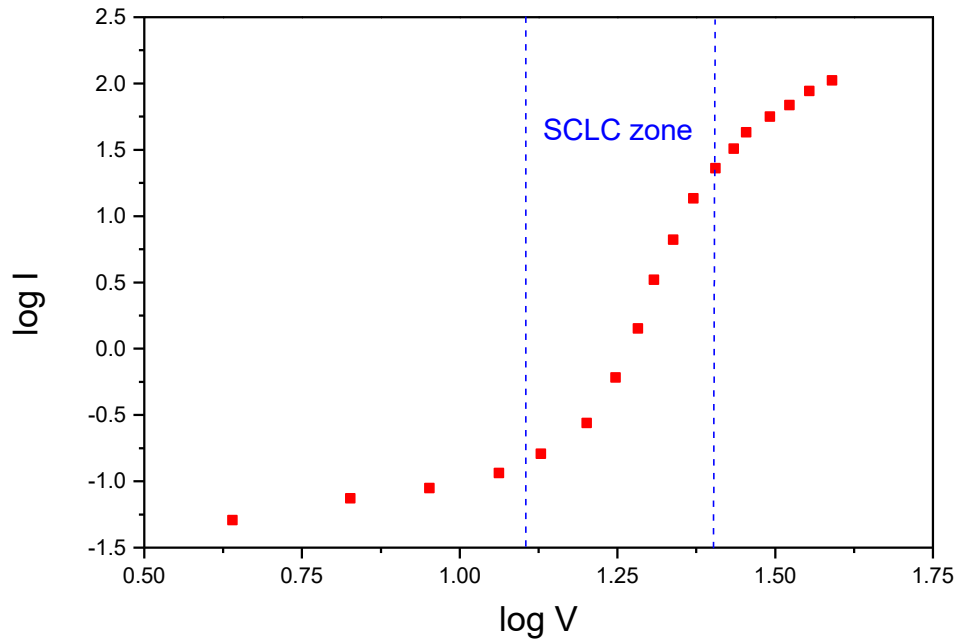


Fig.2.15 Typical I-V characteristics used to SCLC measurements of trap energy of discrete shallow traps

From the slope of the curve at SCLC regime trap energy can be estimated. Differential method has been implemented to observe the signature of trapping in OSCs. Detail measurement calculation and determination process of electrical parameters have been discussed in Chapter III and Chapter IV. Differential method has been implemented to observe the signature of trapping in OSCs.

2.11.1.2. C-V measurements

Density of traps can be determined by using C-V measurements. The experiment is performed at different frequencies. Trap distribution of M-I-S capacitors is obtained by accessing equivalent circuit modeling. The process is simple enough with achieving fast analysis credential but it struggles in determining suitable models to correlate frequency response in optoelectronic devices. C-f modeling optimizes the problem and such modeling is taken into account to estimate trapping-detrapping states with frequency variation. In C-f experiments, external voltage

frequency is swept to obtain characteristic frequency where thermally agitated trapped carriers excited out of trapping states are being recorded.

2.11.2. Optical measurements

2.11.2.1. Photoemission spectroscopy (PES)

PES method follows the principle of photoelectric effect. Carriers trapped in the bulk region of semiconductor are excited by the absorption of light, thereby producing free carriers and gradually enhancing the material conductivity into the sample. This process is known as photoconductivity. Thus by estimating the variation of conduction due to photoconductivity, information about trap distribution can be gathered. The method is generally used to obtain better insight of interfacial DOS spectrum of trapping states of thin film transistors.

2.11.2.2. Charge modulation spectroscopy (CMS)

CMS is another spectroscopic technique used in characterization of trap distribution by probing the variation of optical absorption in OSCs due to electron acquisition/loss from molecular orbital. CMS is well established methodology which provides information about trapping properties [141]. In this process applied voltage is used to modulate carrier concentration that enforces shallow traps to be emptied and subsequently changes the absorption spectrum. Broadening of absorption peak holds with increment of bias voltage that indicates de-trapping of carriers placed in shallow traps. The method is not useful enough to estimate non-radiative trapping states. As a part of such process thermal stimulation current (TSC) is also adopted to resolve the problem of characterization of non-radiative traps. Absorption of light followed by a thermal agitation technique is implemented on trapped carriers to fill up from injection to band gap states. The filling up process runs at a low temperature and subsequently is allowed to be heated until the trapped carriers obtain adequate amount of energy to get rid of trapping states. Conductivity in this process is increased quite naturally and is recorded as function of temperature to extract trap depth and density of traps.

2.11.2.3. Deep Level Transient Spectroscopy (DLTS)

The process is very useful for the characterization of trapping states in inorganic materials. In this process voltage pulse is applied to move the quasi-Fermi energy level towards band gap filling states providing a thermal agitation to the trapped carriers resided at the state. Hence, change of transient capacitance takes place with discharging of excited carriers which collect the information regarding trap related parameters. Electronic trap density and its distribution, evaluation of trap induced energy states can be obtained by utilizing DLTS technique [142].

2.11.2.4. Photo-thermal deflection spectroscopy (PDS)

This process is expensive and takes long time measurement times to achieve high sensitivity in device performance. The process associates with deflection of optical beam of laser source while extrapolating the variation of thermal characteristics of the sample upon light absorption. At first, sample material is immersed into a fluid having temperature dependent highly sensitive refractive index. Monochromatic light beam incidents on the sample form an excitement to transit the trapped carriers in the gap states and subsequently trap DOS are collected by analyzing energy of the aforementioned states [143-144].

2.11.2.5. Scanning probe method based measurement

Scanning probe method based electron force microscopic technique (EFM) and Kelvin probe microscopic technique (KEFM) give images with high quality spatial resolution and construct a topographic mapping of trap prone disordered surface area by identifying with the variation of local contact potential [145]. Surface potential changes due to the existence of trapping sites, so the procedure provides outstanding assistance to extract the spatial distribution of trapping states. EFM and KPFM are used to determine the contribution of grain boundaries on trapping the carriers in thin organic films [98,145].

2.12. Concluding remarks

In present chapter, a detail overview about OSCs has been provided. Past significant works on OSCs based experimental and theoretical research has been discussed. The focus has been given onto the chemical properties of such semiconductors. Illustration of their bond formation in

different small organic molecules has been provided. Subsequently, electronic structure of OSCs has been demonstrated. Depending upon the degrees of disorder, generated by amorphous nature, such materials can be classified into three types: Highly ordered system, Slightly disordered system and Highly disordered system. Purposefully, a brief discussion of these systems has been provided in this chapter. Exciton generation and recombination process in OSCs has been explored in the next section. Relevant comparison in two different type of recombination process (Langevin recombination and Auger recombination) has been obtained in present discussion. Detail theoretical interpretation on charge transport modeling in OSCs has been discussed in next next section. The Gaussian model is well suited to a wide range of organic semiconducting materials. Undoubtedly it is important to consider all necessary consequences when utilizing Gaussian density of states to obtain fruitful outcomes about the charge conduction into organic layers. The conduction mechanism is highly dependent upon diffusion of carrier concentration, drift mobility, temperature and electric field. Charges would prefer to follow simplest way of conduction. Percolation of carriers holds good performance depending upon the thickness of the organic layer. Such percolation effects are naturally less important for thicker organic samples. The process of injection of carriers has been demonstrated along with the discussion of conduction mechanism in further proceeding SCLC zone. Density of current becomes more uniform with the distance from electrodes. Master equation has been approached well for the discussion of the charge transport focusing the aforementioned Gaussian model.

As a consequence of the theoretical ground, details of trapping states in natural organic dyes have also been taken into consideration to cope up with our experimental works described in next chapters. Trapping of carriers is ubiquitous in all OSCs and is definitely a consequence of Van der Waals interactions among molecules. Detail of nature of different type of traps, different sources of traps and their spatial distributions have been focused which have profound influence OSC based charge transport mechanism and related device performance. Effort has been given to address the outcome of the trapping impact on thin OSC film and interfacial regime. Dynamic disorder generated by thermal agitation at tail states has garnered the attention also in this context. In this chapter, a comprehensive overview regarding the fact of trapping has been provided in a nutshell. Starting with the definition of traps, their different source of production has been discussed along with their classification. Finally, trapping theory based most renowned models have been provided with mentioning their several popular determination and

characterization technique. Significant progress has been encountered since last decade on investigation of trap characterization and that has been discussed in terms of different established trap modeling based proposed theory. But, the effect of trap induced states on charge transport in natural dyes still remains a vexed question. Still there is a gap that has been encountered in searching out the way through which trap impacts on different electrical parameters of optoelectronic devices and its recognition at low voltage regime in natural dye. We have started from this point of view to work on the unified realization of traps in organic diode. Our contribution has been discussed in Chapter III, Chapter IV, Chapter V and Chapter VI.

2.13. References

1. K. C. Kao and W. Hwang, M. Pope and C. E. Swenberg, *Electrical Transport in Solids*, (Pergamon, Oxford, 1981)
2. O. H. Le Blanc, *J. Chem. Phys.* 33, 1960, 626
3. K. G. Kepler, *Phys. Rev.* 199, 1960, 1226
4. M. Pope, H. P. Kallmann, and P. Magnante, *J. Chem. Phys.* 38, 1963, 2042
5. D. M. Pai and B. E. Springett, *Rev. Mod. Phys.* 65, 1993, 163
6. C. K. Chiang, C. R. Fincher, Y. W. Park, A. J. Heeger, H. Shirakawa, E. J. Louis, S. C. Gau, A. G. MacDiarmid, *Phys. Rev. Lett.* 39, 1977, 1098
7. A. J. Epstein and Y. Yang, *MRS Bull.*, 22 1997 6
8. N. W. Ashcroft and N. D. Mermin, *Sol. Stat. Phys.*, 1976
9. S. Baranovski, "Charge transport in Disordered Solids with applications in Electronics", (Wiley online library, 1976)
10. C. W. Tang, *Appl. Phys. Lett.* 48(2), 1986, 183
11. C. W. Tang and S. A. VanSlyke, *Appl. Phys. Lett.* 51, 1987, 913
12. H. Koezuka, A. Tsumura, Y. Ando, *Synth. Mat.*, 18, 1987, 699
13. G. Horowitz et al., *Sol. Comm.* 72, 1989, 381
14. J. H. Burroughes et al., *Nature*, 347, 1990, 539
15. F. Garnier et al, *Adv. Mat.* 2, 1990, 592
16. S. Mansurova et al., *JOSA B*, 17 (12), 2000, 1986
17. M. C. Gather, S. Mansurova, K. Meerholz, *Phys. Rev. B.*, 75, 2007, 165203

18. E. Sliwinska et al., Phys. Rev. B, 2009
19. E. Siliwinska et al., Appl Phys., 2009
20. C. L. Braun, J. Chem. Phys. 80, 1984, 41
21. M. J. Tachiya, Chem. Phys. 89, 1988, 6929
22. L. Onsager, Phys. Rev. 54, 1938, 554
23. P. K. Basu and K. Bhattacharya, J Appl Phys. 59, 1986, 992
24. F. R. Shapiro and D. Adler, J Non-Cryst. Sol. 74, 1985, 189
25. B. L. Shklovskii et al., Adv. Disordered. Semicond. 3 (61), 3161, 90
26. Juska, Arlaukas, K. Stuchlik and J. Osterbacka, J. Nob-Crys. Sol. 352, 2006, 1167
27. C. Deibel, A. Baumann, V. Dyakonov, Appl. Phys. Lett. 93, 2008, 163303
28. T. M. Clarke, F. C. Jemieson, J. R. Durrant, J. Phys. Chem. C. 113, 2009, 20934
29. L. Koster et al., Adv. Mat. 1670, 2011
30. C. Deibel, A. Baumann, V. Dyakonov, Phy. Rev. B. 80, 2009, 075203
31. M. M. Mandoc et al. 91, 2007, 263505
32. H. J. Kim et al. Int J Chem Sc, 8, 2013, 8320
33. M. K. Hossain et al. Result I Phys., 7, 2017, 1516
34. A. Dakhel, F. Z. Henan, Mat Sc and Engg, 178, 2013, 1062
35. M. K. Hossain et al. Mat Sc-Pol., 36(1), 2018, 93
36. Z. Ju, J. Sun, Y. Liu, Molecules 24, 2019, 1
37. A. Bouzidi et al., Opt. Quantum Elect. 50 176
38. Basuki, Suyitno, B. Kristiawan , AIP Con. Proceedings, 1931, 2018, 030067-1
39. A. Kojima et al., J. American Chem. Society, 131, 2009, 6050
40. H. S. Kim et al., Sci. Reports, 2, 2012, 591
41. X. Li et al., Science, 353, 2016, 58
42. D. Vasileska, S. M. Goodnick and Gerhard Klimeck, Computational Electronics:, CRC Press, 20
43. Z. B. Wang et al. Phys. Rev. B 80,2009, 235325
44. Z. B. Wang et al. J. Appl. Phys 107, 2010, 034506
45. B. Ruhstaller et al. J. Appl. Phys 89, 2001, 4575

46. J. J. M. van der Holst et al. Phys. Rev. B 79, 2009, 085203
47. J. C. Blakesley, H. S. Clubb, N. C. Greenham, Phys. Rev. B 81, 2010, 045210
48. W. F. Pasveer et al. Phys. Rev. Lett. 94, 2005, 206601
49. S. L. M. van Mensfoort, R. Coehoorn, Phys. Rev. B 78, 2008, 085207
50. M. A. Lampert, P. Mark, Current Injection in Solids, Academic Press Inc, 1970
51. O. Zmeskal, S. Nespurek, M. Weiter, Sol. Frac. 34, 2007,143
52. P N Murgatroyd, J. Phys D: Appl. Phys 3, 1970, 151
53. J. C. Scott, Vac. Surface Film. 21, 2003, 521
54. J. Scott, G. G. Malliaras, Chem. Phys. Lett. 299, 1999, 115
55. P. R. Emtage, J. J. O'Dwyer, Phys. Rev. Lett. 16, 1966, 356
56. Tessler et al. Adv. Mat. 21, 2009, 2741
57. H. Baessler, phys. Stat. sol. 175, 1993, 15
58. C. Tanase, E. J. Meijer, P. W. M. Blom, D. M. de Leeuw, Phys. Rev. Lett. 91, 2003, 216601
59. A. C. Arias, J. D. MacKenzie, I. McCulloch, J. Rivnay and A. Salleo, Chem. Rev., **110**, 2010, 3
60. N. Gasparini, A. Salleo, I. McCulloch and D. Baran, Nat. Rev. Mater., **4**, 2019, 229
61. H. Sirringhaus, Adv. Mater., **26**, 2014, 1319
62. H. Klauk, Chem. Soc. Rev., **39**, 2010, 2643
63. J. E. Anthony, A. Facchetti, M. Heeney, S. R. Marder and X. Zhan, Adv. Mater., **22**, 2010, 3876
64. M. Kuik, G. J. A. H. Wetzelaer, H. T. Nicolai, N. I. Craciun, D. M. De Leeuw and P. W. M. Blom, Adv. Mater., 26, 2014, 512

65. J. L. Bredas, J. P. Calbert, D. A. da Silva Filho and J. Cornil, Proc. Natl. Acad. Sci. U. S. A., **99**, 2002, 5804
66. V. Coropceanu, J. Cornil, D. A. da Silva Filho, Y. Olivier, R. Silbey and J.-L. Bredas, Chem. Rev., **107**, 2007, 926
67. A. Troisi and G. Orlandi, J. Phys. Chem. A, **110**, 2006, 4065
68. S. Fratini, D. Mayou and S. Ciuchi, Adv. Funct. Mater., **26**, 2016, 2292
69. E. A. Silinsh and V. Capek, Organic Molecular Crystals: Interaction Localization, and Transport Phenomena, AIP Press, New York, 1994
70. A. Troisi, Chem. Soc. Rev., **40**, 2011, 2347
71. C. D. Dimitrakopoulos and P. R. L. Malenfant, Adv. Mater., **14**, 2002, 99
72. N. A. Minder, S. Ono, Z. Chen, A. Facchetti and A. F. Morpurgo, Adv. Mater., **24**, 2012, 503
73. S. Ciuchi, S. Fratini and D. Mayou, Phys. Rev. B: Condens. Matter Mater. Phys., **83**, 2011, 081202
74. G. Horowitz and P. Delannoy, J. Appl. Phys., **70**, 1991, 469
75. G. Horowitz, P. Lang, M. Mottaghi and H. Aubin, Adv. Funct. Mater., **14**, 2004, 1069
76. M. C. J. M. Vissenberg and M. Matters, Phys. Rev. B: Condens. Matter Mater. Phys., **57**, 1998, 12964
77. H. f. Haneef, A. M. Zeidell, O. D. Jurchescu. J. Mat. Chem. C. **8**, 2020, 759
78. E. A. Silinsh, Organic Molecular Crystals: Their electronic states, Springer Berlin Heidelberg, Berlin, Heidelberg, 1980
79. E. A. Silinsh, Phys. Status Solidi, **3**, 1970, 817
80. A. R. Vokel, R. A. Street and D. Knipp, Phys. Rev. B: Condens. Matter Mater. Phys., **66**, 2002, 195336

81. J. Rivnay, R. Noriega, J. E. Northrup, R. J. Kline, M. F. Toney and A. Salleo, *Phys. Rev. B: Condens. Matter Mater. Phys.*, **83**, 2011, 121306
82. J. E. Anthony, C. Warwick, L. Jiang, M. Nikolka, Y. Henri Geerts, H. Sirringhaus, G. Schweicher, A. S. Eggeman, A. Troisi, S. G. Yeates and S. Illig, *Nat. Commun.*, **7**, 201610736
83. T. F. Harrelson, V. Dantanarayana, X. Xie, C. Koshnick, D. Nai, R. Fair, S. A. Nun˜ez, A. K. Thomas, T. L. Murrey, M. A. Hickner, J. K. Grey, J. E. Anthony, E. D. Gomez, A. Troisi, R. Faller and A. J. Moule´, *Mater. Horiz.*, **6**, 2019, 182
84. H. T. Yi, Y. N. Gartstein and V. Podzorov, *Sci. Rep.*, **6**, 2016, 23650
85. J. P. Sleigh, D. P. McMahon and A. Troisi, *Appl. Phys. A: Mater. Sci. Process.*, **95**, 2009, 147
86. A. Troisi and G. Orlandi, *Phys. Rev. Lett.*, **96**, 2006, 086601
87. S. Ciuchi and S. Fratini, *Phys. Rev. B: Condens. Matter Mater. Phys.*, **86**, 2012, 245201
88. C. Krellner, S. Haas, C. Goldmann, K. P. Pernstich, D. J. Gundlach and B. Batlogg, *Phys. Rev. B: Condens. Matter Mater. Phys.*, **75**, 2007, 245115
89. S. Haas, A. F. Stassen, G. Schuck, K. P. Pernstich, D. J. Gundlach, B. Batlogg, U. Berens and H. J. Kirner, *Phys. Rev. B: Condens. Matter Mater. Phys.*, **76**, 2007, 115203
90. H. Jiang and W. Hu, *Angew. Chem., Int. Ed.*, 2019, 2
91. S. D. Baranovskii, *Phys. Status Solidi B*, **251**, 2014, 487
92. A. V. Nenashev, J. O. Oelerich and S. D. Baranovskii, *J. Phys.: Condens. Matter*, **27**, 2015, 093201
93. S. S. Lee, C. S. Kim, E. D. Gomez, B. Purushothaman, M. F. Toney, C. Wang, A. Hexemer, J. E. Anthony and Y.-L. Loo, *Adv. Mater.*, **21**, 2009, 3605
94. O. D. Jurchescu, B. H. Hamadani, H. D. Xiong, S. K. Park, S. Subramanian, N. M. Zimmerman, J. E. Anthony, T. N. Jackson and D. J. Gundlach, *Appl. Phys. Lett.*, **92**, 2008, 132103

95. C. P. L. Rubinger, H. F. Haneef, C. Hewitt, D. Carroll, J. E. Anthony and O. D. Jurchescu, *Org. Electron.*, **68**, 2019, 205
96. A. Rose, *Phys. Rev.*, **97**, 1955, 1538
97. L. G. Kaake, P. F. Barbara and X.-Y. Zhu, *J. Phys. Chem. Lett.*, **1**, 2010, 628
98. E. M. Muller and J. A. Marohn, *Adv. Mater.*, **17**, 2005, 1410
99. M. Jaquith, E. M. Muller and J. A. Marohn, *J. Phys. Chem. B*, **111**, 2007, 7711
100. M. J. Jaquith, J. E. Anthony and J. A. Marohn, *J. Mater. Chem.*, **19**, 2009, 6116
101. K. Puntambekar, J. Dong, G. Haugstad and C. D. Frisbie, *Adv. Funct. Mater.*, **16**, 2006, 879
102. G. Horowitz, M. E. Hajlaoui and R. Hajlaoui, *J. Appl. Phys.*, **87**, 2000, 4456
103. M. Tello, M. Chiesa, C. M. Duffy and H. Sirringhaus, *Adv. Funct. Mater.*, **18**, 2008, 3907
104. D. Abbaszadeh, A. Kunz, N. B. Kotadiya, A. Mondal, D. Andrienko, J. J. Michels, G.-J. A. H. Wetzelaer and P. W. M. Blom, *Chem. Mater.*, **31**, 2019, 6380
105. A. Karki, G. A. H. Wetzelaer, G. N. M. Reddy, V. Na'daz'dy, M. Seifrid, F. Schauer, G. C. Bazan, B. F. Chmelka, P. W. M. Blom and T. Nguyen, *Adv. Funct. Mater.*, **29**, 2019, 1901109
106. K. H. Probst and N. Karl, *Phys. Status Solidi*, **27**, 1975, 499
107. O. D. Jurchescu, J. Baas and T. T. M. Palstra, *Appl. Phys. Lett.*, **84**, 2004, 3061
108. P. K. Nayak, R. Rosenberg, L. Barnea-Nehoshtan and D. Cahen, *Org. Electron.*, **14**, 2013, 966
109. G. Zuo, M. Linares, T. Upreti and M. Kemerink, *Nat. Mater.*, **18**, 2019, 588
110. R. R. Dasari, X. Wang, R. A. Wiscons, H. F. Haneef, A. Ashokan, Y. Zhang, M. S. Fonari, S. Barlow, V. Coropceanu, T. V. Timofeeva, O. D. Jurchescu, J. Bre'das, A. J. Matzger and S. R. Marder, *Adv. Funct. Mater.*, 2019, 1904858

111. H. Sirringhaus, *Adv. Mater.*, **17**, 2005, 2411
112. L. Chua, J. Zaumseil, J. Chang, E. C.-W. Ou, P. K.-H. Ho, H. Sirringhaus and R. H. Friend, *Nature*, **434**, 2005, 194
113. Y. Mei, P. J. Diemer, M. R. Niazi, R. K. Hallani, K. Jarolimek, C. S. Day, C. Risko, J. E. Anthony, A. Amassian and O. D. Jurchescu, *Proc. Natl. Acad. Sci. U. S. A.*, **114**, 2017, 6739
114. A. F. Stassen, R. W. I. De Boer, N. N. Losad and A. F. Morpurgo, *Appl. Phys. Lett.*, **85**, 2004, 3899
115. J. Veres, S. D. Ogier, S. W. Leeming, D. C. Cupertino and S. M. Khaffaf, *Adv. Funct. Mater.*, **13**, 2003, 199
116. C. Liu, Y. Xu and Y. Y. Noh, *Mater. Today*, **18**, 2015, 79
117. J. C. Scott, *J. Vac. Sci. Technol., A*, **21**, 2003, 521
118. H. Baessler and G. Vaubel, *Phys. Rev. Lett.*, **21**, 1968, 615
119. J. A. Merlo and C. D. Frisbie, *J. Phys. Chem. B*, **108**, 2004, 19169
120. C. Pannemann, T. Diekmann and U. Hilleringmann, *J. Mater. Res.*, **19**, 2004, 1999
121. T. Komoda, K. Kita, K. Kyuno and A. Toriumi, *Jpn. J. Appl. Phys., Part 1*, **42**, 2003, 3662
122. M. Nikolka, I. Nasrallah, B. Rose, M. K. Ravva, K. Broch, A. Sadhanala, D. Harkin, J. Charmet, M. Hurhangee, A. Brown, S. Illig, P. Too, J. Jongman, I. McCulloch, J. Bredas and H. Sirringhaus, *Nat. Mater.*, **16**, 2017, 356
123. J. A. Merlo and C. D. Frisbie, *J. Phys. Chem. B*, **108**, 2004, 19169
124. Y. W. Wang, H. L. Cheng, Y. K. Wang, T. H. Hu, J. C. Ho, C. C. Lee, T. F. Lei and C. F. Yeh, *Thin Solid Films*, **467**, 2004, 215
125. J. Northrup and M. Chabinye, *Phys. Rev. B: Condens. Matter Mater. Phys.*, **68**, 2003, 041202

126. L. Tsetseris and S. T. Pantelides, Phys. Rev. B: Condens. Matter Mater. Phys., **75**, 2007, 153202
127. D. Knipp and J. E. Northrup, Adv. Mater., **21**, 2009, 2511
128. P.V. Elyuytin, B. Hickey, G. J. Morgan and G. F. Weir, Phys. Stat. Sol. **124**, 1984, 279
129. A. I. Rudenko, V. I. Arkhipov, Philos. Mag. Part B. **45**, 1982, 177
130. A. V. Nenashev et al., Phys. Rev. B. **81**, 2010
131. A. R. Street, J. E. Northrup and A. Salleo, Phys. Rev. B. **71**, 2005, 1
132. R. Noriega et al., Nat. Mater., **12**, 2013, 1038
133. E. M. Conwell, Phys. Rev. **103**, 2010, 51
134. R. Mercus et al., Angew. Chemie. Int. Ed. English., **32**, **1993**, **1111**
135. M. Pollak, I. A. Riess, J. Phys. C., **9**, 1976, 2339
136. S. D. Baranovskii, Phys. Stat. Sol. **251**, 2014, 487
137. A. Rose, Phys. Rev., **97**, 1955, 1538
138. H. Hatta, Y. Miyagawa, T. Nagase, T. Kobayashi, T. Hamada, S. Murakami, K. Matsukawa and H. Naito, Appl. Sci., **8**, 2018, 1493
139. P. P. Boix, G. Garcia-Belmonte, U. Mun˜ecas, M. Neophytou, C. Waldauf and R. Pacios, Appl. Phys. Lett., **95**, 2009, 233302
140. K. Lee, M. S. Oh, S. J. Mun, K. H. Lee, T. W. Ha, J. H. Kim, S. H. K. Park, C. S. Hwang, B. H. Lee, M. M. Sung and S. Im, Adv. Mater., **22**, 2010, 3260
141. B. C. Hoffman, S. Pazoki, A. Apperson and D. B. Dougherty, Phys. Status Solidi RRL, **13**, 2019, 1800486
142. S. Neugebauer, J. Rauh, C. Deibel and V. Dyakonov, Appl. Phys. Lett., **100**, 2012, 263304

-
143. A. Salleo, *Organic Electronics*, Wiley-VCH Verlag GmbH & Co. KGaA, Weinheim, Germany, 2013, 341
144. W. B. Jackson, N. M. Amer, A. C. Boccard and D. Fournier, *Appl. Opt.*, **20**, 1981, 1333
145. O. Gaudin, R. B. Jackman, T. P. Nguyen and P. Le Rendu, *J. Appl. Phys.*, **90**, 2001, 4196
146. Rizvi. S, Mantri. P, Mazhari. B, (2014) Traps signature in steady state current-voltage characteristics of organic diode, *J. App. Phys.* 115: 244502-1.

Chapter-3

Interpretation of Trap Assisted Conduction with Estimation of Electrical Parameters of Thin Indigo Film Based Semiconducting Device

3.1 Introduction

3.2 Experimental arrangement

3.3 Results and discussions

3.4 Conclusive remarks

3.5 References

3.1. Introduction

In previous chapter, we realized the overview of trap states like its origin, theoretical modeling of trapping states and different trap measurement techniques etc. Trap state is basically the energy state below the state of charge transport energy arises due to spatial disorder which has a significant impact on all herbal organic dye based devices. Moreover, field effected lower mobility with respect to the hole mobility is attributed to the presence of huge amount of trap states in organic semiconductors. Current-Voltage (I-V) relationship is distorted also with the existence of high concentration of trap states [7-8]. So knowledge over trap states and their impact into the active thin film made of organic dye is a matter of concern.

In present chapter, we have measured trap energy (E_c) by analyzing logarithmic I-V plot for natural organic Indigo dye based schottky diode. During conduction, E_c produces high value of series resistance (R_s) at the bulk region of the device. R_s is another influential parameter which directly impacts on device efficiency. The main reason of deviation of I-V plot at high voltage regime is the existence of high value of R_s . We have introduced renowned Cheung-Cheung method to measure the value of R_s along with ideality factor (n) and barrier height (ϕ) [9-11]. Schottky effect in electronic structures and charge conduction process and hence related parameters has also been discussed in the rest of the paper. Natural organic semiconductor Indigo dye may have wide possibility in this regard and that has been reported with quantitative information in present investigation. Effectiveness of the dye in electronic devices compared to other reported dyes has also been mentioned in present work. The work will be fruitful enough for further research over its application on other electronic as well as photovoltaic devices, photo diode, photo collector and other photo sensitive devices also.

3.2. Experimental Arrangement:

The section has been divided into two parts such as (i) material description and (ii) details of experiment.

3.2.1. Material description

Indigo dye is a herbal compound with distinctive blue color combination. Chemical formula for indigo is $C_{16}H_{10}N_2O_2$. Indigo is a natural dye extracted from the leaves of certain plants. A

variety of plants have provided indigo throughout history, but most natural indigo was obtained from those in the genus *Indigofera*, which are native to the tropics. The primary commercial indigo species in Asia was true indigo. This dye is taken into consideration for its significant semiconducting properties, good quantum yield and quite satisfactory spectral response [2, 5]. The dye shows the latest peak of absorption spectra at 268 nm at UV light region whereas characteristic peak can be observed at 612 nm in visible light range [2, 32]. Reported optical bandgap of the dye is 1.689 eV [5]. Fig.3.1 shows the chemical structure of Indigo dye.

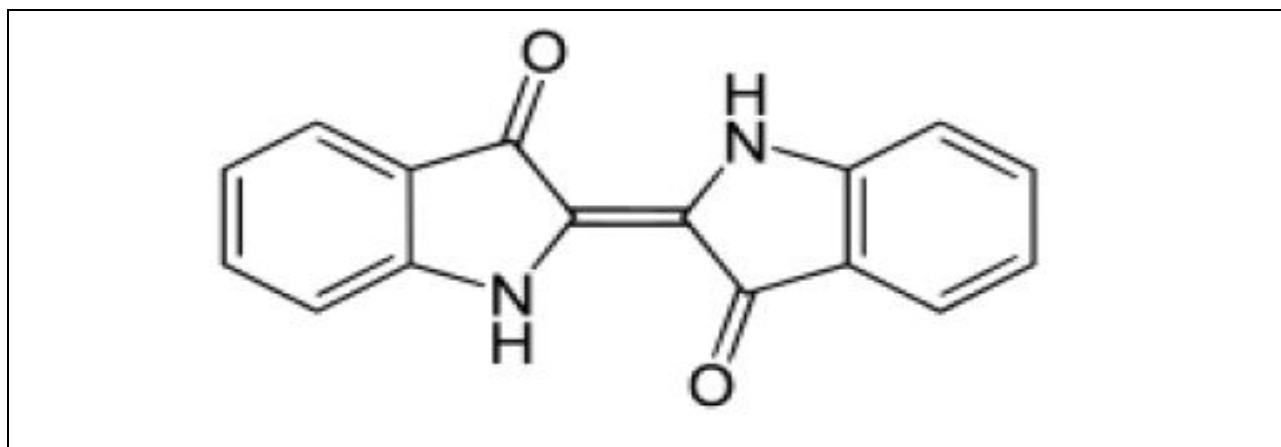


Fig.3.1. chemical structure of Indigo dye

3.2.2. Experimental method

10wt% Indigo solution was prepared from purchased Indigo powder. The mentioned solution was stirred well for 2 hours at room temperature to prepare homogeneous form of solution. Al and Cu electrodes were thoroughly cleaned for 15 minutes by using distilled water in ultrasonic cleaner. The electrodes are then plasma cleaned for 5 minutes after drying. Thermal deposition process was introduced on both substrates at a pressure of 5.5×10^{-5} mbar and rate of deposition was kept 0.1 nm/sec in this process. Thin film of Indigo dye with few μm range of thickness was allowed to be deposited by spin casting process with the angular rotation 2000 rpm in the next stage and hence sandwiched between the substrates. Finally the prepared device is placed at 50°C for one hour to remove the moisture of the evaporated film.

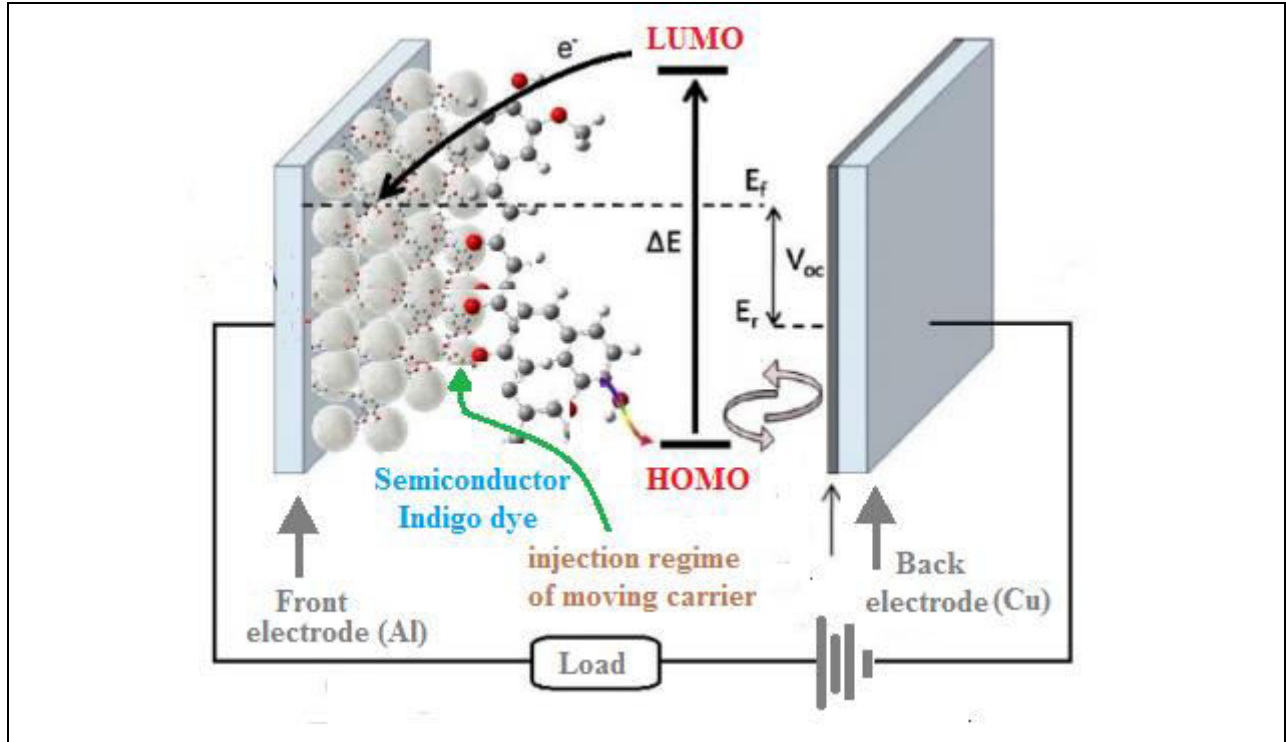


Fig.3.2. Dark current measurement set up where Al and Cu has been used as front and back electrodes respectively whereas the Indigo dye has been selected as active layer sandwiched between the electrodes [6]

3.3. Results and Discussions

To analyze the conduction related properties of Indigo dye based herbal diode of current-voltage (I-V) characteristics has been measured. A non linear behavior of diode has also been observed in the characteristics. This is due to the fact of series resistance R_s which limits the linearity of the plot. So with minimizing the effect of series resistance, greater range of linearity in semilog current-voltage (I-V) plot can be obtained.

The I-V characteristics of organic diode is explained here from the relation [8-10]

$$I = I_0 \exp\left(\frac{q(V-IR_s)}{nKT}\right) \quad (3.1)$$

where IR_s is the drop of voltage across series resistance and I_0 is the saturation current given by

$$I_0 = AA^*T^2 \exp\left(-\frac{q\phi}{kT}\right) \quad (3.2)$$

where q is electronic charge, ϕ is barrier height, A is the device contact area, A^* is the Richardson constant having value $32 \text{ A/cm}^2\text{K}^2$, T is the temperature in K, k is the Boltzmann constant and n is the ideality factor, I_0 is the reverse saturation current. n can be calculated from the linear slope region of the positive bias $\ln I$ - V plot by using eq.(3.3) as follows whereas ϕ can be estimated from eq.(3.4) The typical I-V characteristics have been shown in Fig 3.3.

$$n = \frac{q}{kT} \left(\frac{dV}{d \ln I} \right) \quad (3.3)$$

and

$$\phi = \frac{kT}{q} \ln \left(\frac{AA^*T^2}{I_0} \right) \quad (3.4)$$

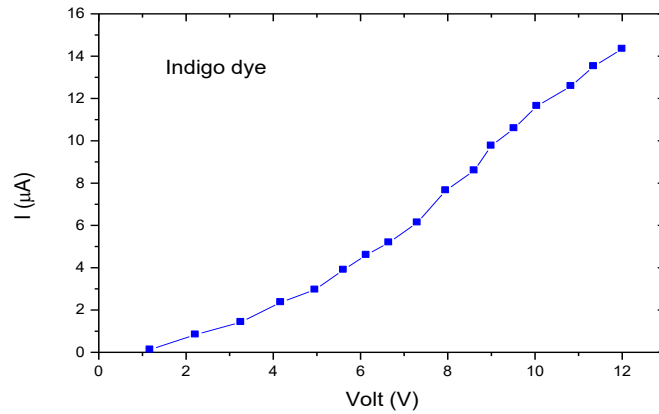


Fig.3.3 I-V Characteristics of Indigo dye based diode

In the present discussion a layer of herbal semiconductor is sandwiched between electrodes having different work function which results a built in voltage (V_{bi}). In the sake of illustration a specific type of carrier is considered to be injected as per choice of electrode workfunctions. Two distinct regions of device operation has been observed specified by voltage V_{bi} . Current shows exponential nature in the region below the value of V_{bi} . The following region is said to be space charge limited in absence of trapping energy which leads to the Mott-Gurney (MG) equation [11, 17]

$$I = \frac{9}{8} A \epsilon \epsilon_0 \theta \mu \frac{V^2}{d^3} \quad (3.5)$$

where V is applied voltage, μ is carrier mobility, ϵ_0 is free space permittivity, θ is trap factor, d is film thickness.

Current above V_{bi} also follows MG law but with a modification as value of V is changed here by an effective voltage V_x where V_x is approximately equal to $(V_{bi}-K)$, where K signifies the factor that implies a transition at a voltage comparatively smaller than built in potential. The modified equation can be described as [11, 18]

$$I = \frac{9}{8} A \epsilon \epsilon_0 \theta \mu \frac{(V-V_x)^2}{d^3} \quad (3.6)$$

Current voltage characteristic exhibits ohmic relation when the value of V is low enough. Carriers are injected into the active region of the device with increasing applied voltage causing enhancement of trapping probability. At higher voltage double logarithmic plot of I-V relation displays $I \propto V^m$, where m shows the increasing value from unity to 2 and then further increment in the value of m can be observed with more increasing value of voltage as well as at the highest region of the characteristic (obtained value of m is 2.87 at this region in this experiment). These interesting result shows the space charge limited current (SCLC) based transport mechanism is dominated by trapped charge limited current (TCLC) with exponential distribution of trap density. When concentration of trap is large enough, distortion in I-V plot becomes significant and distinct regime of current voltage relationship can be determined unambiguously. But it becomes quite difficult to identify the distinct regimes of the plot for low trapping concentration. Since differential technique is very fruitful for the enhancement of small deviations so it can be implemented to reveal the existence of trap states. $G(V)$ - V characteristics has been taken into account for that purpose [11]. Here,

$$G(V) = \frac{d \log(I)}{d \log(V)} \quad (3.7)$$

$G(V)$ actually creates a sharp peak to signify a transition from exponentially rising flow of current to comparatively slower power law dependence above V_{bi} . Peak in the mentioned figure illustrates trap filling states. Hence $G(V)$ vs V plot in Fig.4(a) emphasis on the trap signature allowing relatively easy realization about the nature of traps. A monotonic decrement of function $G(V)$ should be observed in trap free devices but in the aforementioned plot a noticeable amount of distortion exists at different voltage regime which clearly leads to the existence of trapping

states into the device. Trap charge concentration (n_t) can be represented in terms of exponential distribution such as follows [6, 12]

$$n_t(\epsilon) = N_0 \exp \frac{-\epsilon}{kT_c} \quad (3.8)$$

where ϵ represents to the depth of traps below conduction band mobility edge and T_c is trap energy of exponential distribution

where
$$T_c = E_c/k \quad (3.9)$$

here E_c is characteristic trap energy and $E_c = mkT$. The value of trap energy can be estimated from logarithmic current voltage relation is plotted in Fig. 3.4(b).

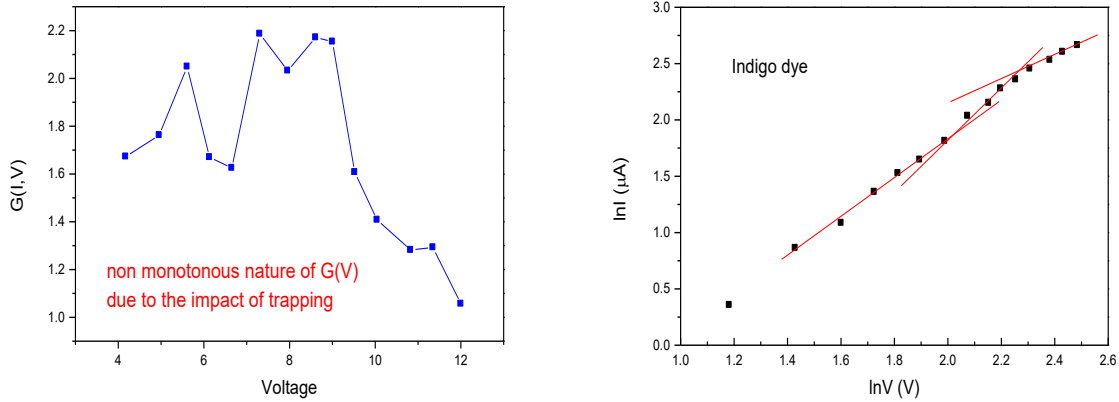


Fig.3.4(a) $G(V)$ - V plot of Indigo dye based diode. Multiple distortions in the figure explain the presence of multiple discrete traps. The first in the plot is quite suppressed and is generated due to V_{bi} . Remaining peaks arise from other deeper traps; Fig. 3.4(b) $\log I$ - $\log V$ plot for Indigo dye based device used to calculate trap energy

Traps play an important role in carrier conduction process in the bulk region of charge transport of such devices. Majority of generated charges suffer with immobilization of their motion due to the existence of traps [12, 30]. These trapping states arises an internal resistive property of organic substances. So it obvious that the movement of free carriers of these devices struggles by high series resistive influence for the presence of trapping states in the active regime [13, 31]. Series resistance is such a parameter which impacts directly on device efficiency and other electrical properties [14, 38]. Series resistance, ideality factor and barrier height can also be

calculated by using well known Cheung-Cheung method and its corresponding equations are given here as follows [14-16]

$$\frac{dV}{d \ln I} = \frac{nkT}{q} + IR_s \quad (3.10)$$

$$H(I) = V - \frac{nkT}{q} \ln \left(\frac{I}{AA^*T^2} \right) \quad (3.11)$$

and

$$H(I) = IR_s + n\phi \quad (3.12)$$

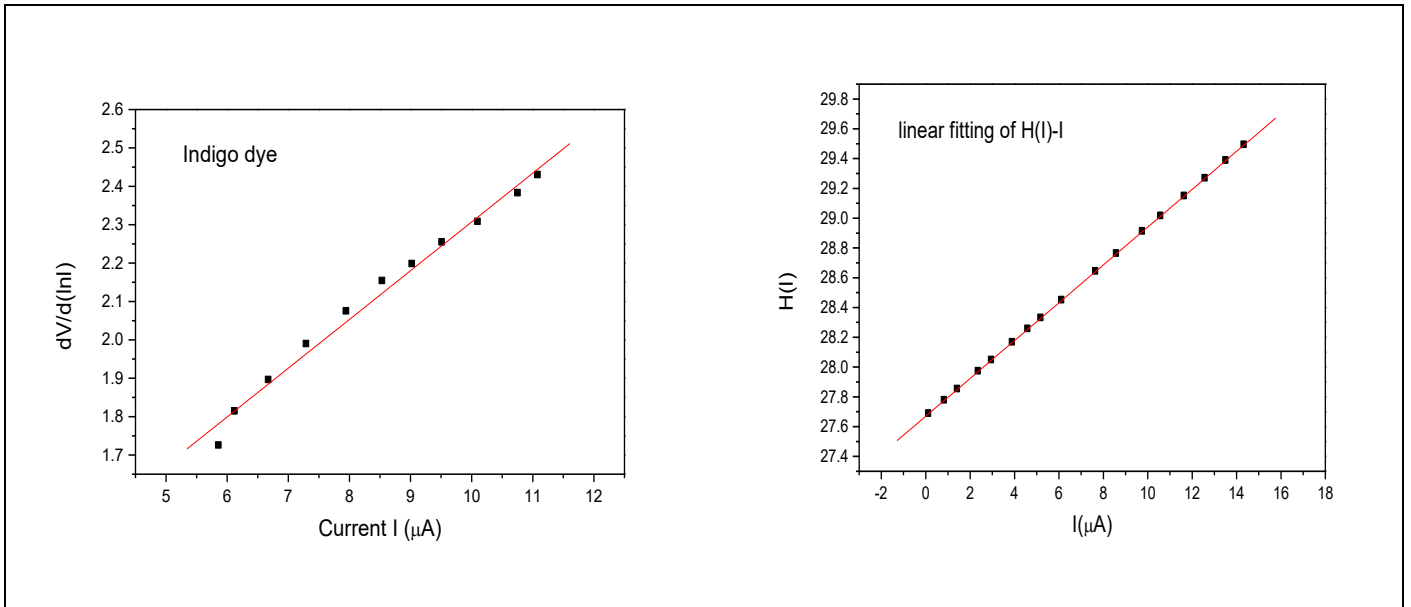


Fig.3.5 (a) $(dV/d \ln I)$ - I plot and (b) $H(I)$ - I plot of Indigo dye based diode

$(dV/d \ln I)$ - I plot has been expressed at high voltage regime of the I - V relation given in Fig.5.5. Value of R_s is estimated from the linear region of the following plot, while n can be extracted from interception with Y axis. R_s is also obtained from the $H(I)$ - I plot [14,20]. $H(I)$ - I plot shows linearity with intercept at the Y axis which is equal to $(n\phi)$. The slope of this plot is basically used for the verification of the accuracy of Cheung function. The results show good agreement with each other. Obtained result containing the value of n expresses the comparison of fabricated diode to the ideal one. Generally the value of ideality factor of organic herbal dye based diode is much greater than unity. High value of ideality factor may be due to different interfacial states or

layer of semiconductor of metal electrode surface and high value of series resistance. Incorporation of amorphous disordered natural organic material between two metal electrodes results high value of R_s . Interaction between conductor-semiconductor interface realign the LUMO-HOMO levels of organic natural semiconductor and work function of metal which changes electron affinity and further results the increment of barrier height (LUMO and HOMO stands for lowest unoccupied molecular orbital and highest occupied molecular orbital respectively) [19, 32-37]. Like other organic devices, the value of R_s is quite high also in this device due to trap prone charge conduction, disordered organic structure and interfacial disorder [14, 36-38]. Value of E_c , R_s , n and ϕ are given in Table 3.1.

Table 3.1.
Estimated electrical parameters for indigo dye based natural organic device

Estimated Parameters	Obtained Values
Trap energy (in eV) (E_c)	0.073
Series resistance (in $k\Omega$) (R_s)	127
Ideality factor (n)	39.87
Barrier height (in eV) (ϕ)	0.87

The electrical parameters show promising results comparatively than other reported organic dyes estimated in the work of Chakraborty et al [12, 21] given in table.3.2. Significant reduction in E_c , R_s and ϕ has been obtained in application of the herbal organic indigo dye over previously reported organic dyes. So the dye under present experiment may have wide possibilities to fabricate organic solar cell, photodiode, OLED etc [22-24, 39].

Table 3.2.

Estimated reduction percentage (%) of electrical parameters obtained in indigo dye based herbal device over other reported organic dye based devices

Electrical parameters	Estimated reduction percentage (%) over Rose Bengal dye	Estimated reduction percentage (%) over Methyl Red dye
Amount of reduction in E_c	16.09	3.95
Amount of reduction in R_s	46.86	72.51
Amount of reduction in ϕ	8.42	12.12

However, its charge transport mechanism can further be predicted with interpretation of semi logarithmic current plotted against square root of voltage before its further application. The current is segmented in two linear distinct regions [25]. Following straight line regions for low and high current region indicate the existence of either Recharadson-Schottky or Pooley-Frankel effect induced carrier flow shown in fig 3.6 [15, 26-27].

The I-V expressions for both the mechanisms are given as follows [28]

$$I = AA^*T^2 \exp\left(\frac{-\phi_b}{kT}\right) \exp\left(\frac{\beta_{RS}V\sqrt{2}}{kTd\sqrt{2}}\right) \quad (3.13)$$

for Schottky effect and

$$I = I_0 \exp\left(\frac{\beta_{PF}V\sqrt{2}}{kTd\sqrt{2}}\right) \quad (3.14)$$

for Poole-Frankel effect.

In the eq.(3.13) and eq.(3.14), ϕ_b represents Schottky barrier height, I_0 means field lowering current, β_{RS} and β_{PF} are Recharadson-Schottky and Poole-Frankel field lowering coefficients respectively. Theoretical value of β_{RS} and β_{PF} can be estimated from the following equation [29]

$$2\beta_{RS} = \beta_{PF} = \left(\frac{q^3}{\pi\epsilon_0\epsilon_r}\right)^{\frac{1}{2}} \quad (3.15)$$

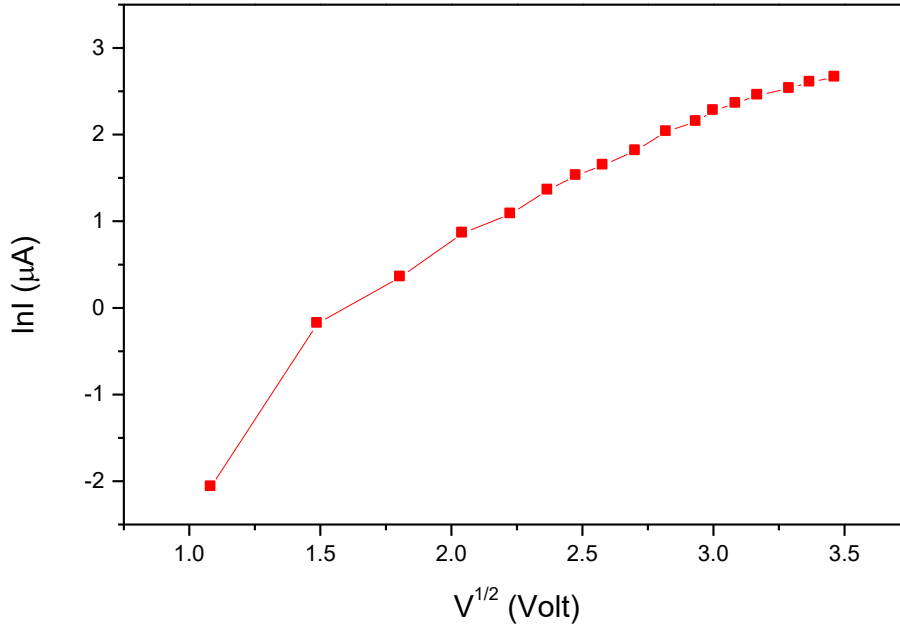


Fig.3.6. $\ln I$ vs $V^{1/2}$ plot for Indigo dye based diode

Theoretically obtained values from eq.(3.15) of β_{RS} and β_{PF} are $2.64 \times 10^{-5} \text{ eVm}^{1/2}\text{V}^{-1/2}$ and $5.28 \times 10^{-5} \text{ eVm}^{1/2}\text{V}^{-1/2}$ where ϵ_r of indigo is considered 7.83. Values of β are further estimated from the slopes at low and high voltage regimes. In this way, experimentally calculated values of β are $\beta_{low} = 1.71 \times 10^{-5} \text{ eVm}^{1/2}\text{V}^{-1/2}$ and $\beta_{high} = 0.96 \times 10^{-5} \text{ eVm}^{1/2}\text{V}^{-1/2}$. It is clearly observed that the experimentally obtained value of β_{high} is 0.36 times of β_{RS} and 0.18 times of β_{PF} . β obtained experimentally at high voltage zone is comparatively close to the theoretical value determined for Recharadson-Schottky effect which leads to bulk limited carrier conduction process [15,29]. In such process, current flow is determined as minority carrier diffusion whereas

production of current is due to flow of majority carriers over extracted potential barrier which usually exists in Schottky barrier diode.

3.4. Conclusive remarks

Fabrication and characterization of Al/Indigo/Cu organic diode has been encountered. Values of R_s , n and ϕ has been estimated from Cheung function and hence verified by H(I)-I plot. Outcome of the estimation shows good agreement together. Obtained results have been compared with other reported organic semiconductor based RB and MR dye. 46.86% and 72.51% improvement has been encountered for R_s whereas ϕ shows 8.12% and 12.12% improvement respectively than RB and MR. Existence of trapping effect of experimental dye has been explained from G(V)-V plot. Considerable amount of trapping defect has been found in the experiment which leads to non ideal conduction procedure as well as hopping mechanism from one to another localized state. Estimated value of E_c is 0.073 eV which shows 16.09% and 3.95% improvement than RB and MR dye. Result shows wide possibilities to introduce it in optoelectronic devices. Bulk limited charge conduction assisted Richardson-Schottky effect has also been examined for the device by using semilog current-voltage plot.

3.5. References

1. Brabec C J, Sariciftci N S, Hummelen J C, 2001 Adv. Funct. Mater. 11 15
2. Ju Z, Sun J, Liu Y, 2019 *Molecules* 24 1
3. Yu G, Heeger A J. 1995 J Appl Phys. 78 4510
4. Feron K, Belcher W, Fel C J, Dastoo P C. 2012. Int J Mol Sci. 13 17019
5. Bouzidi A, Yahia I S, Zilani W, El-Bashir M, Alfaify S, Algarni H, Guermazi H, 2018 Opt. Quantum Elect. 50 176
6. Chakraborty K, Das. A, Mandal. R, Mandal D K, 2020 Trans. Tianjin Univ. 26 265
7. Cui J, Wang A, Edleman N L, Ni J, Lee P, Adv. Mater. 13 1476
8. Petraki F and Kennou S 2009 Org. Electron. 10 1382–7

9. Wan A S, Makinen A J, Lane P A and Kushto G P 2007 Chem. Phys. Lett. 446 317
10. Shah M, Sayyad M H, Karimov Kh S and Tahir M M 2010 Physica B 405 1188
11. Rizvi S M H, Mantri P, Mazhari B, 2014 J. Appl Phys. 115 244502
12. Chakraborty S, Manik N B, 2016 Physica B. 481 209
13. Chakraborty K, Das A K, Mandal D K, Mondal R 2019 IJIKC 7 170
14. Cheung S K, Cheung N W. 1986 Appl Phys Lett 49 85
15. Shah M, Sayyad M H, Karimov Kh S 2010 J Phys D. 43 405104
16. Yakuphanoglu F 2010 Synthetic Metals. 160 1551
17. Mott N F and Gurney R W (International Series of Monographs on Physics), second edition, 1948. Electronics Process in Ionic Crystals (Oxford University Press, London, U.K)
18. Rizvi S M H, Mazhari B 2018 IEEE Trans Elect Dev. 99 1

19. Yang J, Jun shen J 1999. J.Appl.Phys. 85(5) 192699.

20. Shah M, Karimov K S, Ahmad Z 2018 Chin Phys Lett 27 106102

21. Chakraborty K, Chakraborty S, Manik N B, 2018 J Semiconduct. 39 094001-1
22. Mark P, Helfrich W, 1962 J. Appl. Phys., 33-1 205
23. Das A K, Mondal R, Chakraborty K, Mandal D K 2019. IJIKC. 7 178
24. Chakraborty K, Malakar S, Mandal D K, Mondal R, Maiti A K 2019 Int J Adv. Sci Eng. 6 42
25. Baranovskii S D, Cordes H, Hensel F, and Leising G 2000 Phys Rev. B, Condens. Matter, 62 793
26. Sathyamoorthy R, Senthilarasu S, Lalitha S, Subbarayan A, Natarajan K and Mathew X 2004 Sol. Energy Mater. Sol. Cells 82 169–77
27. Gao W and Khan A 2002 Org. Electron. 3 53
28. Riad A S 1999 Physica B 270 148
29. Aydin S, Yildiz D, Cavus H K, Sahigoj R, 2014 Bul. Mat Sc. 37 1563
30. Kawano K, Sakai J, Yahiro M, Adachi C. 2009 Sol.Energy Mater.Sol.Cells 93 514

31. Benanti T, Venkataraman D. 2006 Photosynth. Res. 87 73

-
32. Basuki, Suyitno, Kristiawan. B, 2018 AIP Con. Proceedings, 1931 030067-1
 33. Zhu L, Zhou J, Guo Z, Sun Z, 2015 J. Materiomics, 1 285
 34. Oehzelt M, Koch N, Heimel G, 2014 Nat. Comm. 5 4174
 35. Bruyn P, Rest A H P, Wetzelaer G A H, Leeuw D M, Blom P W M, 2013 Phys. Rev. Lett. 111 186801-1
 36. Shang J et al., 2014 Adv. Func. Mater. 24 2171-9
 37. Hu C, McDaniel M, Posadas A, Demkov A, Ekerdt J G, Yu E T, 2014 Nano Lett. 14 4360-7
 38. Lien C D, So F C T, Nicolet M A, 1984 IEEE Elect. Dev. 31 (10) 1502
 39. Haldar A, Maity S, Manik N B, 2008 Ionics 14 427

Chapter-4

Investigation on Trapping Signature in Organic Semiconductor Turmeric Film Introducing Different Current-Voltage Analysis

4.1 Introduction

4.2 Materials and experiments

4.3 Results and discussions

4.4 Conclusive remarks

4.5 References

4.1. Introduction

In earlier Chapter-III, we have reported the characterization and measurement of electrical parameters of Indigo dye based Schottky contact and hence explained the trap assisted charge conduction into the device.

In present study, experiments has been worked out to investigate the signature of traps and its effect on other charge transition related electronic parameters of natural organic Turmeric film. There are different methods what can be executed to obtain the signature of traps but steady state analysis of I-V characteristics is attractive enough here regarding this issue. As mentioned in earlier chapter, I-V plot distorts in presence of high trapping concentration [9]. But when trapping concentration is small enough, their impact can't be determined prominently and naturally it becomes quite difficult to obtain the imperfection due to traps from the shape of the characteristics. So development of more concise measurement over the existing idea needs to be executed to better understand the fact. Presence of small trapping density can be encountered with the implementation differential technique [10]. The following technique is utilized to detect the precise change occurred by distortion in current relative to voltage due to trap filling conditions. Value of E_t has been estimated from $\log I$ - $\log V$ plot [11]. It has been found that value of E_t is much lower for natural turmeric dye based organic semiconductors than many other reported organic semiconducting dyes. Lower value of E_t has effective contribution to the reduction of barrier height and hence comparatively smoother charge conduction [12]. Evaluation of present study on the dye may indicate wide possibilities in device fabrication and further different optoelectronic application.

4.2. Materials and Experiments

Turmeric is natural compound with bright yellow color belongs to the botanical Curcuminoid group. The chemical compounds of the dye extracted from *Curcuma Longa* consist mainly of diarylheptanoid and natural phenol. Chemical formula of Turmeric is $C_{21}H_{20}O_6$ [13]. The dye shows promising semiconducting properties besides several medical applications. Recently, the dye under consideration is utilized as natural semiconductor in organic photovoltaic devices [14-

16]. It has excellent UV absorption property [14-15]. Estimated Optical band gap of turmeric dye solution is 2.85 eV [16]. Structure of the chemical configuration of the dye has been shown in Fig.4.1.

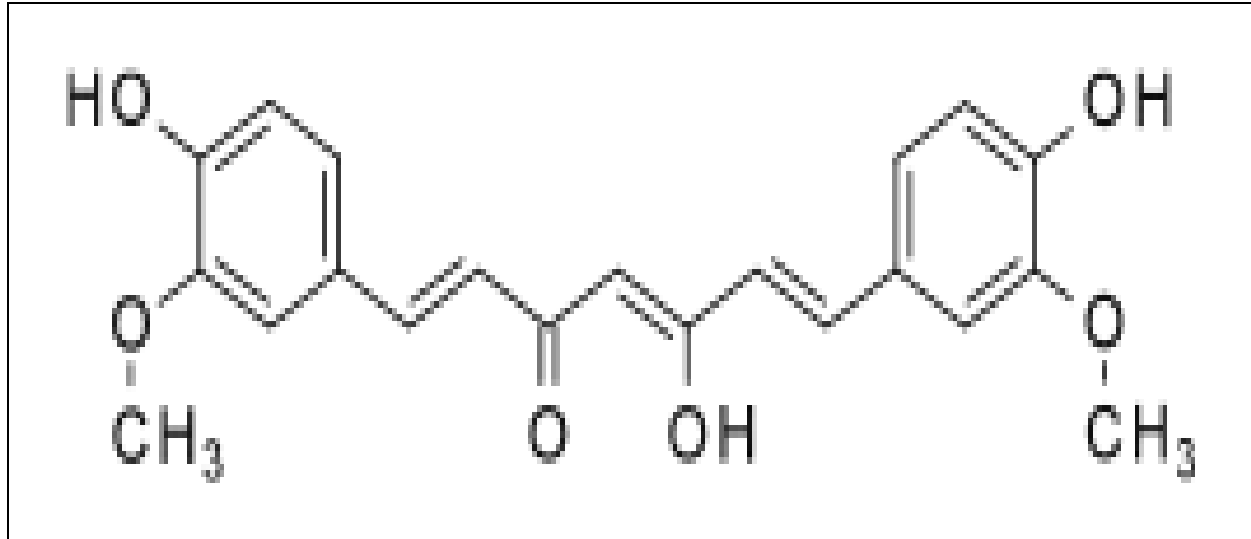


Fig.4.1 Chemical structure of Turmeric dye

10g Turmeric powder formed from pure natural turmeric root is mixed properly in 100 ml of ethanol solution at 60° c for 3 hours to prepare a dye solution. The mixture is then left to stir with a magnetic stirrer for next half an hour to have the homogeneity of the solution. The Al and Cu substrates are then cleaned well for 15 minutes in distilled water by ultrasonic cleaner and hence left to dry. The substrates are then etched with HF: H₂O (in ratio 1:10) to remove native oxide from those substrates. Film of prepared solution is then allowed to coat on the substrates with the help of spin coater with 1000 rpm angular rotation at normal temperature. Pressure remains at 5.5×10^{-5} mbar during the time of film deposition with a few μm thickness ranges. The device is then fabricated and kept at a temperature 50° c for at least one hour. Hence the device is finally ready for experiment.

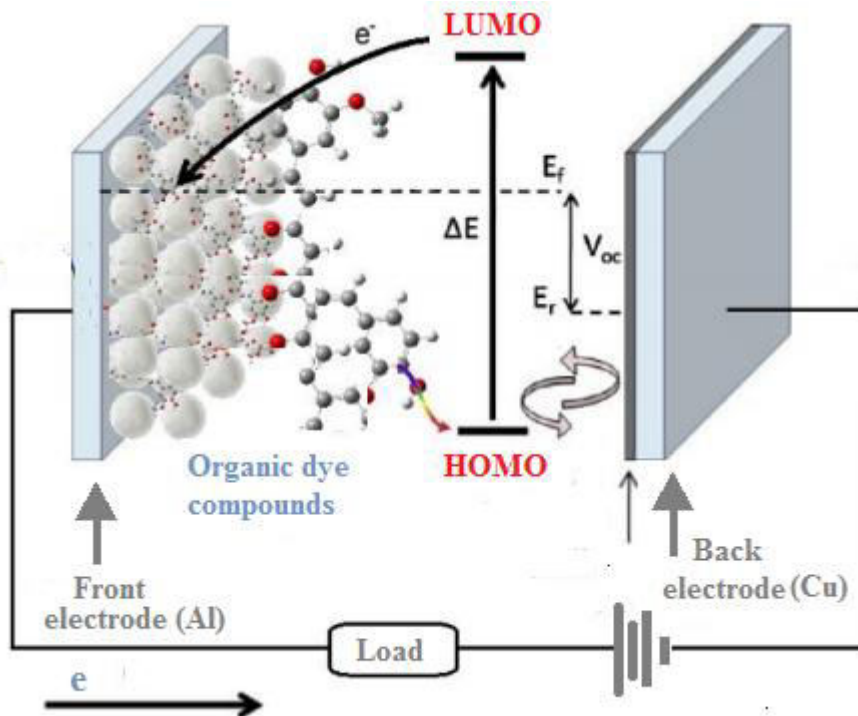


Fig.4.2 Schematic current-voltage measurement set up where Al and Cu are selected to utilize as front and back electrodes respectively. Thin film Turmeric dye is used as active semiconducting layer deposited between the mentioned electrodes

4.3. Results and Discussions

Geometry of natural organic device may be used to have a better insight about traps. A sandwich configuration has been taken into account where a natural semiconducting layer has been incorporated between the electrodes having different work function. In ideal condition, both electrodes form good interfacial contact along with the sandwiched semiconducting material which results zero built in potential (V_{bi}). A trap free conduction always follows the space charge limited current (SCLC) behavior with quadratic current voltage relation in such kind of devices [17]. But the charge conduction process becomes relatively complex in presence of trapping states in organic semiconductors [18]. Such conduction process has been demonstrated by different mechanisms like hopping transport based disordered model [19], MTR (multiple trap release) model [20] and even both of their combination generates another explanation [21]. All of the mechanisms clearly generalize that trap assisted charge conduction leads to the quadratic

dependence of current on voltage. In present illustration we introduce V_x -V plot and differential current voltage relationship to analyze the trap signature explaining the distortion in I-V characteristics [10, 22-23]. The following characteristics of the device contain several regimes at different power law exponent m . SCLC in the device follows quadratic behavior beyond V_{bi} maintaining the relationship $I \propto (V - V_{bi})^2$ [24-25]. Trap filling conduction state can be expected to follow on progress of further certain voltage. The different conduction mechanism is circumvented by considering I-V plot follows a specific power law beyond threshold voltage V_{th} [22]

$$I \propto (V - V_{th})^m \quad (4.1)$$

Derivative of the function w.r.t voltage gives

$$\frac{dI}{dV} \propto m(V - V_{th})^{(m-1)} \quad (4.2)$$

To correctly classify the different power law regimes of we introduce the differential function where $\frac{dI}{dV}$ expresses the incremental conductance and V_x can be termed as

$$V_x = \frac{V - V_{th}}{m} \quad (4.3)$$

Comparative analysis of V_x -V characteristic and differential G(V)-V plot indicates the difference of interpretations provided by the mentioned techniques. The proposal of the first approach classifies the whole characteristics to be divided into three regimes as illustrated in Fig.4.3.

Flat portion of V_x in zone-I is the part of characteristic having exponential nature that is observed below the range of V_{bi} . In this region linearity can be observed due to the shunt leakage network and very small amount of charge injection [24]. A dramatic change of ohmic region towards exponential zone has been encountered in the transition of area of threshold voltage. The transition is related to the voltage drop across injecting front electrode and trap assisted conduction. Current in this region faces distortion due to the presence of trapping states and high value of m can also be encountered in this region which is very indicative about signature of traps. Traps in this zone are filled partially and trap density varies accordingly with change of voltage and consequently leads to a close quadratic dependence of carrier conduction relative to the applied voltage. With further progress of applied voltage, most of active traps are getting

filled which leads to a comparatively flatter slope in region III [22]. Relative high power exponent can be observed there when applied voltage exceeds trapped filled limit of voltage. All the regimes in the experiment has been encountered sharply in the abovementioned characteristic which indicates the trapping distribution in different segments of conduction. For a trap free device, the plot should be straight line with a slight non-linearity at the beginning zone below the threshold voltage regime as the value of m remain constant everywhere because of the proportional I-V relationship and that has been drawn by red line in the following figure.

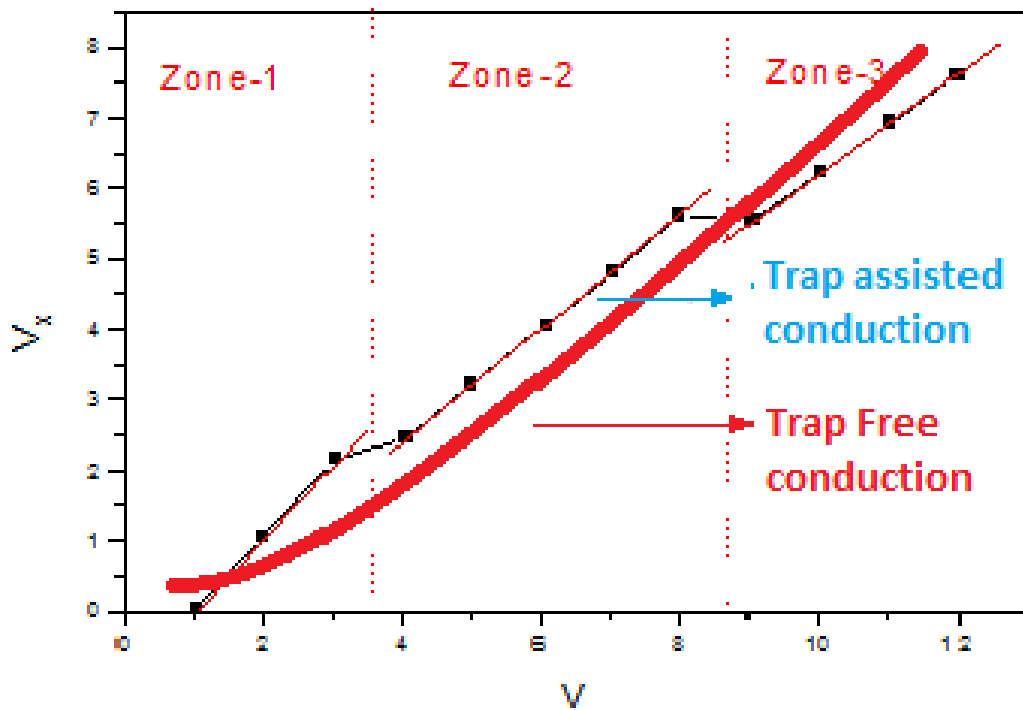


Fig.4.3 V_x - V Characteristics of Al/Turmeric/Cu device where trap assisted charge conduction with distinct nature at different regime has been shown with clear signature of trapping distribution is shown with comparison to ideal trap free conduction for better realization

A differential $G(V)$ - V plot can also be introduced for the verification of trap signature into the conduction process of the device also. In sake of this illustration we consider current in V_{bi} regime is expected to have space charge limited conduction with obvious exponential type in absence of traps following MG (Mott-Gurney) relation [26-27,34]

$$I = \frac{9}{8} A \epsilon \epsilon_0 \theta \mu \frac{V^2}{d^3} \quad (4.4)$$

Above the transition region of built in potential, current maintains modified MG law with an effective voltage $V_x = (V_{bi} - K)$, where K means transition voltage factor relatively smaller value than V_{bi} . MG law with further modification expressed such as follows [10,28]

$$I = \frac{9}{8} A \epsilon \epsilon_0 \theta \mu \frac{(V - V_x)^2}{d^3} \quad (4.5)$$

where V is potential difference across the two terminal of the device, μ is dynamic charge mobility, ϵ_0 signifies permittivity of free space, θ is trap factor, d is film thickness.

Outcome of the I-V plot indicates SCLC conduction is dominated by TCLC (trapped charge limited current) with distribution of exponential trapping states. Distortion in the following plot can clearly be observed with the orientation of large trapping concentration and unambiguously distortion affected distinct regions can be observed. But problem arises about their identification when the concentration of trap density is very low. As mentioned earlier, differential technique is very efficient to determine the small deviation introducing its enlargement in the plot that it can reveal the trapping states clearly during conduction of charges. Hence, in Fig.4.4, $G(V)$ - V plot is used regarding this purpose where [29]

$$G(V) = \frac{d \log(I)}{d \log(V)} \quad (4.6)$$

Differential analysis leads to the formation of sharp peak to elaborate the switching from exponential nature of charge conduction towards relative slower law of power dependence regime above built in potential. Peak in the characteristics signifies the filling of traps. From this approach it is needless to mention that the plot under consideration is very indicative about the presence of trapping states with easy understanding of nature of its distribution. Monotonic decrement of differential parameter relative to applied voltage should be seen for trap free conditions but noticeable distortion of $G(V)$ with non-monotonous shape appears at distinct voltage region [10,29] which concludes the distribution of trapping during conduction into the device and the plot has been shown in Fig.4.4.

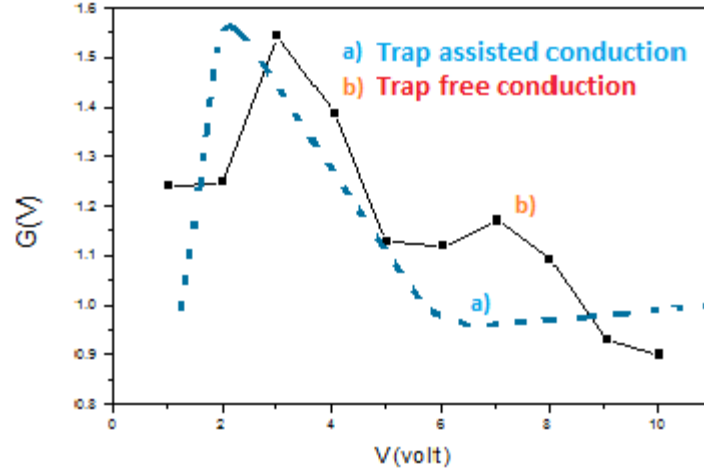


Fig.4.4 G(V)-V characteristics of Al/Turmeric/Cu based device. Multiple distortions in such figure represent multiple discrete traps, first of which is quite suppressed and is generated due to V_{bi} . Remaining peaks arise due to the existence of other deeper traps

Trap influenced charge conduction at different voltage region can be explained by energy band diagram. Starting from quasi equilibrium state in Fig.4.5(a), the current generally exhibits ohmic behavior at low applied voltage region. Amount of carrier concentration is increased with injection of more carriers with increasing voltage. I-V relationship in this state is explained by modified MG law in eq.(4.6). Trap factor θ in that expression is termed as [30-31]

$$\theta = \frac{P_f}{P_f + P_t} \quad (4.7)$$

As outcome of the increasing carrier density the fermi level moves closer to the valence band or HOMO (highest occupied molecular orbital) as shown in Fig.4.5(b). Fermi level E_F exists considerably above the level of trap E_{TD} . θ , termed as free carrier (P_f) to the total carrier ($P_f + P_t$) ratio, is independent at low voltage but acquires a minimum value expressed by the following equation [22]

$$\theta_{min} = \frac{1}{1 + \frac{N_{TD}}{N_V} \exp\left(\frac{-E_{TD}}{kT}\right)} \quad (4.8)$$

where N_{TD} is density of traps and N_V is effective density of states of HOMO. The curve of E_F is getting sufficiently close to E_{TD} with increasing voltage as shown in Fig.4.5(c). Value of θ starts to vary eventually with further enhancement of voltage that result strong dependence

comparatively than quadratic dependence is observed. All the trap states fill and consequently E_F goes below to the level of E_{TD} [see Fig.4.5(d)]. θ becomes close to unity in this region. θ can be approximated from logrhythmic current-voltage characteristics.

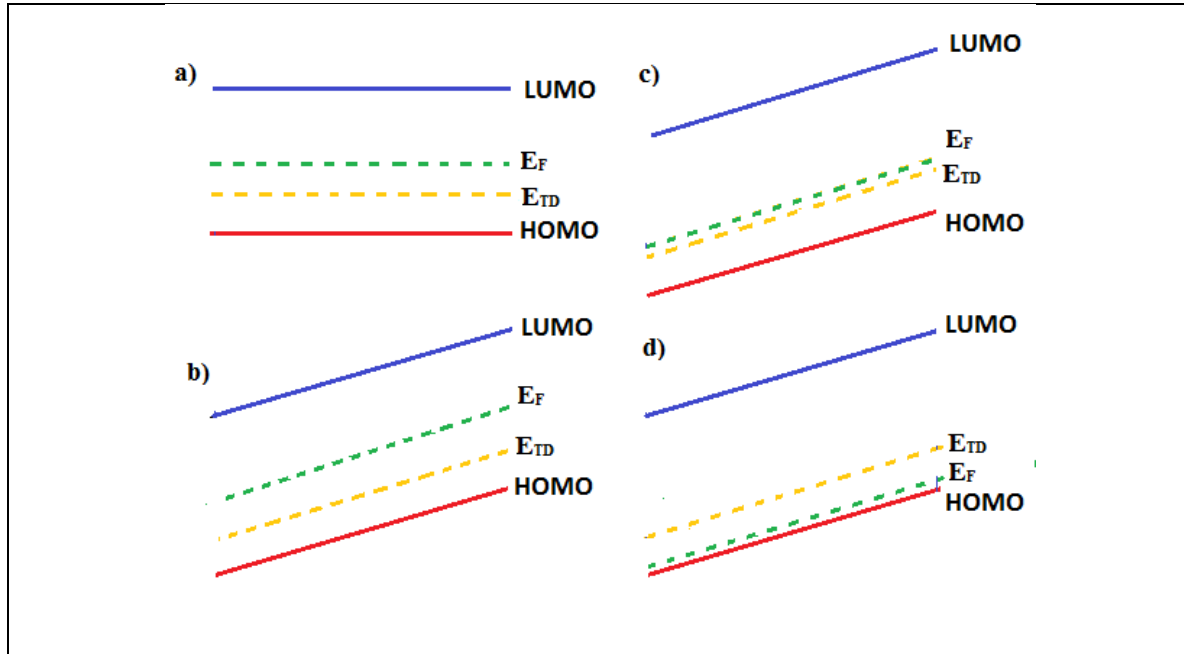


Fig.4.5 Energy band diagram at different states at different voltage limit. a) Quasi equilibrium, b) $E_F < E_{TD}$, c) $E_F \approx E_{TD}$, d) $E_F > E_{TD}$

After having good realization about trap signature, it is quite important to have a better insight about the influence of trapping. Amorphous disordered orientation of carrier state of distribution accelerates the possibility of trapping due to what organic dye based such device is prone to traps. Traps are distributed randomly at the energy states located between LUMO and HOMO. Traps carry a very crucial role when conduction occurs [10,12]. The concerned parameter impacts on the fluent flow of carriers during conduction and is also the reason of high value of series resistance and barrier height at the bulk transport of the device. Traps can be distributed as discrete as well as following Gaussian distribution or exponential distribution. The parameter has been considered to explain in the aforementioned form of distribution in present study.

Exponential trap distribution along with concentration of trapping (N_t) can be expressed as [10, 32]

$$N_t(\epsilon) = N_0 \exp\left(-\frac{\Omega}{kT_c}\right) \quad (4.9)$$

Where t is trap function, Ω means trap depth below the edge of conduction band mobility and k means Boltzman constant and T_c is characteristic energy of the following distribution function and is represented as [33]

$$T_c = \frac{E_t}{k} \quad (4.10)$$

and

$$E_t = mkT \quad (4.11)$$

Here, E_t represents trap energy and the following parameter can be determined from the slope of $\ln I$ - $\ln V$ plot.

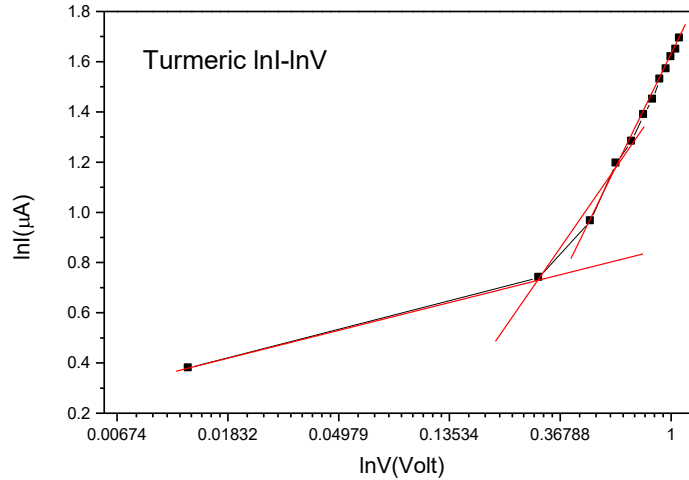


Fig.4.6 $\ln I$ - $\ln V$ plot of Al/Turmeric/Cu based device

SCLC conduction in organic semiconductors is very interesting for its renewed optoelectronic application. Conduction in such intrinsic semiconductor is limited due to the formation of space charge [1]. Using MG law in eq. (4.5), dependence of drift current on applied voltage has been

shown for organic semiconductors. But diffusion current contribution in the following law has been neglected because its influence is restricted at very low voltages only. Solution of drift and diffusion current combination has not found for SCLC conduction in absence of trapping states even in an ideal device. However, contribution of diffusion current density in organic diode can be explained by the following equation [28, 34-35]

$$J_{diff} = \frac{q\mu N_v(\phi_{bi}-B-V)[\exp(\frac{qV}{kT})-1]}{L[\exp(\frac{q\phi_{bi}}{kT})-\exp(\frac{q(V+B)}{kT})]} \quad (4.12)$$

Where ϕ_{bi} is the interfacial barrier height and B denotes band bending parameter follows the expression

$$B = \frac{kT}{q} [\ln\left(\frac{q^2 N_v L^2}{2kT\epsilon}\right) - 2] \quad (4.13)$$

L is the distance between the electrodes. Band bending takes place by accumulation of carriers at region of ohmic injection contact. V_{bi} appears from difference of Fermi level to the contact and is expressed with a relation between V_{bi} and ϕ_{bi} given by, $B = (\phi_{bi} - V_{bi})$. As mentioned earlier, trap has some definite impact on the barrier height. High value of barrier height (ϕ_{bi}) often can be observed at metal-semiconductor interface due to the presence of trapping in organic semiconductors. In almost all organic film based devices, presence of localized trap states distributed between the gap of LUMO (lowest unoccupied molecular orbital) and HOMO (highest unoccupied molecular orbital) impacts on the performance of charge conduction. Recombination of carriers at the trap centre results the degradation of free charge concentration and reduction of mobility of charge carriers. The injection of charges at this interfacial contact region has a good contribution on other electrical properties. Interfacial potential barrier is the reason of the difference of energy of Fermi level to the organic layer energy band. The aforesaid parameter signifies the one of the most important properties that impacts upon threshold voltage and leakage current.

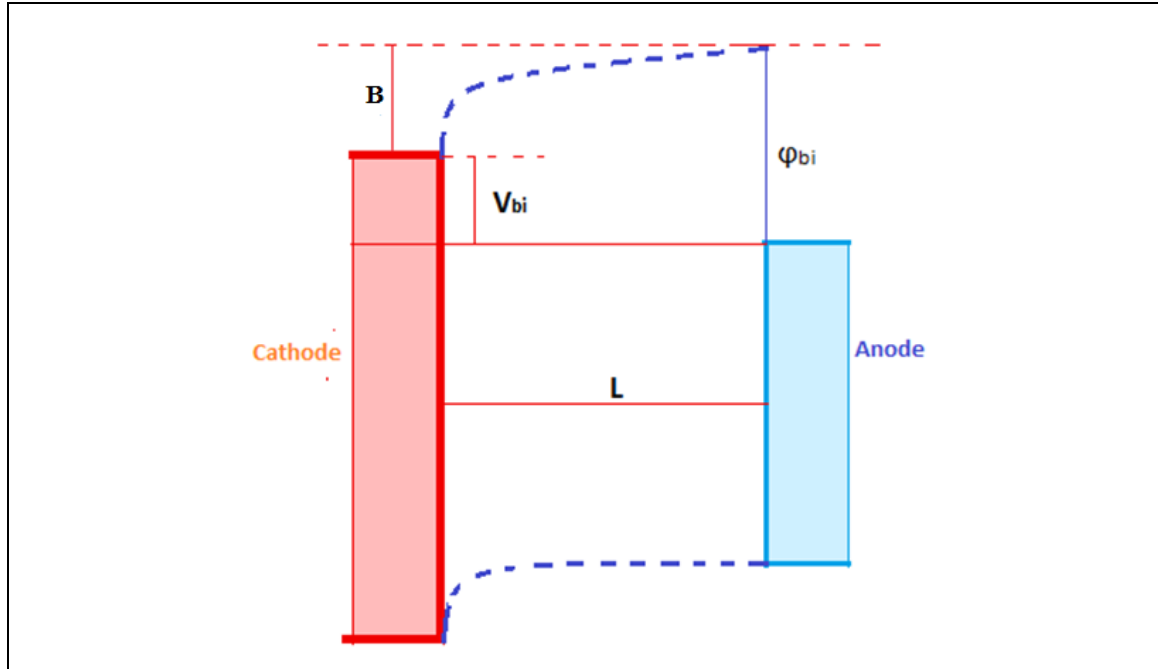


Fig.4.7 Schematic representation of interfacial band bending at electrodes having different work function along with relating built in potential and barrier height together

Current into the metal-semiconductor interfacial contact is represented by the following expression as follows [12, 30-31]

$$I = I_0 \left[\exp\left(\frac{qV}{nkT}\right) - 1 \right] \quad (4.14)$$

and

$$I_0 = AA^*T^2 \exp\left(-\frac{q\phi_{bi}}{kT}\right) \quad (4.15)$$

Where I_0 is reverse saturation current, q is electronic charge, V is applied voltage, A is Recharldson constant, A is effective area of the device and ϕ_{bi} is corresponding barrier height. Further, ϕ_{bi} can be estimated from the equation

$$\phi_{bi} = \frac{kT}{q} \ln\left(\frac{AA^*T^2}{I_0}\right) \quad (4.16)$$

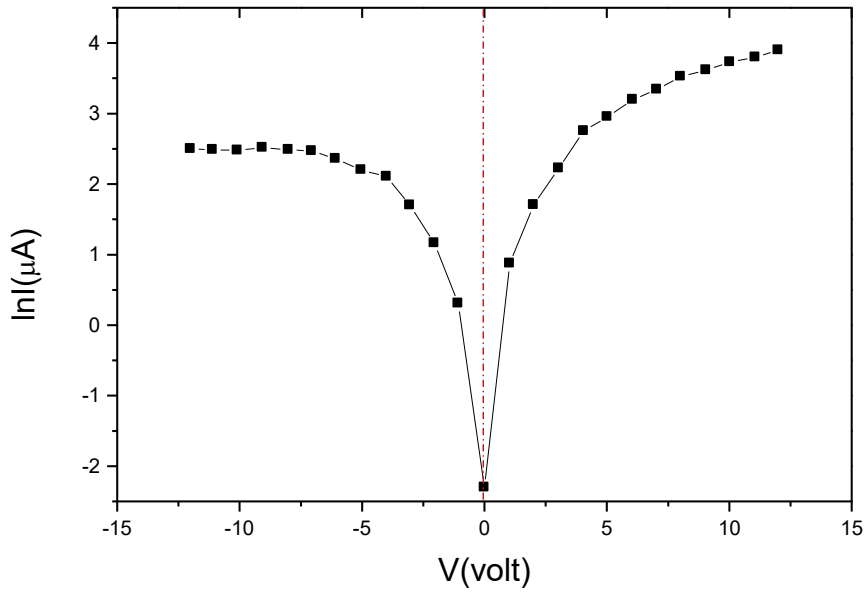


Fig.4.8 Semilog I-V plot of Al/Turmeric/Cu based device

Estimated value of Trap energy (E_t), Trap factor (θ) and barrier height (ϕ_{bi}) has been shown in the table given below.

Table 4.1.

Estimated electrical parameters for Turmeric dye based natural organic device

Estimated Parameters	Obtained Values
Trap energy (in eV) (E_t)	0.028
Trap factor (θ)	0.88
Barrier height (in eV) (ϕ)	0.825

A very promising outcome of the parameters of the experimental dye based device has been encountered comparing to the previously reported results of Chakraborty et al. [12,32]. Comparison indicates enormous decrement of Trap energy and Barrier height in the present experiment over previously reported semiconducting organic Rose Bengal (RB) and Methyl Red (MR) dye based organic diodes. Present data may lead to the possibility to introduce this dye in vast optoelectronic applications in future. However, there should be the consideration of other relevant electrical parameters like series resistance, shunt resistance, ideality factor also to achieve final conclusion in such applications. Estimated comparison has been given in Table 4.2.

Table 4.2.
Estimated reduction percentage (%) of E_t and ϕ obtained in Al/Turmeric/Cu device over RB and MG dye based organic diodes

Electrical parameters	Estimated reduction percentage (%) over Rose Bengal dye	Estimated reduction percentage (%) over Methyl Red dye
Reduction in E_t	67.81	63.16
Reduction in ϕ	13.68	17.17

Trap affected disordered energy level typically explained by Gaussian distribution proposes that charges populate at the lower energy states at extremely small concentration of carriers and go towards highly available hopping transport with enhancing density of injected carrier mobility. Enhanced mobility with increasing bias voltage can heuristically be described by the Poole-Frankel model and Recharadson- Schottky model. Exponential dependence of current proposes strongly Schottky or Poole-Frankel mechanisms applicable at the junction. Semilog current w.r.t $V^{1/2}$ plot has been depicted in Fig. 4.9. I-V expression for both mechanisms is given by [30, 36-37]

$$I = AA^*T^2 \exp\left(\frac{-\phi_b}{kT}\right) \exp\left(\frac{\beta_{RS}V^{1/2}}{kTd^{1/2}}\right) \quad (4.17)$$

for Schottky effect and

$$I = I_0 \exp\left(\frac{\beta_{PF}V^{1/2}}{kTd^{1/2}}\right) \quad (4.18)$$

for Poole-Frankel effect.

β_{RS} denotes Richardson-Schottky coefficients and β_{PF} denotes Poole-Frankel field lowering coefficients respectively. Relation between β_{RS} and β_{PF} is given as follows

$$2\beta_{RS} = \beta_{PF} = \left(\frac{q^3}{\pi\epsilon_0\epsilon_r}\right)^{1/2} \quad (4.19)$$

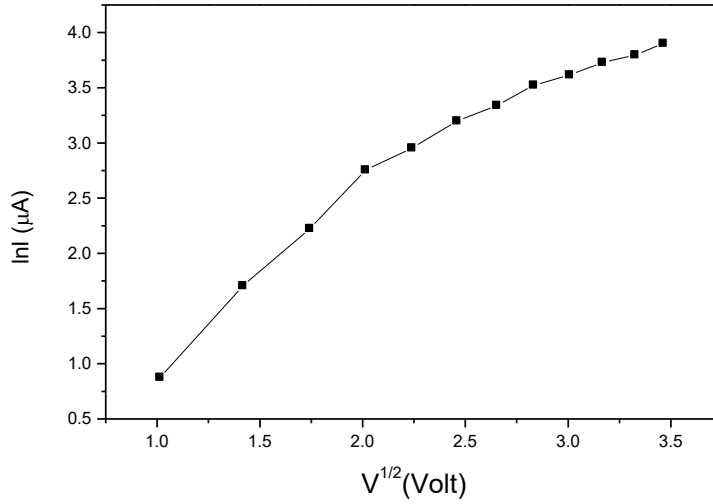


Fig.4.9 $\ln I$ vs $V^{1/2}$ plot for Al/Turmeric/Cu based diode

Theoretical values of β_{PF} and β_{RS} can be estimated from above equations considering the relative permittivity, ϵ_r of Turmeric is 54.2 [15]. Reported value of ϵ_r of the experimental dye is high enough than other natural semiconductors. However, the theoretically obtained values of β_{RS} and β_{PF} are $3.06 \times 10^{-6} \text{ eVm}^{1/2}\text{V}^{-1/2}$ and $6.12 \times 10^{-6} \text{ eVm}^{1/2}\text{V}^{-1/2}$. Approximation of experimental outcomes at high voltage linear zone of I-V relation shows the value of β is $0.95 \times 10^{-6} \text{ eVm}^{1/2}\text{V}^{-1/2}$. Extracted value of β is linear region is 0.31 times of β_{RS} and 0.62 times of β_{PF} . So it is clearly indicative that β obtained experimentally is quite closer to β_{RS} which ensures

Reichardson-Schottky mechanism is comparatively dominant in the present discussion. The following mechanism suggests bulk limited charge conduction process of the device.

4.4. Conclusive remarks

Turmeric dye based organic device has been taken into account to realize the trap assisted conduction mechanism at different regime of organic semiconducting device. Signature of trapping states has been verified by introducing V_x - V plot and differential $G(V)$ - V analysis. Explanation of both analysis leads to the confirmation of trap signature into the bulk region of the device. Hence the value of trap energy (E_t), barrier height (ϕ) and trap factor (θ) be encountered. Dependence of barrier potential on trap states has also been explained considering drift diffusion current equation and modified Mott-Gurney law. Comparison of the estimated data with other reported dyes shows possibility to introduce the dye in further electronics and semiconductor application. Reichardson-Schottky based conduction mechanism has been found dominant analyzing $\ln I$ vs $V^{1/2}$ plot in charge conduction process over Poole-Frankel process in this device.

4.5. References

1. Brabec C J, Sariciftci N S, Hummelen J C, Plastic solar cells, *Adv Funct Mater.*,2001, 11(1):15-26
2. Kawano K, Sakai J, Yahiro M, Adachi C, Effect of solvent on fabrication of active layers in organic solar cells based on poly (3-hexylthiophene) and fullerene derivatives. *Sol.Energy Mater.Sol.Cells*, 2009, 93:514-518
3. Yu G, Heeger A J, Charge separation and photovoltaic conversion in polymer composites with internal donor/acceptor heterojunctions, *J Appl Phys.*, 1995, 78:4510-4515
4. Feron K, Belcher W, Fel C J, Dastoo P C, Organic solar cells: understanding the role of Förster resonance energy transfer, *Int J Mol Sci.*, 2012, 13:17019-17047

5. Carbone A, Pannetta C, Reggiani L, Traping-detraping fluctuations in organic space-charge layers, *Appl. Phys. Lett.*, 2009, 95:233303
6. Carr J A, Chowdhury S, On the identification of deeper defects levels in organic photovoltaic devices. *J. Appl. Phys*, 2013, 114:064509-7
7. Nicolai H T, Kuik M, Wetzelaer G A H, Boer B, Campbell C, Risko C, Bredas J L, and Blom P W M, Unification of trap-limited electron transport in semiconducting polymers, *Nature Mater.* 2012, 11:882
8. Scheinert S, Paasch G, Doll T, The influence of bulk traps on the subthreshold characteristics of an organic field effect transistor, *Synthetic Met.*, 2003, 139:233
9. Xu M L G., et al., "Bulk-Like electrical properties induced by contactlimited charge transport in organic diodes: revised space charge limited current," *Adv. Electron. Mater.*, 2018, 4:1700493
10. Rizvi S M H, Mantri P, Mazhari B, Traps signature in steady state current-voltage characteristics of organic diode, 2014, 115:244502-(1-9)
11. Ahmed Z, Sayya M H, Electrical characteristics of a high rectification ratio organic Schottky diode based on Methyl red. *Optoelectron Adv Mater*, 2009, 3:509
12. Chakraborty K, Chakraborty S, Manik N B, Effect of single walled carbon nanotubes on series resistance of Rose Bengal and Methyl Red dye-based organic photovoltaic device, 2018, 39: 094001-(1-7)
13. Kim H J., et al. "Curcumin Dye Extracted from Curcuma Longa L Used as Sensitizers for Efficient Dye-Sensitized Solar Cells", *Int J Chem Sc*, 2013, 8:8320-8328
14. Hossain M K., et al. Effect of Dye extracting solvents and sensitization time on photovoltaic performance of natural dye sensitized solar cells, *Result I Phys.*, 2017, 7:1516-1523
15. Dakhel A, Henan F Z, Extraction and dielectric properties of curcuminoid films grown on Si substrate for high-k dielectric applications, *Mat Sc and Engg*, 2013, 178, 1062-1067
16. Hossain M K., et al. Influence of natural dye absorption on the structural, morphological and optical properites of TiO₂ based photoanode of dye-sensitized solar cell, *Mat Sc-Pol.*, 2018, 36(1): 93-101
17. Mott N. F. and Gurney R. W., *Electronics Process in Ionic Crystals*. Oxford, U.K.: Oxford Univ. Press, 1948
18. Li L, Lu N, and Liu M, "Limitation of the concept of transport energy in disordered organic semiconductors," *Europhys. Lett.*, 2014, 106(1):17005-

19. Blakesley J C, Clubb H S, and Greenham N C, "Temperature dependent electron and hole transport in disordered semiconducting polymers: Analysis of energetic disorder," *Phys.Rev. B, Condens. Matter*, 2010, 81(4):45210
20. Baranovskii S D, Cordes H, Hensel F, and Leising G, "Charge-carrier transport in disordered organic solids," *Phys Rev. B, Condens. Matter*, 2000, 62(12):793
21. Mensfoort S L M, Billen J, Vulto S I E, Janssen R A J, Coehoorn R, "Electron transport in polyfluorene-based sandwich-type devices: Quantitative analysis of the effects of disorder and electron traps," *Phys. Rev. B, Condens. Matter*, 2009, 80(3):33202
22. Rizvi S M H, Mazhari B, "Investigation of Traps in Thin-Film Organic Semiconductors Using Differential Analysis of Steady-State Current–Voltage Characteristics", *IEEE Trans Elect. Dev.*, 2018, 65(8):3430
23. Vries R J, Mensfoort S. L M V, Janssen R A J, Coehoorn R, "Relation between the built-in voltage in organic light emitting diodes and the zero-field voltage as measured by electroabsorption," *Phys. Rev. B, Condens. Matter*, 2010, 81(12):125203
24. Bruyn P D, Van Rest A H P, Wetzelaer G A H, De Leeuw D M, Blom P W M, "Diffusion limited current in organic metal-insulator-metal diodes," *Phys. Rev. Lett*, 2013, 111(18):186801
25. Hwang. J, Wan A, Kahn A, "Energetics of metal–organic interfaces: New experiments and assessment of the field," *Elsevier Mater. Sci. Eng., R, Rep*, 2009, 64(1–2):1
26. Poplavskyy D, Nelson J, Nondispersive hole transport in amorphous films of methoxy-spirofluorene-arylamine organic compound, *J App Phys*, 2003, 93(1):341
27. Ishihara S, Hase H, Okachi T, Naito H, Demonstration of determination of electron and hole drift-mobilities in organic thin films by means of impedance spectroscopy measurements, *Thin Sol Films*, 2014, 554:213-217
28. Wetzelaer G A H, "Analytical description of the current-voltage relationship in organic-semiconductor diodes", *AIP Adv.*, 2018, 8:035320-(1)
29. Mantri. P, Rizvi S M H, Mazhari B, Estimation of built-in voltage from steady-state current-voltage characteristics of organic diodes, *Org Elect*, 2013, 14(3):2034-2038
30. Shah M, Sayyad M H, Karimov Kh S, Wahab F, Electrical characterization of the ITO/NiPc/PEDOT: PSS junction diode, *J of Phys D: Appl Phys*, 2010, 43:405104-(1)
31. Yakuphanoglu F, Shah M, Farooq W A, Electrical and Interfacial Properties of p-Si/P3HT Organic-on-Inorganic Junction Barrier, *Acta Phys Pol A*, 2011, 120(3):558-562

32. Chakraborty S, Manik N B, Effect of single walled carbon nanotubes on the threshold voltage of dye based photovoltaic devices, 2016, 481:209-216
33. Scher H, Montroll E W, Anomalous transit-time dispersion in amorphous solids, *Phys Rev B*, 1975, 12(6):2455-2477
34. Shfai T S, Thomas A L, Junction properties of nickel phthalocyanine thin film devices utilizing indium injecting electrodes, *Thin Sol Films*, 2001, 398-399:361
35. Solak S, Blom P W M, Wetzelaer G A H, Effect of non-ohmic contacts on the light-intensity dependence of the open-circuit voltage in organic solar cells. *Appl Phys Lett*. 2016, 109(5), 053302
36. Riad A S, Influence of dioxygen and annealing process on the transport properties of nickel phthalocyanine Schottky-barrier devices, *Physica B*, 1999, 270:148
37. Aydin A B K., Yildiz D E, Xanvus H T, Sahingoz R, “ALD TiO₂ thin film as dielectric for Al/p-Si Schottky diode”, *Bull Mat Sc*, 2014, 37(7):1563

Chapter-5

Utility of Carrier Transportation Layer P3HT:PCBM for Efficiency Improvement of Organic Photovoltaic Devices using GPVDM Modeling

5.1 Introduction

5.2 Numerical Modeling and Experiments

5.3 Results and discussions

5.4 Conclusive remarks

5.5 References

5.1. Introduction

In last two chapters, illustration has been pointed out the influence of trapping states on charge conduction related issues of natural organic diode configurations. So it will be convenient to validate the aftermath of trapping states in industrialized application of organic dye based device.

In this perspective, GPVDM modeling technique has been introduced to calibrate the photovoltaic configuration and accordingly obtain the different electrical and photovoltaic output parameters. Incorporation of buffer layer has been taken into account also to verify the efficiency improvement. Outcome of present experimental modeling shows consistency with numerous previously reported such attempts.

In present chapter, the physics of photo conversion efficiency (PCE) enhancement with insertion of electron transportation layer along with photoactive layer has been described. The parameters have been measured by modeling the devices using simulation technique. The fact of realization should be started from the illustration of dark current-voltage (I-V) curve of the diodes, which shows linearity in semilog range of measurements below threshold voltage. But the characteristic deviates from linearity with increasing bias voltage. Presence of series resistance is one of the most significant factors which basically results this deviations [3]. Since absorbance of organic thin films is high enough and excitons dissociation process is very fast for dissociation efficiency to achieve unity, the performance gradually becomes limited by short exciton diffusion length and very low charge collection due to high value of series resistance. Even series resistance of the bulk region of the film resists photo generated charges at the level of donor-acceptor interface from reaching to the electrode. In the bulk region traps play an important role in the carrier conduction process. At below threshold voltage region of I-V curve, effect of trap is negligible and current exhibits ohmic nature. Charge injection at this regime is too low and transport mechanism is explained by well-known Mott-Gurney's equation. Influence of trap on I-V characteristics can be understood above threshold voltage regime. Majority of generated charges face immobilization of motion due to the reason of trap existence above threshold voltage regime [4]. Such trapping states create an internal resistive property of organic substances. So it is obvious that the movement of free carriers of these devices struggles by high series resistive influence due to the presence of trapping states in the active regime. Investigation of the present report suggests that both of R_s and E_t has been reduced with incorporation of blend composite of

P3HT:PCBM with active material through which charges will be passed. Lowering of trap energy inherently lowers the influence of R_s which is the reason of enhancement of fill factor as well as efficiency of the solar cell.

5.2. Numerical Modeling and Experiments

GPVDM (General Purpose Photovoltaic Device Model), a very renowned, recently updated and reliable simulation modeling technique [5-6], has been introduced for current research to understand the physics of the charge transport mechanism and measurement for comparison of electrical as well as photovoltaic parameters of single and bi-layer photovoltaic devices. This modeling technique brings a revolution in research of organic photovoltaic devices by providing numerous advantages like device characterization by analyzing simulation outcome, ease programming of device modeling, prediction of improved device designing and its application and realization of charge conduction physics in organic photovoltaic devices finally. Numbers of typical relevant parameters have been taken into account to execute GPVDM successfully (given in supplementary file). Active layer of the experimental devices is considered to be sandwiched between the front and back electrodes. Thickness of the active layer is a very important issue on which device efficiency basically depends [7]. If active semiconductor layer regime is thin enough then efficiency is found to be low because of less absorption of photon whereas with enhancement of layer thickness leads to recombination of photo-generated carriers before reaching polymer/heterojunction interface which is unintended for improvement of efficiency. It has been observed that device performs better between thickness range 200nm-250nm [5, 16]. The devices under experiment have been performed considering layer thickness 220nm in this work. I-V characterization has been simulated and the data has been extracted using Graph extractor and plotted accordingly. Series resistance (R_s) of the devices has been determined theoretically by analyzing $I dV/dI-I$ plot whereas trap energy (E_t) has been estimated from log I-V characteristics. From outcome of simulation modeling, photovoltaic parameters has been extracted and compared for both type of devices. The only photoactive layer (PAL) based device is abbreviated as PALD and electron transport layer (ETL) added with PAL is named as ETLD.

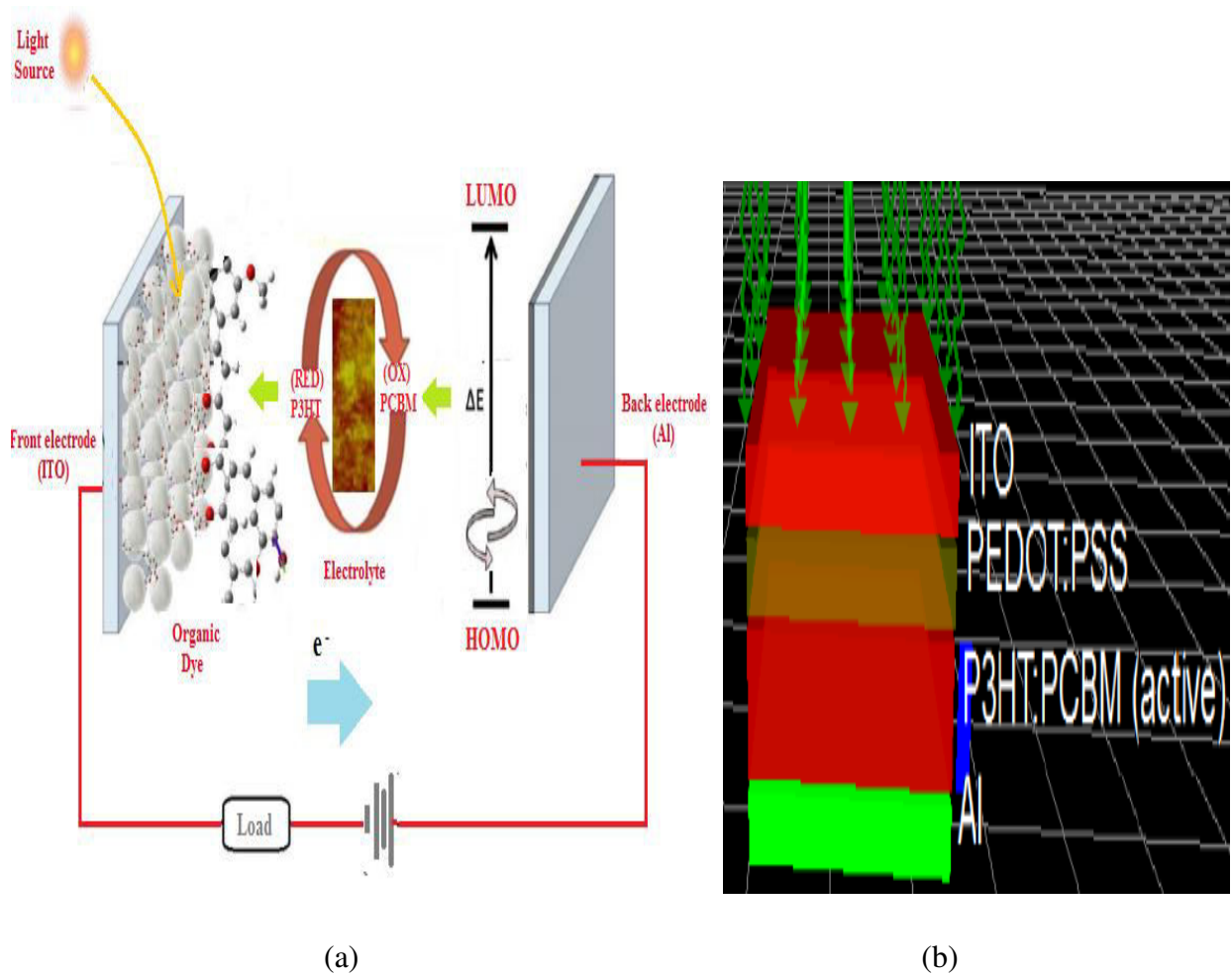


Fig.5.1 Block diagram representation of organic dye based photovoltaic measurement setup (a) in experiment and (b) in GPVDM simulation

5.3. Results and Discussions

Output of simulation indicates that the effectivity of electrical parameters as well as device efficiency is improved enough for bi layer device. To have a better insight of the result, current-voltage (I-V) characteristics have been taken into account. Evaluation of the data shows that current has considerably increased for ELTD. The following I-V characteristic is shown in Fig.5.2.

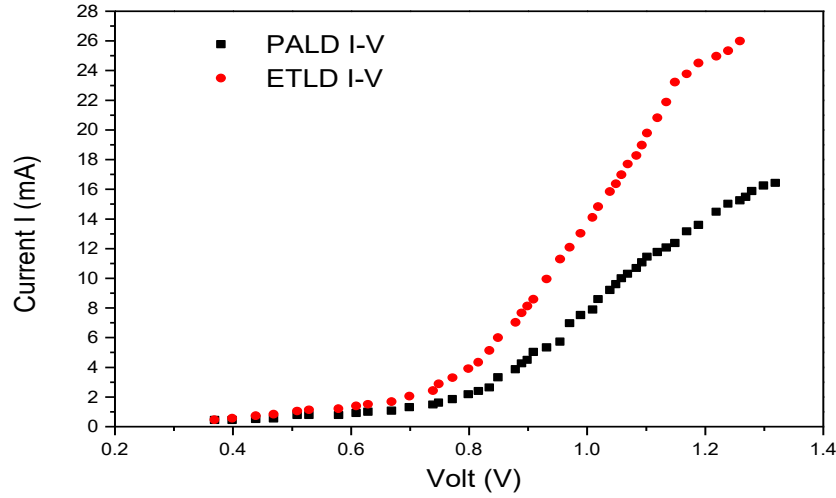


Fig.5.2 I-V characteristics of PALD and ETLD obtained in GPVDM (plotted in origin 5.0)

There are various factors actually affecting the current conduction procedure of organic device. But the factor has the major impact on the conduction of carriers is termed as R_s . The parameter is considered as a crucial reason of non ideal behavior of organic devices. R_s directly impacts on fill factor and explicitly on device efficiency. Therefore, device efficiency is expected to be improved with decrement of the parameter R_s . In order to estimate R_s , approach of estimation of the parameter deals with I-V characteristics using the formula of Rakhshani et al [8]. I-V characteristics for high value of R_s of photovoltaic device can be expressed by [8-10]:

$$I = I_0 [e^{q(V-IR_s)} - 1] \quad (5.1)$$

Whereas voltage can be explained in terms of current as follows

$$V = \frac{nkT}{q} \ln \left(\frac{I}{I_0} + 1 \right) + I R_s \quad (5.2)$$

Derivative of voltage with respect to current can be written as

$$\frac{dV}{dI} = \frac{nkT}{q} \frac{1}{\left(\frac{I}{I_0} + 1\right)} \frac{1}{I_0} + R_s \quad (5.3)$$

Since current I is high enough than reverse saturation current I_0 (i.e., $I \gg I_0$) at the high current regime. So the Eq. (5.3) can be expressed as

$$I \frac{dV}{dI} = R_s I + \frac{nkT}{q} \quad (5.4)$$

From above consideration at high current zone, $I \frac{dV}{dI}$ is linearly dependent on total current I . R_s can be extracted from the slope by introducing a linear fit in the high current region whereas ideality factor n can be estimated from the intercept of the linear fit using Eq. (5.4). Dark I - $I \frac{dV}{dI}$ characteristics for both devices are shown in Fig. 3.

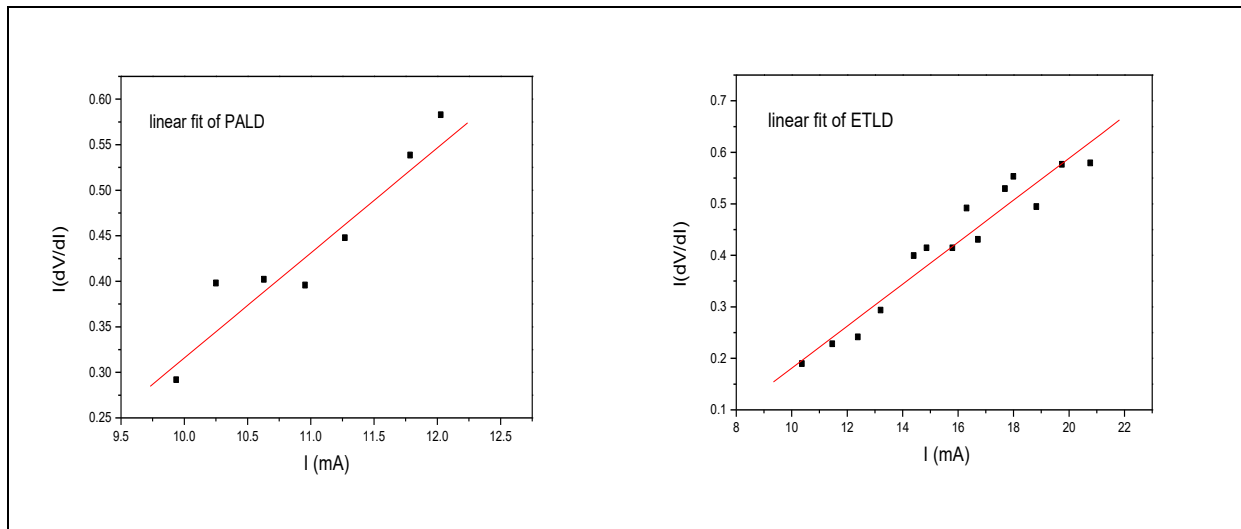


Fig.5.3. $I \frac{dV}{dI}$ vs I characteristics of PALD and ETLD

n is such a parameter which indicates the tendency of linearity of ideal diode. The value of n is usually very high in organic devices due to the distortion of current-voltage characteristics generated by interfacial disorder, mismatch in metal-semiconductor interface, hopping carrier transport and high series resistive impact [10, 32]. It has been found that the value of ideality factor reduces drastically with insertion of charge transportation layer based ETLD. R_s is closely related also with another important parameter, named as Trapping effect which has high influence on organic photovoltaic devices. Presence of significant concentration of trapping states becomes a factor in organic semiconducting devices which appears due to the disordered elementary structures of organic molecules and has a significant contribution to produce high

value of R_s . The role of trap is a matter of concern in carrier conduction mechanism of organic dye based devices [4, 10, 19]. Charges interact with these traps when conduction occurs. Injected carriers depend on the trap energy for a particular distribution. For bulk transport process, it is a vital function which controls current flow by providing resistive influence. Basically charges are trapped and recombined in presence of huge amount of traps concentration. Hence conductivity gradually becomes limited which gradually results low device efficiency. Existing trap concentration deliberately adds resistive impact which prevents smooth flow of the carriers into bulk transport regime. It has been observed in present experiment that incorporation of a polymer layer (P3HT:PCBM) which acts as interfacial electron transportation layer with PEDOT:PSS reduces the amount of trap energy E_t in ETLD. It will be rather convenient to describe the fact from Fig. 4.

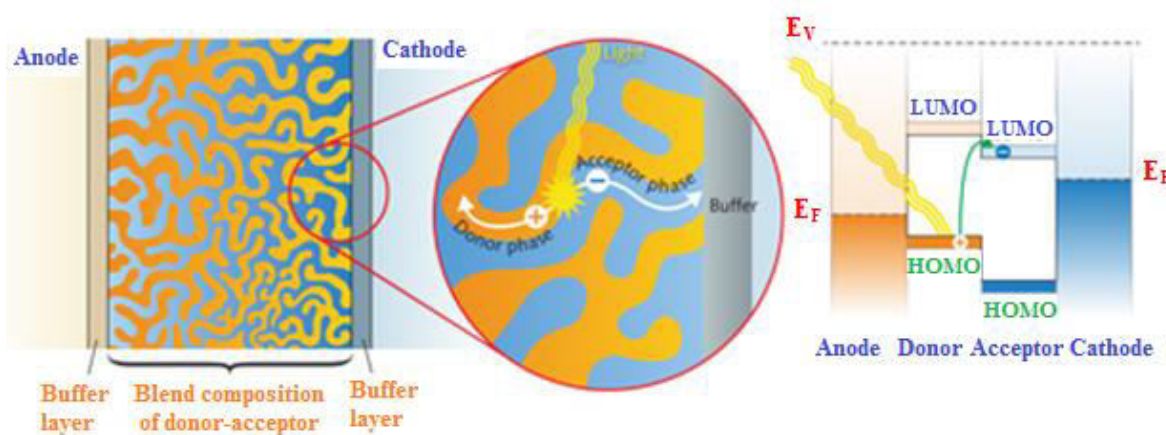


Fig.5.4. absorption of photon energy generates dynamic holes and electrons that travel through acceptor and donor phases and its consequent energy level diagram where E_V represents the energy at vacuum level and E_F expresses the energy of Fermi level [6, 28, 31]

Electrons move from highest occupied molecular orbital (HOMO) of donor molecules towards lowest unoccupied molecular orbital (LUMO), leaving a positive carrier “hole” on donor molecule during absorption of photon energy. Holes and electrons move along opposite directions together and simultaneously captured by anode and cathode [4, 24-26]. The interfacial transition between electrode and organic dye is critical enough for efficient collection of carriers. Such charge transformation causes significant drop of voltage and moreover, leakage current impact on electrodes, resulting decrement of PCE. Incorporation of charge transportation buffer

layer (P3HT: PCBM) in ETLD, plays crucial role to minimize the effect of voltage drop and leakage current. The layer permits interfacial alignment of energy-level providing rectification and additional percolation network to trapped charges and on the other hand, absorption of more optical energy by this layer results comparatively greater range of free carriers [10-27-28]. Increasing tendency of free carrier concentration reduce the energy of trapping states and hence series resistance also. Moreover, insertion of buffer layer in ETLD results high value of J_{sc} and Fill factor (FF) which inherently improve the device efficiency comparatively than PALD [4, 29]. Carrier transportation buffer layer acts as a bridge between the work function differences to provide suitable charge transport into the bulk region which seems to another probable reason of reduction the trapping states consecutively. Fig.5.5 can be effective in this regard to show the charge hopping mechanism on the basis of work function of materials [5, 20-22] into the device. Fermi level energy of materials are parameterized by their work function [11, 25-26]. Work function determines the amount of energy loss when removing or adding an electron from a substance. Maximum value of open circuit voltage (V_{oc}) can be found with greater value work function of anode over ionization energy of donor atoms and low value of cathode work function than acceptor electron affinity [7, 23-24].

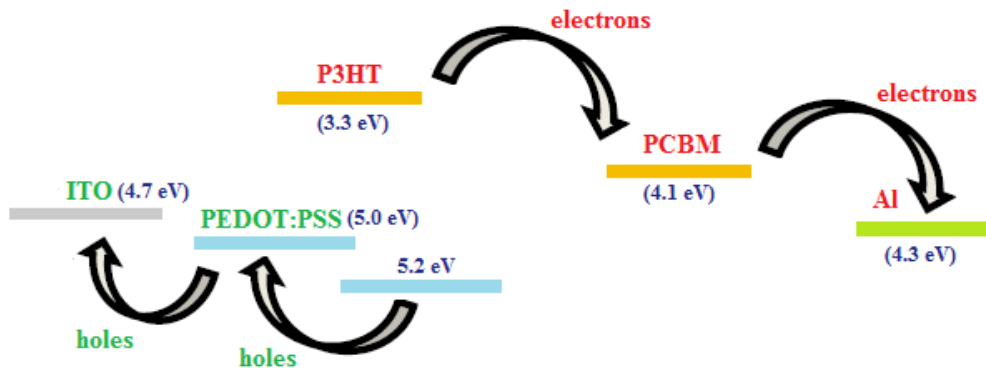


Fig.5.5 hopping movement of carriers in different materials as par work function into ETLD

Exponential distribution of trapping concentration and its solution relates current density and applied voltage in such a way that they maintains the following relation $J \sim V^{m+1}$, where $m = T_c/T$, T_c is the characteristic temperature and T is room temperature and Trap energy

$E_t = mkT$. Value of m is calculated from $\ln I - \ln V$ plot and hence E_t is extracted from the value of m using the relation mentioned above [4, 11]. Trapping carrier concentration (n_t) can be explained by exponential distribution as follows [12, 19]

$$n_t(\epsilon) = N_0 \exp \frac{-\epsilon}{kT_c} \quad (5.5)$$

where ϵ expresses the traps depth below conduction band mobility regime and T_c is the trap energy of the following distribution. Impact of trapping on I-V characteristics can be described from the modified version of well known Mott-Gurney relation and is given by [13]

$$I = \frac{9}{8} A \epsilon \epsilon_0 \theta \mu \frac{(V - V_x)^2}{d^3} \quad (5.6)$$

where V is applied voltage, ϵ_0 is free space permittivity, μ is carrier mobility, d is thickness of the semiconducting and θ is trap factor. Values of θ can be estimated from logarithmic representation of I-V plot. θ has significant signature about the indication of improvement of trapping states. Aforementioned parameter denotes the ratio of the amount of trapped charges (P_t) to total number of free charges participated in conduction process (P_f) as well as the trapped charges and can be represented as [13-14]

$$\theta = \frac{P_t}{P_f + P_t} \quad (5.7)$$

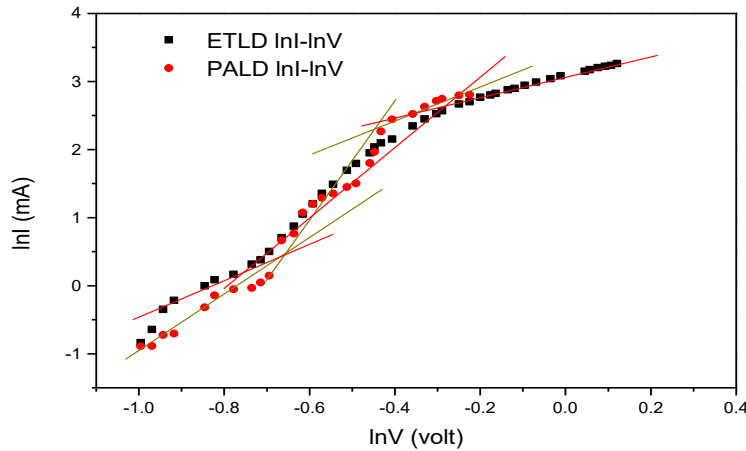


Fig.5.6 $\ln I - \ln V$ characteristics of PALD and ETLD

To have a better insight about the trapping distribution into the devices a differential technique should be implemented. Distortion in I-V curve is clearly observed in presence of large trap

concentrations and distinct regions containing distortions can be unambiguously predicted. But the prediction becomes quite problematic to recognize the distortions in the plot for low trap density. Differential technique is fruitful in this context for enhancement of the small deviations so it has been introduced to reveal the orientation of distribution of trap states. $G(V)$ - V plot is explained regarding this purpose where [12,15]

$$G(V) = \frac{d \log(I)}{d \log(V)} \quad (5.8)$$

A transition of exponentially rising current flow to power law dependence regime about built in potential voltage (V_{bi}) is marked by sharp peak of $G(V)$. Filling of trap states can be illustrated by such peak which signifies easy identification of transition voltage related to voltage V_{bi} . The distinct peak of $G(V)$ - V curve explains the nature of trapping distribution where monotonous decrement from sharp peak of $G(V)$ with increasing voltage denotes the trap free conduction into the device.

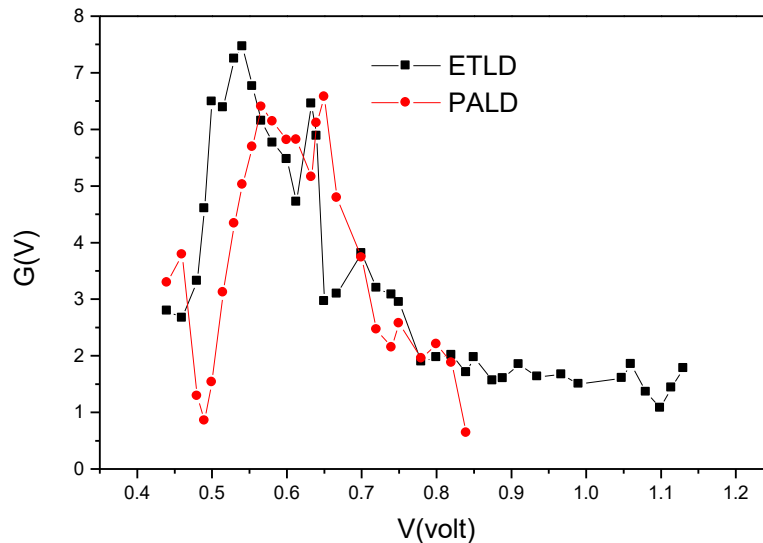


Fig.5.7 $G(V)$ - V characteristics of PALD and ETLD

Exponential behaviour at power law regime with sharp peaks are noticeable clearly for both devices in Fig.5.7. Sharp peak of $G(V)$ indicates the change in slopes from exponential regime to power law regime as mentioned earlier. Decrement of trapping density can be clearly concluded

with comparatively greater monotonic decremental orientation of $G(V)$ at high voltage for bilayer devices. Height of trap peaks depend upon the slope of current voltage relationship which can be measured by the variation of θ . Traps are progressively got filled with increasing voltage which leads to the enhancement of θ from its minimum value towards unity. A relatively smooth conduction procedure can be expected with increasing value of θ . ETL D comprises of two distinct organic layers in which one layer having high ionization potential and electron affinity acts as acceptor while the other layer acts as donor of excitons. Electrostatic force arises in such configuration is strong enough to break the exciton pairs much efficiently than PALD. The thickness of acceptor layer is ranged in such a way that large amount of photons are absorbed and transported through acceptor successfully [16]. In this process, amount of recombination is comparatively small than PALD configuration so greater range of charge can be transported from one electrode towards another. Improvement in carrier conduction is caused by low value of trapping energy. Since organic structures are disordered and prone to traps, they usually have high resistive impact. The trapping problems can be optimized by the insertion effective polymer layer which leads to reduction of series resistance also and electrical parameters as well as device efficiency enhances gradually.

Table 5.1.

Comparison of electrical parameters of PALD and ETL D

Electrical parameters	PALD	ETLD	% improvement in ETL D
Trap Energy, E_t (in eV)	0.040	0.014	65.0
Series resistance, R_s (in Ω)	115	40	65.2
Ideality factor, n	30.88	8.73	71.7
Trap factor, θ	0.275	0.342	24.4

Photovoltaic parameters have been obtained from the output result of simulation technique. Obtained values of the parameters have been given in Table 5.2. Efficiency of solar cell (η) can

be defined as ratio of maximum power of the device to the power of incident photons and is expressed as [4, 17-18]

$$\eta = \frac{J_{sc} \times V_{oc} \times FF}{\phi} \times 100 \quad (5.6)$$

where ϕ is intensity of incident photons, J_{sc} is short circuit current, V_{oc} is open circuit voltage and FF is fill factor of the device. FF can be estimated from the following relation

$$FF = \frac{V_m \times J_m}{V_{oc} \times J_{sc}} \quad (5.7)$$

where J_m and V_m are maximum current density and voltage at maximum power rectangle.

Table 5.2.

Comparison of photovoltaic parameters of PALD and ETLD

Photovoltaic parameters	PALD	ETLD	% improvement in ETLD
V_{oc} (V)	0.602	0.668	10.9
J_{sc} (A/m ²)	111.63	220.52	97.5
FF	67.11	74.19	10.5
PCE	4.51	10.93	142.9

The result shows consistency with the analytical illustration stated earlier and also with previously reported experimental outcomes [4, 32-36]. Fill factor is observed to increase in the ETLD due to less number of recombination and lower trapping concentration. Though V_{oc} does not change significantly with insertion of ETL but a considerable increment of J_{sc} is observed in ETLD structure which suggests that photo generated carrier is enhancing with addition of that corresponding layer in the aforementioned device.

5.4. Conclusive remarks

Improved device performance with insertion of semiconducting polymer layer between PEDOT:PSS and electrode has been explained. Electrical parameters like E_t , R_s , n and θ are

obtained from by analyzing different I-V characteristics for both devices. It has been found that electrical parameters are improved for ETLD. Trapping orientation has been demonstrated by introducing differential technique for both devices. Greater range of monotonic decrement of $G(V)$ has been found better for bi-layer devices which leads relatively trap free smooth conduction at higher voltage regime. Photovoltaic parameters have been encountered for single and bi-layer devices respectively. Physics of the PCE of ETLD has been vividly illustrated. It has been observed that J_{sc} , fill factor is enhanced for ETLD structures with reduction of R_s as well as E_t which is inherently the reason of device efficiency.

5.5. References

1. Brabec. C J, Sariciftci. N S, Hummelen. J C, (2001) Plastic solar cells Adv. Funct. Mater. 11: 15-26.
2. Yu. G, Heeger. A J,(1995) Charge separation and photovoltaic conversion in polymer composites with internal donor/acceptor heterojunctions, J Appl Phys. 78: 4510–4515.
3. Shah. M, Sayyad. M H, Karimov. Kh S and Tahir. M, (2010) Investigation of the electrical properties of a surface-type Al/NiPc/Ag Schottky diode using $I-V$ and $C-V$ characteristics, *Physica B* 405: 1188–92.
4. Chakraborty. S, Manik. N B, (2016) Effect of single walled carbon nanotubes on the threshold voltage of dye based photovoltaic devices, *Physica B*. 481: 209-216.
5. MacKenzie. R, Kirchartz. T, Dobb. G, and Nelson. J, (2011) Modeling Nongeminate Recombination in P3HT:PCBM Solar Cells, *J. Phys. Chem. C*, 115 (19): 9806-9813.
6. Sims. L, Hörmann. U, Hanfland. R, MacKenzie. R, Kogler. F, Steim. R, Brütting. W, Schilinsky. P, (2014) Investigation of the s-shape caused by the hole selective layer in bulk heterojunction solar cells, *Org Elect*. 15: 2862-2867.

7. Chakraborty. K, Malakar. S, Mandal. D K, Mondal. R, Maiti. A K, (2019) Experimental Prediction of Effect of Thickness of Active Layer of Photovoltaic Device on a series of Electrical Parameters using GPVDM Software Int J Adv. Sci Eng. 6: 42-46.
8. Rakhshani. A E, (2001) Heterojunction properties of electrodeposited CdTe/CdS solar cells, J App Phys, 90 (8): 4265-4271.
9. Shen. Y, Li. K, Majumdar. N, Campbell. J C, Gupta. M C, (2011) Bulk and contact resistance in P3HT:PCBM heterojunction solar cells, Sol Mat. Sol Cell, 95: 2314-2317.
10. Chakraborty. K, Chakraborty. S, Manik. N B, (2018) Effect of single walled carbon nanotubes on series resistance of Rose Bengal and Methyl Red dye-based organic photovoltaic device J Semiconduct. 39: 094001 1-7. 7
11. Scher. H, Montroll. E W, (1975) Anomalous transit-time dispersion in amorphous solids, Phys Rev B, 12(6): 2455–2477.
12. Rizvi. S, Mantri. P, Mazhari. B, (2014) Traps signature in steady state current-voltage characteristics of organic diode, J. App. Phys. 115: 244502-1.
13. Rizvi. S, Mazhari. B, (2018) Investigation of Traps in Thin-Film Organic Semiconductors Using Differential Analysis of Steady-State Current–Voltage Characteristics, IEEE Trans Elect. Dev. 65(8) : 3430-3437.
14. Shah. M, Sayyad. M H, Karimov. K, (2011) Electrical characterization of the organic semiconductor Ag/CuPc/Au diode, Journal of Semiconductors, 32: 4. [http://doi: 15](http://doi:15). Mantri. P, Rizvi. S, Mazhari. B, (2013) Estimation of built-in voltage from steady-state current-voltage characteristics of organic diodes, Org. Elect, 14(3): 2034-2038.
16. Deschler. F, Riede. D, Ecker. B, Como. E D, Hauff. E, MacKenzie. R, (2013) Increasing organic solar cell efficiency with polymer interlayers, P Chm Chm P., 15(3): 764-769.
17. Chakraborty. S, Halder. A, Manik. N B, (2014) Size Effect of Multi-walled Carbon Nanotubes on the Performance of Malachite Green Dye Based Photovoltaic Devices, J. Basic App Engg Res. 1(4): 85-89. 18. Wetzelaer. G J, Blom. P WM, (2014) Diffusion-driven currents in organic semiconductor diodes, N. Asia. Mat., 6: 1-13.

19. Kim. C H, Yaghmazadeh. O, Bonnassieux. Y, Horowitz. G, (2011) Modeling the low-voltage of organic diodes: Origin of the ideality factor 110 : 093722(1-8)
20. Fan. X, Nie. W, Tsai. H, Wang. N, Huang H et al. (2019) PEDOT:PSS for Flexible and Stretchable Electronics: Modifications, Strategies, and Applications: Adv. Sci. News., 6 : 1900813 (1-41)
21. Greiner. M T, Helander. M G, Tang. W M, Wang. Z. B, Qiu. J, Lu. Z H, (2017) Universal energy-level alignment of molecules on metal oxides: Nature. Mat., 11 : 76-81.
22. Ullah. N, Shah. S M, Hussain. H, Ansir. R, Husain. M N, (2020) Pyrocatechol violet sensitized Ho-TiO₂/ZnO nanostructured material: as photoanode for dye sensitized solar cells, Mater. Res. Express., 7 : 035003 (1-15).
23. Farjamtalab. I, Kashaniniya. A, Nadooshan. R S, (2015) Improving power conversion efficiency in bulk heterojunction P3HT: PCBM organic solar cells by utilizing RGO-TiO₂, IOSR-JAP., 7:(41-48).
24. Park. M, Chin. B D, Yu. J W, Chun. M S, Han. S H, (2008) Enhanced photocurrent and efficiency of poly (3-hexylthiophene)/ fullerene photovoltaic devices by the incorporation of gold nanoparticles, J. Industrial and Engg. Chem. 14 : 382-386.
25. Elumalai. N K, Vijila. C, Jose.R, Zie. Z, Ramakrishna. S, (2014) Effect of trap depth and interfacial energy barrier on charge transport in inverted organic solar cells employing nanostructured ZnO as electron buffer layer, J. Nanotech. 11: 322-332.
26. Ratcliff et al. (2011) Challenges and Oppurtunities in Light and Electrical Energy Conversion, 2 : 1351-1352.
27. Gershon. T, (2011) Metal oxide applications in organic-based photovoltaics, Mat. Sci. Tech., 27 : 1357-1371.
28. Groves. C, (2013) Developing understanding of organic photovoltaic devices: KINETIC Monte Carlo models of geminate and non-geminate recombination, charge transport and charge extraction, Energy. Envior. Sci., 6 : 3202-3217.
29. Tengstedt. C, (2006) Fermi-level pinning at conjugated polymer interfaces, Appl. Phys.Lett., 88 : 053502.

30. Wang. Z, Yin. H, Tang. Y, Ren. X, Yuan. H, Yan. N, (2020) Design of TiO₂-based nanocomposite via two-step method on Aland Fe-doped Ti₃SiC₂ ceramic for photo-electrode, SN App.Sc., 2 : 1121
31. Homepage (detectors and imaging), ORGANIC PHOTOVOLTAICS: Transition metal oxides increase organic solar-cell power conversion, Laser Focus World (webpage)
32. Almeida. B M, M. Jr. M A, Bettini. J, Beneditti. J E, Nogueira. A F, (2014) A novel nanocomposite based on TiO₂/Cu₂O/reduced graphene oxide with enhanced solar-light-driven photocatalytic activity, App. Sur. Sc. 324: 419-431.
33. Ismail. Y A M, Soga. T, Jimbo. T, (2009) Improvement in light harvesting and performance of P3HT:PCBM solar cell by using 9,10-diphenylanthracene, Sol. Mat. Sol. Cell. 93: 1582-1586.
34. Li. F, Zhao. J, Tao. K, Chen. Y, (2012) Origin of the efficiency improvement in pre-annealed P3HT/PCBM solar cells with LiF/Al electrodes, Chem. Phys. Lett. 553: 36-40.
35. Sen. S, Manik. N B, (2019) Effect of Carboxyl-Functionalized Single Walled Carbon Nanotubes on the Interfacial Barrier Height of Malachite Green Dye Based Organic Device, Phys. Int. 10: 1-6.
36. Lee. H Y, Huang. H, (2014) Investigation Performance and Mechanisms of Inverted Polymer Solar Cells by Pentacene Doped P3HT : PCBM, Int. J. Photoenergy., 2014: 1-9.

Chapter-6

An Analytical Study on Low Voltage Regime of Natural Organic Semiconductor Based Device: Physics of Trap energy and Ideality Factor

- 6.1. Introduction**
- 6.2. Materials and methods**
- 6.3. Results and discussions**
- 6.4. Conclusive remarks**
- 6.5. References**

6.1. Introduction

In present chapter, focus has been given on low voltage regime to observe the trap assisted charge conduction and effect of trapping states. Amount of current is too small at the aforesaid regime when the applied bias is less than built-in potential level and usually it was late attracted issue to the researchers. Except some few works (like as Kim et al. and Wetzelaer et al.), not much study can be found which interprets the physics of this regime. Present investigation has been started in this context to provide some relevant information of trap dominated charge transport. Diffusion driven states of current flow has been taken into consideration of organic semiconductor diode in this regard which provides significant information regarding the physics of charge transport. Semiconducting layer based organic dye sandwiched between two metals of different work function is used to explain the following facts. The device comprises an ohmic injection interface while the other interface is non-ohmic in nature. Due to the introduction of different work function, internal electric field grows up which results the formation of built-in potential V_{bi} across the metal-semiconductor interfacial contact. At a high value of positive bias, greater than V_{bi} , flow of current is described as drift current in this region. Current is restricted by the impact of injected carriers leading to SCLC (space charge limited current) conduction proposed by Mott –Gurney equation [6.1]

$$J = \frac{9}{8} \mu \varepsilon \frac{(V - V_{bi})}{L^3} \quad (6.1)$$

where μ is mobility of charge carrier, ε is related permittivity, V is applied voltage and L is transition width of interface. Variation and inter-dependence of electrical parameters in this region can be predicted very easily by analyzing current-voltage (I-V) relationship.

At this regime, appeared electric field is negative and hole density gradient leads to diffusion dominated carrier flow towards the interfacial contact. Diffusion limited conduction in organic diode can be analyzed by classical Shockley equation where ideality factor (n) is highly expected to be unity in absence of trapping states and is indicated to bimolecular recombination. n provides crucial information about carrier transport and process of recombination in organic semiconductors. Presence of trapping states is another limitation of organic semiconductor based device. Trapping distribution in such semiconductors is generally described as Gaussian distribution at band bending edges. Therefore finding a relation between ideality factor and trap

energy will be very fruitful matter of concern from theoretical prediction and verification of its validation from experimental outcomes.

6.2. Materials and Methods

This section has been divided into two parts. In the first part, Modeling of GPVDM simulation has been described while detail of sample preparation for experimental study has been shown in the second part.

6.2.1. GPVDM simulation

GPVDM simulation, a renowned simulation approach [2-3], used for modeling of optoelectronics devices, has been taken into consideration. The technique has been introduced for measurement of electrical parameters and understanding the physics of carrier conduction of single layer organic device. Standard amount of device parameters have been set to run the simulation and calculate accordingly the related parameters. Simulation modeling based device is abbreviated as SM. The list of the parameters is given below. Estimated value of barrier height (ϕ_{bi}) of SM is 0.598 eV and it can easily be found from I-V plot of SM device. Data consisting current voltage relationship is extracted from the output of simulation modeling and plotted accordingly by Origin software.

6.2.2. Experimental arrangements:

Indigo dye (chemical formula- $C_{16}H_{10}N_2O_2$) and Turmeric dye (chemical formula- $C_{21}H_{20}O_6$) are the natural dyes used to fabricate the devices in the present experiment. Instead to using any chemical dyes, these mentioned natural dyes have been taken into consideration as the dyes show promising semiconducting properties reported in earlier investigations [4-7].

10gm of powder of aforementioned semiconducting elements is properly mixed in ethanol solution at 60° temperature for 3 hours. The formed solution is allowed for next 30 minutes to make the concentration homogeneous. Al and Cu substrates are cleaned then for next 15 minutes by using ultrasonic cleaner in distilled water. Then substrates are etched with HF: H₂O (in ratio of 1:10) to wash away oxides from the substrate. Prepared thin film is now coated using spin coater onto the substrate with 1000 rpm at room temperature. Pressure should be held at 5.5×10^{-5} mbar during deposition of film. Substrates coated with film are allowed to be attached together. The fabricated device is then placed at 50° C for two hours. Finally devices are ready for characterization to extract current voltage relationship.

6.3. Results and discussions

To have a better insight over the low voltage regime, present discussion has been confined from injection limited region to the starting of exponential region. I-V plot exhibits two discernable regions on the basis of n . The low voltage regime has been categorized in region-1 and region-2. Flow of current happens in region-1 by parasitical conduction, named as leakage current and n shows incremental tendency here in this region. Diffusion dominated current flow has been observed below V_{bi} in region-2. n decreases in this region with increasing applied voltage where current just starts to move towards exponential zone as shown in Fig.6.1. In the work of Sah et al. [8], n is affected by trap assisted mechanism of recombination in exponential regime. Immobilized electron in this regime faces recombination with free holes which leads to SRH (Shockley_Read_Hall) model [9, 10]. Value of n finds to nearly be equal to 2 in loss mechanism following SRH model. However, in practical cases of organic semiconductors, n is much larger than 2. Ideality factor thus be regarded as an efficient tool for trap-assisted recombination.

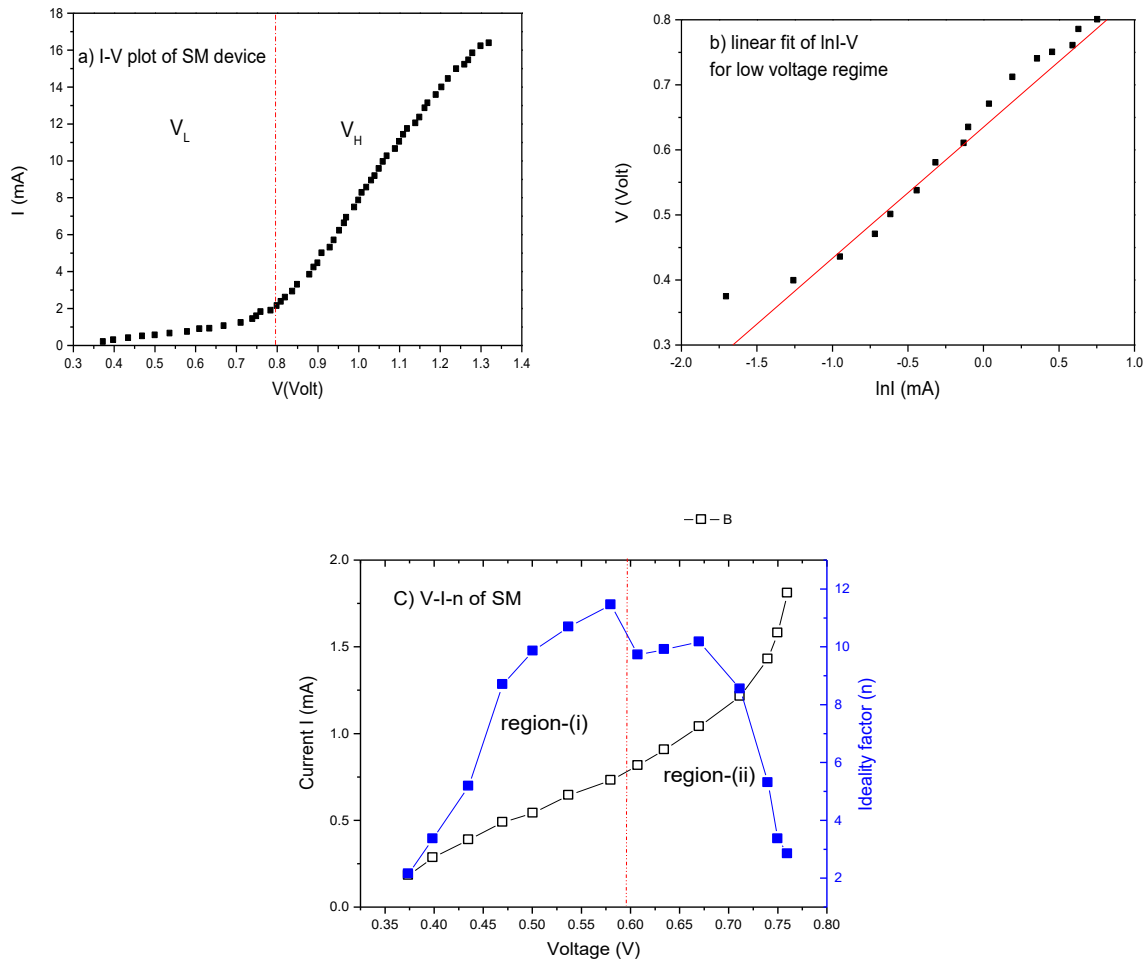


Fig.6.1 (a) Dark I-V characteristics obtained for SM (simulation modeling is abbreviated as SM) based device. V_L and V_H notify are low and high voltage zone respectively and the mentioned zones are separated by dotted line in first figure. V_L is basically diffusion conduction dominated regime whereas V_H is influenced by drift dominated conduction regime. Fig.6.1 (b) $\ln I$ -V characteristics of SM based device at low voltage regime. From the slope of the characteristics ideality factor is determined. Fig.6.1 (c) I and n has been plotted with respect to V. In region-(i) n is increasing with increasing voltage while reduction of n is found with increasing voltage in region-(ii). Dotted line in this figure is used to distinguish these two regions.

n can be estimated by linear fitting the experimental data of semilog I-V relationship following equation $n = kT/q \cdot (dV/d \ln I)$. Usually, at low voltage, conduction shows linear dependence with voltage but the magnified view of fig.1 shows the deviation of linearity at region-(i) and region-(ii) of organic semiconductors. As described by Wetzelaer et al. [11], n is such a parameter,

deviation of which from unity could be the result of violation of Einstein equation which shows the relation between diffusivity and mobility of carriers such as follows [12]:

$$\frac{D}{\mu} = \frac{kT}{q} \quad (6.2)$$

where D is diffusion constant. Validity of Einstein relation faces serious challenge when it is employed to explain the facts related to such parameters in disordered organic materials. The parameters suffer significant deviation from Einstein model when conduction mechanism in disordered amorphous organic systems is explained by the process of hopping transport between the localized states in Gaussian DOS (density of state) distribution [13-15]. Gradually the approachability of this equation in disordered structures is a matter of concern. Several experimental and theoretical research reports that the equation can't be fit to define charge transport in organic medium because of large disorder affected non equilibrium hopping even it requires serious modification for quasi-equilibrium condition [16-19]. Subsequently DOS distribution of organic semiconductor is approached to explain the modification of Einstein relation such as [20]:

$$\frac{D}{\mu} = \frac{p}{q \frac{\partial p}{\partial E_f}} = g(p, T) \frac{kT}{q} \quad (6.3)$$

where E_f denotes the quasi Fermi level and p is charge density. $g(p, T)$ is a dimensionless function which is defined as enhancement function of Einstein relationship. Proposed approach of Baranovskii et al. [16] states the deviation of modified approach is valid for energy states not associated with hopping transport in exponential regime but practical evidence doesn't hold good with that statement [21]. Demonstration through the measurement of I-V plot at diffusion prone regime of single carrier device may be fruitful as one significant method to probe Einstein relation, suggested by Harada et al. [22] and it can be represented as

$$J = J_0 \left\{ \exp\left(\frac{qV}{gkT}\right) - 1 \right\} \quad (6.4)$$

where J_0 is density of saturation current. Comparing to the ideal diode equation, it can be taken into consideration that ideality factor is equivalent to the enhancement factor g in organic semiconductor which is dependent on carrier density and temperature as mentioned in the work of Harada et al. Experimental observation of present study also supports the above discussion of

high value of n at low voltage regime and it not only depends on carrier density or temperature but it also has strong dependence on trap energy (E_t). Simulation based outcome of the present observation shows good consistency with the experimental study in this context. Schottky diffusion equation [23] is useful to start the discussion regarding this purpose. Theory of the equation deals with the configuration where organic semiconducting compound is sandwiched between metal contacts. Majority of carriers suffer diffusion at metal-semiconductor interface in such device where they face some deep trapping at the injection contact. Injected charges lead to formation of resultant electric field at the depletion regime which is the reason of band bending. Alternative statement of thermionic emission in Schottky theory is only applicable for high mobility concentration whereas diffusion current is described only as limiting case of low mobility induced organic semiconductors. Proper explanation of band bending is relatively absent in this regime. But the previous discussion shows the existence of band bending occurs in low voltage regime also. Classical differential Schottky equation can be introduced to clarify the confusion such as follows [24]:

$$J_p = \mu_p kT \left(\frac{p}{kT} \frac{dE_v}{dx} - \frac{dp}{dx} \right) \quad (6.5)$$

Since the conduction in organic structure strongly depends upon the thickness L , hence the following equation is further modified to set a range upto L in integration to obtain the total current density which leads to:

$$J_p = \int_0^L \exp\left(-\frac{E_v}{kT}\right) dx = -\mu_p kT p(x) \exp\left(-\frac{E_v(x)}{kT}\right) \Big|_0^L \quad (6.6)$$

Solution of the given equation can be stated as:

$$J_p = \frac{q\mu N_v(\phi_{bi}-V)\left[\exp\left(\frac{qV}{kT}\right)-1\right]}{L\left[\exp\left(\frac{q\phi_{bi}}{kT}\right)-\exp\left(\frac{qV}{kT}\right)\right]} \quad (6.7)$$

The above equation was valid for charge diffusion area where the mobility concentration is constant, Pasveer et al.[25]. Since band bending occurs near the injection contact which reduces the effect of built-in-potential in that region, hence the eq (6.7) needs to be modified slightly and the expression was found from the work of Bruyn et al. [26]:

$$J_{diff} = \frac{q\mu N_v(\phi_{bi}-b^*-V)[\exp(\frac{qV}{kT})-1]}{L[\exp(\frac{q\phi_{bi}}{kT})-\exp(\frac{q(V+b^*)}{kT})]} \quad (6.8)$$

where b^* means the amount of band bending and is defined as [27,28]

$$b^* = \frac{kT}{q} [\ln\left(\frac{q^2 L^2 N_v}{2kT\epsilon}\right) - 2] \quad (6.9)$$

Band bending is basically the resultant value of interfacial potential and V_{bi} . The term interfacial potential can be termed as a reason of the difference of Fermi level energy and energy of active organic layer. Significant impact of trap concentration can be encountered on the value of interfacial potential. Increment of its influence can be observed at the metal-semiconductor interface in presence of trapping. Energetic disorder along with interfacial contact causes accumulation of charges in band bending zone in presence of more hopping sites. Band bending has definite impact to reduce the value of V_{bi} as well as on the current density below V_{bi} . Figure of band bending has been shown in Fig.6.2. On the basis of b^* affected thickness parameter, conduction follows an inverse relation with L in diffusion regime. Since penetration of free carriers through the interfacial thickness increases quite naturally with increasing voltage so density of trapped charge should decrease with the applied voltage in that region. Fig.3 shows the consistency of above discussion which also leads to the reliability of present experiment where the following parameters for simulation are considered such as effective density of state (N_v), carrier mobility (μ), trapping density (N_t), Richardson constant (A^*) and characteristic temperature (T_c) are 10^{20} cm^{-3} , $2.48 \times 10^{-7} \text{ m}^2 \text{ V}^{-1} \text{ s}^{-1}$, $1.45 \times 10^{25} \text{ m}^{-3} \text{ eV}^{-1}$, $5.4 \times 10^{-4} \text{ A/m}^2 \text{ K}^2$ and 1200 K respectively.

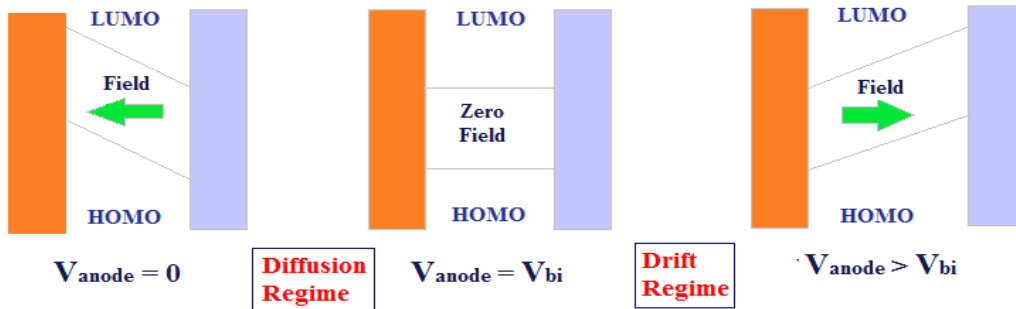


Fig.6.2 Schematic diagram of band bending at diffusion regime towards drift regime [30]

The above discussion can also be expressed in terms of theoretical approximation. In this context, Boltzmann approximation will be useful enough which signifies certain relationship between density of holes and potential:

$$p = p_0 e^{-(qV)/kT} \quad (6.10)$$

Where $p_0 = N_v e^{-\phi_{bi}/kT}$ is hole density at initial regime of carrier injection and ϕ_{bi} is barrier potential at anode-semiconductor interface.

At low voltage, total current density can be estimated from the carriers started to flow from anode and cathode together along opposite direction. As can be seen in Fig.6.3, due to the low amount of voltage applied across anode than V_{bi} , only carriers having high thermal energy results anode current along the direction of electric field followed in such condition $V_{anode} < V_{bi}$. Works of skinner [29] subsequently following Mott-Gurney had predicted the general solution of electric field which writes such as follows:

$$F(x) = -\frac{2kT}{q} m \coth m(x + x_1) \quad (6.11)$$

where $x_1 = \frac{arm \sinh gx_0}{m}$, x_0 denotes Debye length and m is constant.

Potential across that regime can easily be estimated by simply integrating the electric field in such a manner

$$V(x) = \int_0^x F(x) dx = \frac{2kT}{q} \ln \frac{\sinh(mx + arm \sinh mx_0)}{mx_0} \quad (6.12)$$

In present context, x of $V(x)$ ranges between 0 to V_{bi} . In such range of diffusion regime theoretical prediction can't reach any specific conclusion, according to Kim et al. [30]. So to have better insight regarding the purpose to solve the concerned problem, numerical simulation based modeling and verification of the result of modeling by experimental outcome perhaps the possible approach to set any relation between trapping states and ideality factor with relevant theoretical interpretation.

Existence of distribution in disordered organic structures has already been reported in several studies but its effect at diffusion regime is still remains a vexed question about its significance in

diffusion regime. However, exponential DOS distribution in this case gives the following equation mentioned below [31]:

$$N(E) = \frac{N_t}{kT_c} e^{-\frac{(E-E_v)}{kT_c}} \quad (6.13)$$

where N_t is density of trapping states, T_c is characteristic temperature. The trapped hole density is calculated from FD (Fermi & Dirac) distribution over given energy range

$$p_t(E_F) = \int_{-\infty}^{+\infty} \frac{N'(E)dE}{1+e^{-(E-E_F+qV)/kT}} \quad (6.14)$$

where E_F is Fermi energy. Kim and co-workers predicts [30] that for the condition when $T_c > T$, relation between trapped hole concentration (p_t) and applied voltage can be approximated as

$$p_t = p_t^0 e^{-(qV)/kT} \quad (6.15)$$

where $p_t^0 = N_t e^{-\phi_{bi}/kT}$, p_t^0 denotes amount of trapped hole at $x=0$. Semilog plot of trapped hole density with applied voltage (V) at concerned regime has been shown in Fig.6.3.

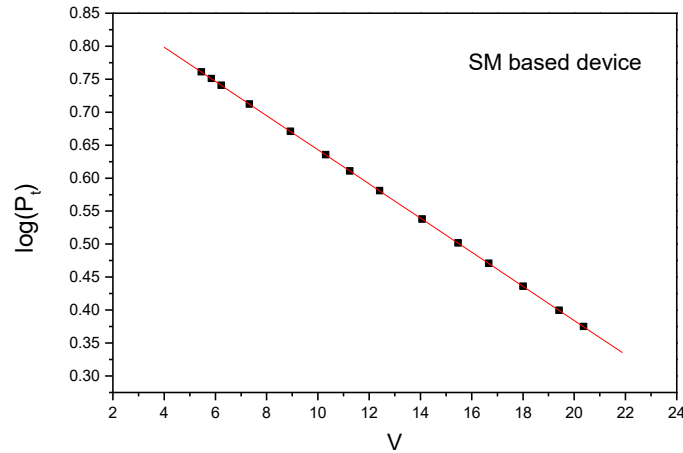


Fig.6.3 $\log(P_t)$ vs V plot of SM based device. $\log(P_t)$ follows inverse linearity with increasing voltage which shows consistency with the theoretical aspect.

Several fact of realization to have better insight about the impact of traps and the difference between trap assisted states with conduction states has already been proposed. ME (mobility-

edged) model [32] is one of the renowned model among those descriptions which was also the very first model regarding organic semiconductors. Starting from the fact of disordered materials, this can also be introduced to an extension of crystalline elements. The model has likely been followed in MTR (Multiple trapping-releasing) model [33]. It can be stated from the proposal of the model that hopping transport of the conducting carriers take place in the localized states which is negligible in comparison to the conduction in further extended states. However, to solve this consequence TE (transport energy states) model based Gaussian distribution in localized state has more conceptual relevance, according to Zhao et al [34]. Transport energy level is basically a temperature dependent level. Electrons start hopping from upper energy states towards a particular energy state. After facing number of hopping it transits in a state near the TE level where relaxation process changes and corresponding transport mechanism follows MTR model. Ideality factor and energy of trapping states are the fundamental factors described in such different models related to carrier conduction and also in present illustration so it may have scientific relevance for organic devices to find a relation between these two parameters. As the simulation based outcome obtained in fig.3 matches with the earlier theoretical illustrations, investigation to predict a relation between the parameters has been approximated on the basis of the outcome of the simulation technique. Experiments have also been done on a pair of natural dye based single layer organic device for verification of simulation outcome which satisfactorily matches with the obtained relation. Discussions over the fact have been presented in next section of the work.

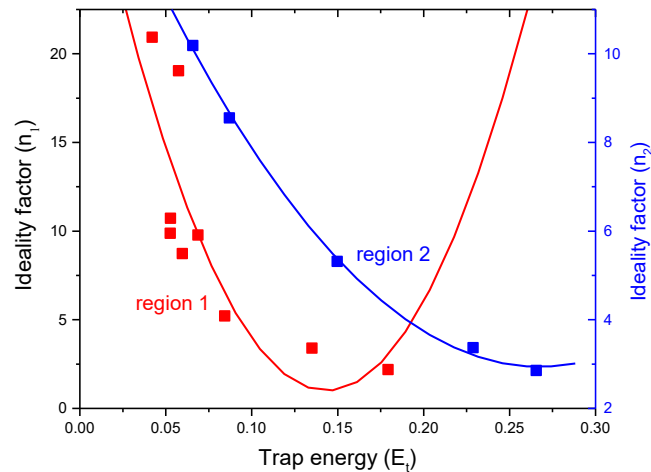


Fig.6.4 E_t vs n plot of SM based device at low voltage zone. Low voltage zone has been segmented into two different regions. In region 1, the plot n shows highly disordered nature with increasing E_t whereas n faces exponential decay in region 2 with increasing value of E_t .

Fig.6.4 represents the profile of n - E_t plot of SM based device. From the aforementioned plot it can be predicted that as charge population is said to happen at band bending regime of injection contact, recombination takes place with opposite charges and also due to multiple disordered hopping based conduction towards transport energy state, conduction is highly non linear which leads to repeated dramatic variation of n with respect to trap energy in region 1. In region 2, the plot indicates quite interesting nature. n follows an inverse exponential relation with E_t in region 2. As transition occurs from band bending dominated injection contact towards relatively linear diffusion zone below V_{bi} , ideality factor is facing exponential decrement from high value towards unity with relatively prone deep trapping states. Hence trap dominated ideality factor can gradually be elucidated from region 2. There are several study available which signifies the abovementioned parameters but no prominent explanation was put forwarded relating the parameters yet at diffusion regime. It is predicted that the outcome of present data provides relevant information probably for first time which shows inter-dependence between these two measured parameters. The obtained results have also been verified by estimation in experimental devices.

Indigo and Turmeric dye based natural organic semiconductors are taken into account for experimental verification. These experimental dyes are easily available. Moreover, inexpensive such common natural ingredients show promising semiconducting nature [5-6, 35]. Research over these dyes may provide significant information which may be valuable enough for future application in different electronic devices. Since earlier investigations have reported that these two dyes have more wide possibilities among other natural dyes so the present study has taken into consideration the mentioned dye based organic devices in this regard for characterization. However, for making the illustrations convenient, indigo dye based device is named as ID and Turmeric dye based device is abbreviated as TD. Fig.6.5 shows current voltage relation for ID and TD based devices. I and n have been plotted accordingly with respect to voltage at diffusion regime. Comparison of figures indicates similar conduction mechanism as depicted in Fig.6.3. It is quite natural that the values obtained in experiment should differ from the values obtained

from simulation but the focus should be given on the nature of charge conduction and obviously on ideality factor based on earlier discussion.

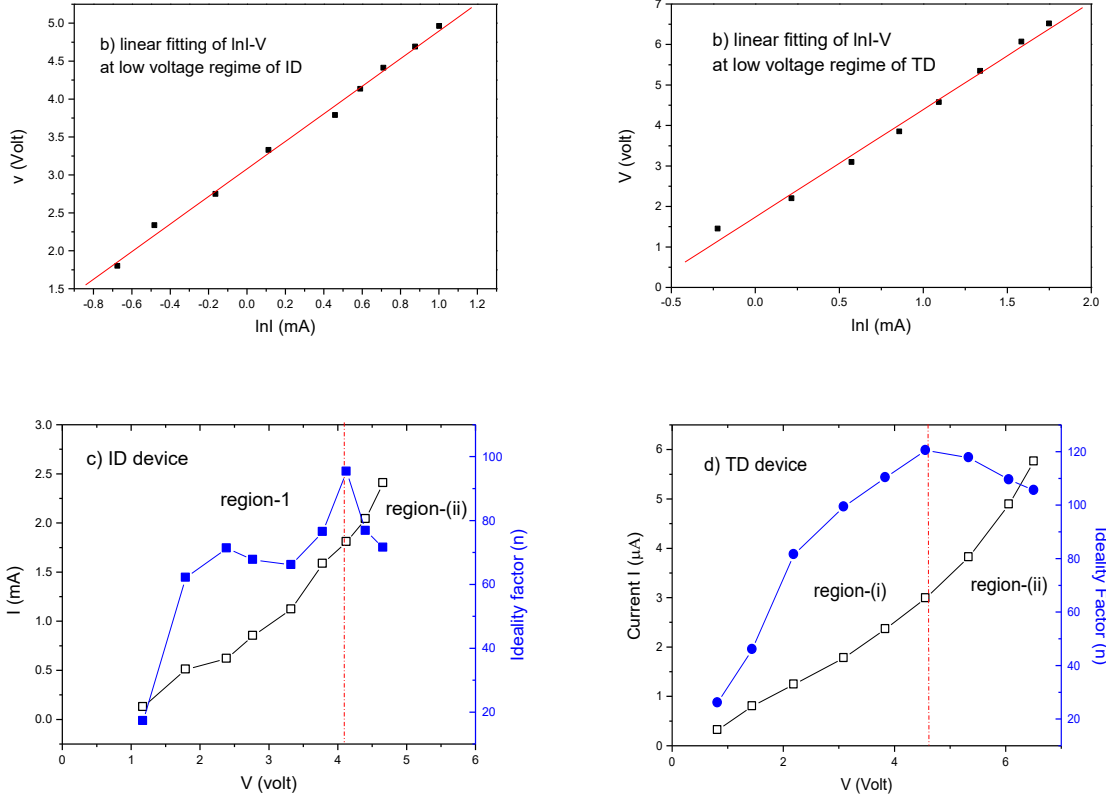


Fig.6.5 $\ln I$ -V characteristics at low voltage regime of 5.(a) ID based 5.(b) TD based device. From the slope of the characteristics ideality factor is determined for both devices. V-I-n plot of 5.(c) ID based 5.(d) TD based device

Result of the experiment shows good consistency with the simulation outcome profile. The outcome of the experimental characterizations fairly agrees with the theory of modified Einstein equation. For both devices (ID and TD), ideality factors show far deviation from unity at highly disordered injection zone of diffusion regime mentioned as region-(i) in the figure. Similarity has also been encountered in the region-(ii) for ID and TD device. This region denotes the extended state where charges start to flow overcoming the carrier accumulation assisted disordered

hopping. TE in this regime leads to relative linearity which results initiation of corresponding decrement of ideality factor nearly built-in-potential zone of diffusion regime.

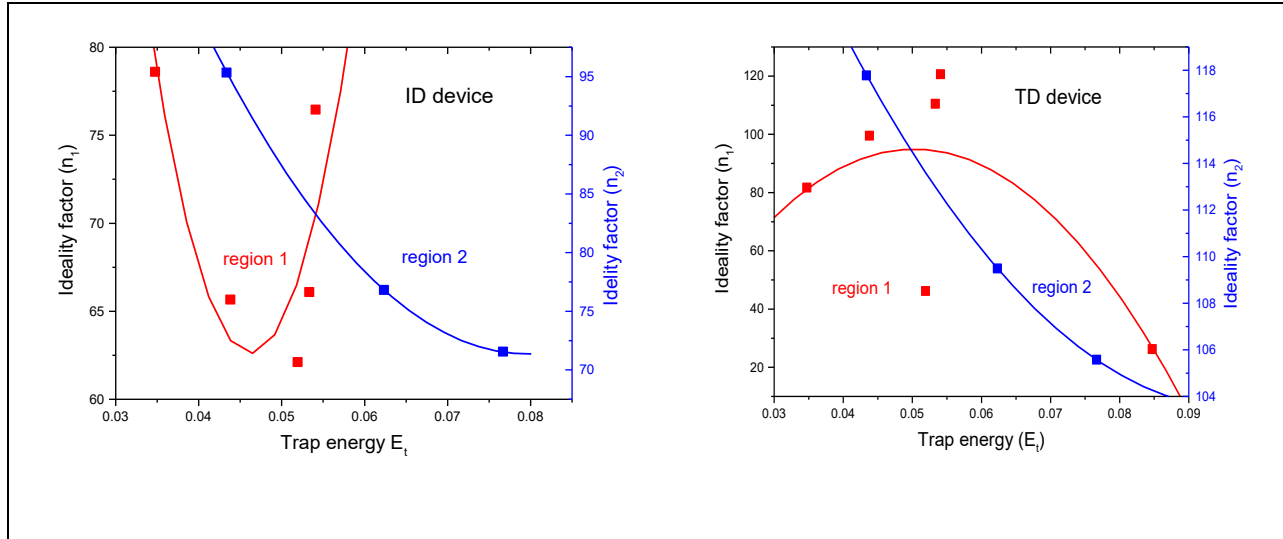


Fig.6.6 E_t vs n plot of ID and TD based devices at low voltage zone

Subsequently, experimental observation on dependence of n on E_t , interpreted on the basis simulation approach in Fig.6.4, shows convincing similarity with practical application of ID and TD devices depicted in Fig.6.6. As illustrated from simulation outcome, result of the experiments on ID and TD devices to relate n and E_t also can't predict any definite relation at region-1 due to interfacial mismatch at injection contact generated high level of disordered hopping nature of charges. In region-2 of diffusion dominated conduction, n shows inverse exponential relation with E_t . The following aspect supports the prediction ascribed in n - E_t characteristics of SM based device model.

6.4. Conclusive remarks

Conduction mechanism at low voltage of natural dye based organic semiconducting devices has been reported. Current in this regime follows diffusion dominated conduction. Simulation output on this occasion has been verified by theoretical models to search for the reliability of our experimental outcome. Simulation outputs shows consistency with the theoretical relations.

Hence the experimental work has been performed on a pair of natural organic devices to further study the validation of the prediction. Experimental observation on both devices also shows satisfactory similarity with the plot of simulation result. In present investigation, large deviation of n from unity is at diffusion regime has been encountered and possible reasons have been explained leading to the practical implementation of modified Einstein equation. Relation between n and E_t has been approximated at the aforementioned regime. No specific relationship can be established between these two parameters analyzing the simulation as well as experimental data of devices at the leakage flow assisted interfacial injection zone. Possible reasons of high variation of n at this regime have been discussed over this issue. An inverse exponential decay of n has been encountered with respect to E_t at the diffusion dominated extended regime of the previous state. Conduction with relative linearity at this extend state comprises less accumulation of charge concentration, more hopping tendency and trapping orientation by appeared directional electric field which leads at such a transition energy level, where carrier mobility is getting enhanced towards exponential switch. The fact has been interpreted as the possible cause of such exponential decay of high range ideality factor near the transition regime.

6.5. References

1. S.M.H. Rizvi, P. Mantri, B. Mazhari, Traps signature in steady state current-voltage characteristics of organic diode, J. Appl. Phys. 115, (2015), 244502-(1-9)
2. R. MacKenzie, T. Kirchartz, G. Dibb, and J. Nelson, Modeling Nongeminate Recombination in P3HT:PCBM Solar Cells, J. Phys. Chem. C, 115 (19), (2011), 9806-9813
3. L. Sims, U. Hörmann, R. Hanfland, R. MacKenzie, F. Kogler, R. Steim, W. Brütting, P. Schilinsky, Investigation of the s-shape caused by the hole selective layer in bulk heterojunction solar cells, Org Elect. 15 (2014) 2862-2867
4. A. K. Rajan, L. Cindrella, Studies on new natural dye sensitizers from *Indigofera tinctoria* in dye-sensitized solar cells, Opt Mat. 88 (2019) 39-47

5. A. Bouzidi et al., Electronic conduction mechanism and optical spectroscopy of Indigo carmine as novel organic semiconductors, *Opt Quant Elect.* 50 (176) (2018) 1-15
6. Md K. Hossain et al., Effect of Dye extracting solvents and sensitization time on photovoltaic performance of natural dye sensitized solar cells, *Result I Phys.* 7 (2017) 1516-1523
7. A. Dakhel, F Z. Henan, Extraction and dielectric properties of curcuminoid films grown on Si substrate for *high-k* dielectric applications, *Mat Sc and Engg*, 178 (2013) 1062-1067
8. C. T. Sah, R. N. Noyce, W. Shockley, Carrier generation and recombination in P-N junctions and P-N junction characteristics, *Proc. IRE.* 45 (1957) 1228–1243
9. W. Shockley, W T. Read, Statistics of the recombinations of holes and electrons, *Phys. Rev.* 87 (1952) 835–842
10. R N. Hall, Electron-hole recombination in germanium. *Phys. Rev.* 87 (1952) 387
11. G. A. H. Wetzelaer, L. J. A. Koster, P. W. M. Blom, Validity of the Einstein Relation in Disordered Organic Semiconductors, *Phys. Rev.Lett.* 107, (2011), 066605-(1-4)
12. Y.Q. Peng et al., Einstein relation in chemically doped organic semiconductors, *Appl. Phys. A.*, 86, (2007) 225-229
13. H. Bassler, Charge transport in disordered organic photoconductors a Monte Carlo simulation study. *Phys. Stat. Sol. B* 175 (1993) 15–56
14. S. V. Novikov, et al., Essential role of correlations in governing charge transport in disordered organic materials. *Phys. Rev. Lett.* 81 (1998) 4472–4475
15. M C J M.. Vissenberg, M. Matters, Theory of the field-effect mobility in amorphous organic transistors, *Phys. Rev. B* 57 (1998) 12964–12967
16. R. Richert, L. Pautmeier, H. Bassler, Diffusion and drift of charge carriers in a random potential: deviation from Einstein's law. *Phys. Rev. Lett.* 63 (1989) 547–550
17. S. D. Baranovskii, T. Faber, F. Hensel, P. Thomas, G. J. Adriaenssens, Einstein's relationship for hopping electrons. *J. Non-Cryst. Solids* 198-200 (1996) 214-217

18. Y. Roichman, N. Tessler, Generalized Einstein relation for disordered semiconductors implications for device performance. *Appl. Phys. Lett.* 80 (2002) 1948–1950
19. D. Ritter, E. Zeldov, K. Weiser, Ambipolar transport in amorphous semiconductors in the lifetime and relaxation-time regimes investigated by the steady-state photocarrier grating technique. *Phys. Rev. B* 38 (1988) 8296–8304
20. G.-J. A.H. Wetzelaer, P. W. M. Blom Diffusion-driven currents in organic-semiconductor Diodes, *NPG. Asia. Mat.* 6 (2014) 1-13
21. O. Tal. et al, Measurements of the Einstein relation in doped and undoped molecular thin films. *Phys. Rev. B* 77 (2008) 201201
22. K. Harada. et al., Organic homojunction diodes with a high built-in potential: interpretation of the current-voltage characteristics by a generalized Einstein relation. *Phys. Rev. Lett.* 94, (2005) 036601
23. N. I. Craciun, J. Wildeman, P. W. M. Blom, Universal Arrhenius temperature activated charge transport in diodes from disordered organic semiconductors, *Phys. Rev. Lett.* 100 (2008) 056601
24. L. J. A. Koster, E. C. P. Smits, V. D. Mihailetschi, P. W. M. Blom, Device model for the operation of polymer/fullerene bulk heterojunction solar cells. *Phys. Rev. B* 72 (2005) 085205
25. W. F. Pasveer et al., Unified description of charge-carrier mobilities in disordered semiconducting polymers. *Phys. Rev. Lett.* 94(2005) 206601:
26. P. de Bruyn, et al. Diffusion-Limited Current in Organic Metal-Insulator-Metal Diodes, *Phys. Rev. Lett.* 111 (2013) 186801-(1-5)
27. G. A. H. Wetzelaer, Analytical description of the current-voltage relationship in organic-semiconductor diodes, *AIP Adv.* 8 (2018) 035320-(1-5)
28. [M. Kröger](#), et al. Role of the deep-lying electronic states of MoO₃ in the enhancement of hole-injection in organic thin films, *Appl. Phys. Lett.* 95 (2009) 123301

29. S. M. Skinner, Diffusion, Static Charges, and the Conduction of Electricity in Nonmetallic Solids by a Single Charge Carrier. I. Electric Charges in Plastics and Insulating Materials, *J. App. Phys.* 26 (1955) 498
30. C. H. Kim, O. Yaghmazadeh, Y. Bonnassieux, G. Horowitz, Modeling the low-voltage regime of organic diodes: Origin of the ideality factor, *J. App. Phys.* 110 (2011) 093722-(1-8)
31. V. Kumar, S. Jain, A. Kapoor, J. Poortman, R. Merten, Trap density in conducting organic semiconductors determined from temperature dependence of J–V characteristics, *J. App. Phys.* 94 (2003) 1283
32. J. Cottaar, L. J. A. Coster, R. Coehoorn, P.A. Bobbert, Scaling Theory for Percolative Charge Transport in Disordered Molecular Semiconductors, *Phys. Rev. Lett.* 107 2011 136601
33. N. Felekidis, A. Melianas, M. Kemerrink, Non equilibrium drift-diffusion model for organic semiconductor devices, *Phys. Rev. B.* 94 (2016) 035205
34. C. Zhao, C. Li, L. Duan, A competitive hopping model for carrier transport in disordered organic semiconductors, *Phy. Chem. Chem. Phy.* (2019)
35. K. Uehara, K. Takagishi, M. Tanaka, The Al/Indigo/Au photovoltaic cell, *Sol. Cells*, 22 (1987) 295-301

Chapter-7

Conclusion of the thesis

- 7.1. Introduction**
- 7.2. Work summary**
- 7.3. Concluding remarks**
- 7.4. Scope of the future work**

7.1. Introduction

Technological development in recent area is the witness of conceptual invention of application of nano-level organic semiconductor based devices. The area of research has indicated tremendous potential over last few decades. Physics of charge transport mechanism with proper study on optoelectronic properties at different regime of OSC based devices harvests a fascinating field in material science based research. Analytical elucidation based on these materials exhibit the opening of many enfolded avenue to the researchers. The justification of distinct properties of such materials differentiates them from inorganic one which claims the novelty about the judgment of their applicability in device application. Still the organic materials are required yet to be researched more extensively since the fabricated devices are facing fundamental limitations about their rapid development. The proper way of orientation the whole study requires establishing a bridge to relate the experimental techniques with theoretical aspects followed by simulation modeling to fruitfully validate the overall outcome. Following this manner, in depth explanation has been initiated focusing on discussion over different chemical and electronic properties of organic semiconductors. Theory based on charge transport modeling at different regime of OSCs has been incorporated with the aforesaid discussion in the thesis. It has been observed that the OSCs mainly struggle in order to maintain consistent device efficiency due to trap prone conduction appeared by its disordered nature. Conduction into the process faces high impact of series resistance driven by the existence of traps. Non-radiative recombination takes place during trap assisted charge conduction thus by decrementing the device efficiency. Based on the consideration of the following fact, it is truly required to carry out investigation over the detail of charge trapping in OSCs. Emphasis should be given on role of traps and its impact on charge conduction mechanism of organic semiconductors to resolve the problem. The outcomes of the whole research work in this context are intended to elucidate at various sections of the thesis.

7.2. Work summary and objectives

The aim of the research has been expressed in Chapter-I. Discussions are given on the entire work embedded in the thesis and represented in compact form of the total work in present

chapter. The analytical explanation over the organic semiconductor based trap prone charge conduction is aimed to be discussed vividly.

Detail overview of OSCs has been given in chapter-II. Review on past background consisting significant research works with theoretical and experimental elucidation has been explained. Properties of OSCs have been categorized into two sections: chemical and electrical structure. On the other hand, based on the tendency of disordered orientation, such materials are classified into three different sections: high ordered system, slight disordered system and high disordered system. The process of production of excitons and their recombination process have been focused. A comprehensive explanation on different types of recombination process has been provided also. It has been mentioned that Langevin recombination is the reason of recombination at interfacial regime whereas Auger recombination leads to the thermal agitation producing phonons. Focus has been concentrated on different theoretical modeling related to charge transport mechanism into OSCs. The Gaussian model is said to be one of the most fundamental method describing such charge transport. Equally all other essential consequences are considered utilizing Gaussian DOS. Diffusive charge concentration, concerned temperature and applied electric field highly influence the charge conduction. In general, percolation of carriers takes place depending upon the layer thickness in OSCs. The transition of the nature of diffusive flow turns into drift current when charges enter into SCLC regime from injection regime. Master equation approach has been well introduced in this context to demonstrate charge conduction in SCLC regime.

Charge trapping is ubiquitous in all OSCs which has a definite impact on the devices based on this materials. Detail nature of shallow and deep level trapping and their spatial distributions have been studied. Effort has been focused to address the aftermath of the trapping impact at interfacial regime. Disorder driven thermal agitation at band tail states has garnered the attention also in this context. A comprehensive discussion on different trap induced effect has been mentioned by describing some renowned theoretical model. Critical review on Anderson localization model leads to the separation between delocalized to localized states below the mobility edge (ME) range. Theory of ME model is mentioned in this context to explain the trapping induced conduction at the energy states placed above the extended delocalized mobility range with continuous band distribution. Thermal activated charge tunneling in localized states

followed by Miller-Abraham (MA) expression has been termed in order to elucidate hopping transport model. Hopping takes place at extended ranges of different energy sites. Percolation model becomes meaningful as an advancement of such hopping transport. Combining the theoretical analysis, it was reasonable to conclude that the conduction mechanism in disordered structure based OSCs is disturbed mainly due to contribution of shallow trapping and such trapping has inherent impact comparatively much greater than deep trapping. Chemistry insight of how trapping states play its role in OSCs was yet to be investigated. The objective of our work concentrates on that point of view to fill up the gap between conduction mechanism of OSCs and role of traps on such mechanism. Different trap measurement techniques have been introduced to characterize traps, among which renowned SCLC measurement technique has been taken into account in our experimental works described in chapter III to chapter VI.

Based on the objective to cope with the set point of the motivation, natural organic $C_{21}H_{20}O_6$ (Turmeric dye) and $C_{16}H_{10}N_2O_2$ (Indigo dye) has been taken into consideration to have unified realization of the trap assisted charge transport at different regime of such material based device. Verification of trap signature has been experimented by introducing different Current-Voltage relationship. Estimation of trap related electrical parameters such as trap energy, barrier height, trap factor and trap energy has been encountered from different analytical treatment. Dependence of barrier potential on trap energy during conduction has been elucidated by considering Mott-Gurney law and drift-diffusion equation. Richardson-Schottky based charge transport mechanism is observed dominant analyzing $\ln I$ vs $V^{1/2}$ plot in conduction process over Poole-Frankel process in this device. The following consequence has been described in Chapter III and IV.

As an application of the experimental outcome described in Chapter-III and Chapter IV, has been validated with analyzing the simulation output of GPVDM modeling in Chapter V. GPVDM (General Purpose Photovoltaic Device Model), a very well known, updated and reliable simulation modeling technique, is introduced for current research to have better insight on the physics lies on the carrier transport mechanism and estimation of comparison of photovoltaic and electrical parameters of single and bi-layer photovoltaic devices. Dark output current obtained from simulation modeling is considered to explain the orientation of trapping sites by introducing differential technique. Greater range of monotonic lowering of the $G(V)$ vs V curve

conclude reduced trapping influence for bi-layer device which inherently enhances the charge conduction. Reduced effect of trapping explicitly results better device efficiency with improvement of different electrical and photovoltaic parameters in bi-layer devices in comparison to single layer device.

Chapter VI deals with charge transport at low voltage regime. The work comprises a combination of theoretical illustration with experimental outcome. Current obtained at low voltage is found as diffusion driven in nature. Observation in this context shows consistency among different aforementioned approaches undertaken to elucidate the fact. Significant deviation of ideality factor from unity at diffusion dominated conduction regime has been obtained and the physics held behind the reasons have been expressed leading to the practical implementation of modified Einstein equation. No specific theoretical inter-relation between trap energy and ideality factor can be approximated analyzing the obtained data prone to distorted discrete leakage current at low voltage zone. But an inverse exponential decay of ideality factor has been encountered with respect to trap energy at an extended low voltage state have been observed in our experimental interpretation. The possible fact of elucidation has been discussed in the abovementioned chapter VI.

7.3. Concluding remarks

The entire work involves in organic semiconductor based diode fabrication, its characterization and trap related electrical parameters measurement techniques. In most of the cases SCLC measurement has been implemented for elucidation of analytical outcome of trap induced current-voltage characteristics. Basically, like all other reports, space charge limited regime has been into account for realization of charge transport mechanism of Turmeric and Indigo dye based natural organic diodes. Signature of trapping states has been intended to identify by analyzing differential I-V curve. Non-monotonic distortion holds in such curve implies the existence of trapping sites at the interfacial transport regime of OSCs. Role of trapping energy on barrier potential and interfacial band bending has been elucidated in order to illustrate the conduction in OSCs. It has been observed that trap energy has enormous impact on electrical parameters mainly such as: series resistance and ideality factor. Interpretation of GPVDM simulation based output has been provided comparing the analytically measured performance of

single layer and bi-layer organic device to validate the aforementioned observation. Finally, trap effect on charge transport at low voltage regime has been reported. Conduction follows diffusion driven mechanism at the mentioned regime. Significant consistency have been obtained in experimental observation and theoretical elucidation concluding trap induced exponential decay of ideality factor at extended state of diffusion dominated distorted carrier injection zone. It is expected that the thesis will be helpful to the researchers working over the application of organic semiconductor based photovoltaic devices, photo diode, photo collector and other photo sensitive devices.

7.4. Scope of the future work

It is needless to mention that grown up interest on organic semiconductor based devices will lead them towards an efficient replacement of inorganic one in near future. Our contribution is intended to accelerate the motion of the occurrence being a catalyzer in this aspect. In addition, focus has also been reflected even such on some facts (like conduction in low voltage regime) which were less attracted earlier. But it is believed that ever growing science lies into the research will further update more aspects which may draw the significant attention of the researcher community. But despite of numerous investigations, there is still exists the persistence of some vexed questions. Plenty of unsolved studies are proposed which could act as continuation from the investigation described in the thesis.

Remarkable progress can be observed over several years in terms of trap characterization reducing unintended effects through introducing implementation of novel techniques in trap characterization and fabrication of the device. Proper understanding of the issue leads to novelty in the context of new design formation. Systematic research involving in trap induced nature of DOS spectrum with variation of temperature should be taken into concern as an extension of future scope. Though we have provided a comprehensive discussion by comparing the extracted data that indicates improvement of trap assisted electrical parameters, but still common natural semiconducting dyes are primary level of research. A very few manuscripts can be found that discusses the positivity and negativity of such dyes. So that realization of intermolecular interaction, interfacial charge coupling, surface morphology, analysis of thin film imaging should be carefully reported to have a better insight on the applicability of such elements in commercial device application. On the other hand, trap generated from variation of different disordered system should be theoretically correlated to resolve the trapping problem. Precise theoretical modeling supported by experimental validation should be developed. In addition, studying the improvement of trap energy of these materials with incorporation of different nano-particles and nano-tubes are to be investigated properly and the obtained data should be procured to analyze the reason of quality improvement of conduction mechanism. Furthermore, effect of such nano-elements on charge conduction with temperature variation should be recorded. In order to resolve the following facts, development and characterization coupled with progressive outcome, leads

to significant performance improvements enabling full potential to be realized in real world application.

-----***-----

LIST OF PUBLICATIONS INCLUDED IN THESIS

1. “A Comprehensive Study on Utility of Carrier Transportation Layer for Efficiency Improvement of Organic Photovoltaic Devices using GPVDM Modeling”- **K. Chakraborty**, R. Mondal, D. K. Mandal, *Int. J. Engg. Appl. Phys.* (2022)
2. “Interpretation of Trap Assisted Conduction with Estimation of Electrical Parameters of Thin Indigo Film Based Semiconducting Device”- **K. Chakraborty**, A. Das, R. Mondal, D. K. Mandal, *Bull. Mat. Sc*, 2021
3. “An analytical study on low voltage regime of natural organic semiconductor based device: Physics of trap energy and ideality factor”- **K. Chakraborty**, A. Das, R. Mondal, D. K. Mandal, *Sol. Stat. Comm.* 2021
4. “Investigation on the Trap Signature in Organic Semiconductor Turmeric Film Through Current–Voltage Analysis”- **K. Chakraborty**, A. Das, R. Mondal, D. K. Mandal, *Trans. Tianjin. Univ.* 2020

LIST OF PUBLICATIONS NOT INCLUDED IN THESIS

1. “A Unified Realization of the Modified Einstein Equation Approach in Organic Semiconductors: Theoretical Interpretation and Experimental Validation”- **K. Chakraborty**, R. Mondal, A. Das, D. K. Mandal, *Ind. J. Phys.* (2023)
2. “Effect of single walled carbon nanotubes on series resistance of Rose Bengal and Methyl Red dye-based organic photovoltaic device”- **K. Chakraborty**, N. B. Manik, S. Chakraborty, *J. Semiconductors* (2018)

3. **“Impact of ZnO nanoparticles on electrical characteristics of herbal dye based Schottky Diode”**- A. Das, R. Mondal, **K. Chakraborty**, D. K. Mandal, **Bull. Mat. Sc.**(2022)

4. **“Electrical Characteristics of Turmeric dye based organic thin film diode and effect of light on barrier height”**- A. Das, R. Mandal, **K. Chakraborty**, D. K. Mandal, **Mat. Proceeding.** (2022)

5. **“Design and Fabrication of Indigo Dye Based Organic Thin Film”**- A. Das, R. Mondal, **K. Chakraborty**, D. K. Mandal, **IJKC** (2019)

LIST OF PRESENTATIONS IN INTERNATIONAL CONFERENCES

1. **“Experimental Prediction of Effect of Thickness of Active Layer of Photovoltaic device on a series of electrical parameters using GPVDM software”**- **K. Chakraborty**, D.K. Mandal, R.Mondal, A. Maiti, **2ND** International Conference on **“Innovation in Science and Technology”** (SPECTRUM-2019), **Int.J.Adv.Sci.Engg. 2019, IEM, Kolkata**

2. **“Estimation of Series Resistance in Different Organic Compound Dye based Organic Diodes”**- **K. Chakraborty**, R. Mondal, D. K. Mandal, S. Gangopadhyay, International Conference on (RAICMHAS-2019), **IJKC, (2019), Brainware University, Barasat, Kolkata**